biomolecules

Review

Madecassoside Part I: From Biosynthesis to Druggability

Yuping Li [1,2,3], Mengdan Xu [4], Yuting Yang [1], Shanshan Liang [1,5], Yucui Lu [1,3], Xianmei Lin [1,3] and Lichun Zhao [1,3,*]

[1] Research Center of Trace Elements and Health Development, Guizhou University of Traditional Chinese Medicine, Guiyang 550025, China
[2] School of Basic Medicine, Guizhou University of Traditional Chinese Medicine, Guiyang 550025, China
[3] School of Pharmacy, Guizhou University of Traditional Chinese Medicine, Guiyang 550025, China
[4] Guiyang Institute of Information Science and Technology, Guiyang 550025, China
[5] Resource Institute for Chinese and Ethnic Materia Medica, Guizhou University of Traditional Chinese Medicine, Guiyang 550025, China
* Correspondence: hyzlc@gzy.edu.cn

Abstract

Background: Madecassoside (MA) is the core bioactive pentacyclic triterpenoid saponin and a key quality control marker of *Centella asiatica* (L.) Urb. Its material basis and druggability profiles are fundamental prerequisites for pharmacological research and clinical translation. Although several reviews have covered selected aspects of MA chemistry and pharmacology, no systematic review has comprehensively covered the full chain from chemical structure to in vivo disposition exclusively for MA monomer. **Objective:** As the first part of a two-part series, this review aims to systematically integrate evidence on the chemical basis, biosynthesis, green preparation, and pharmacokinetic characteristics of MA and clarify the core druggability bottlenecks of this compound. **Methods:** The literature search was conducted in PubMed, Web of Science, and China National Knowledge Infrastructure (CNKI) up to 31 August 2026. Studies focusing on the chemistry, biosynthesis, extraction/purification, and pharmacokinetics of MA were included and critically analyzed. Evidence was stratified into four predefined levels: Level A (clinical trials), Level B (in vivo animal studies), Level C (in vitro cell/molecular studies), Level D (computational prediction). The limitation of Chinese literature to Peking University core journals is acknowledged as a potential source of publication bias. **Results:** Current evidence supports that the C-6 β-hydroxyl group on the ursane-type aglycone skeleton and the intact linear trisaccharide chain at the C-28 position are the major structural correlates of MA's biological activity (working hypothesis based on natural analog comparisons). The backbone cyclization and glycosylation steps in the MA biosynthetic pathway have been largely characterized, but the specific enzymes responsible for C-2 α- and C-6 β-hydroxylation remain to be fully identified. Green extraction technologies such as ultrasound-assisted extraction, microwave-assisted extraction, and deep eutectic solvent extraction have been well optimized, and multiple purification strategies can yield high-purity monomers. In rats, the oral absolute bioavailability of the pure MA prototype is less than 1%, with extensive intestinal metabolism and enterohepatic circulation, representing the core druggability bottleneck. Human pharmacokinetic data remain very limited, and rat values cannot be directly extrapolated to humans. **Conclusions:** This review establishes a full-chain material basis framework for madecassoside spanning from molecular structure to in vivo disposition, systematically integrating evidence on structural activity determinants, biosynthetic pathways, green extraction and purification technologies, and pharmacokinetic profiles. Extremely low oral bioavailability and extensive in vivo metabolic transformation are confirmed as the core druggability bottlenecks. These findings lay the essential foundation for elucidating pharmacological mechanisms, optimizing

Academic Editors: Hilal Zaid, Zipora Tietel and Akhilesh K. Tamrakar

Received: 20 October 2026
Revised: 9 November 2026
Accepted: 11 November 2026
Published: 14 November 2026

Copyright: © 2026 by the authors. Licensee MDPI, Basel, Switzerland. This article is an open access article distributed under the terms and conditions of the Creative Commons Attribution (CC BY) license.

delivery systems, and advancing clinical translation in the second part of this series. To our knowledge, this is the first two-part systematic review focused exclusively on the MA monomer that covers the full translational spectrum from chemical fundamentals and druggability profiles to pharmacological mechanisms and clinical translation.

Keywords: madecassoside; chemical basis; structure–activity relationship; biosynthesis; green extraction; pharmacokinetics; druggability

1. Introduction

1.1. Traditional Uses and Modern Medicinal Value of Centella Asiatica

Centella asiatica (L.) Urb. is one of the most historically used traditional medicinal plants worldwide. In traditional medical systems across Asia—particularly in China, India, and Southeast Asia—it has been widely used to treat wounds, burns, skin infections, and inflammation, and to promote wound healing. It is also commonly used as a brain tonic due to its purported effects of enhancing brain function, improving memory, and relieving anxiety. In folk medicine, it is also applied for psoriasis, scleroderma, leprosy, fever relief, detoxification, and gastrointestinal and urinary tract disorders [1,2].

Modern pharmacological research has confirmed that the core active constituents of *C. asiatica* are triterpenoids, including madecassoside (MA), asiaticoside (AS), and their respective aglycones madecassic acid (MAA) and asiatic acid (AA). These compounds endow *C. asiatica* with a broad spectrum of pharmacological activities, making it one of the most evidence-based single herbs in the field of burn therapy [3,4]. Although isolated case reports have suggested potential hepatotoxicity [5], *C. asiatica* still holds broad modern application prospects in wound healing, neuroprotection, and anti-inflammatory therapy.

1.2. Discovery and Status of MA as a Core Active Constituent of C. asiatica

The discovery and status of MA as a core active component have been gradually established through chemical isolation and pharmacological validation. In 1981, researchers first isolated and identified MA from total AS fractions [6]. Subsequent studies have confirmed that MA not only promotes fibroblast proliferation and collagen synthesis (especially type I and type III collagen) [7,8] but also possesses anti-inflammatory [9,10], antioxidant [11,12], neuroprotective [13,14], antidepressant [15], cardiovascular protective [16], and wound-healing/anti-scarring activities [17,18]. Some studies indicate that MA is superior to its homolog AS in promoting collagen synthesis and exerting anti-inflammatory effects [7,17], and the two often exhibit synergistic effects [19]. Its mechanisms of action involve multiple key signaling pathways such as Nuclear factor-κB (NF-κB), Mitogen-Activated Protein Kinase (MAPK), and Nuclear factor erythroid 2-related factor 2 (Nrf2)/Heme Oxygenase-1 (HO-1) [9,12,20].

Taken together, MA is not only a quality control marker for *C. asiatica* but also the core driver of its broad pharmacological efficacy [2,21,22]. However, the exertion of its efficacy fundamentally depends on its material properties: chemical structure determines target interaction, biosynthesis and preparation determine supply stability, and in vivo disposition determines druggability potential. A systematic clarification of these material foundations is a prerequisite for in-depth exploration of its pharmacological mechanisms and clinical translation.

1.3. Limitations of Existing Reviews and the Scope and Innovations of This Review

Despite the growing depth of MA research, as of 31 August 2026, prior reviews have either focused on total *C. asiatica* extracts or covered only selected pharmacological aspects of MA. No narrative review has focused specifically on MA monomer and covered the full chain from chemical basis to druggability profiles. A systematic analysis of the available literature reveals three core research gaps in the material foundation field, aligned with the logical chain from molecular structure to biosynthetic production, and then to preparation and in vivo disposition. These gaps correspond to the three core domains covered in Sections 3–6 of this review.

1.3.1. Chemical Fundamentals and Structure–Activity Relationships

Current evidence on MA's structural characteristics, isomer diversity, structure–activity rules, and structural modification strategies remains fragmented. Most studies focus on a single pharmacological activity or isolated structural analog, rather than establishing a systematic framework linking specific functional groups to activity intensity and druggability. There is also a lack of critical evaluation of the methodological limitations of natural analog-based structure–activity inferences. Readers cannot readily identify the core structural determinants of MA's biological activity from a single publication [6,23].

1.3.2. Biosynthetic Pathways and Raw Material Supply Systems

Although core enzymes in the MA biosynthetic pathway have been progressively identified, a full-chain review spanning upstream precursor supply, midstream skeleton modification, and downstream glycosylation processing is still lacking. In addition, there is no systematic cross-comparison of technical maturity, yield level, and industrialization bottlenecks across different production systems (field cultivation, hairy root culture, cell suspension, and microbial heterologous synthesis). This lag in basic biosynthetic research directly restricts the stable and controllable supply of high-quality MA raw materials [24].

1.3.3. Green Preparation Technologies and Druggability Profiles

Existing reviews of extraction and purification technologies are predominantly process-oriented and fail to establish the linkage between preparation process parameters, product purity/impurity profiles, and downstream druggability characteristics. Meanwhile, pharmacokinetic studies of MA are scattered across individual pharmacological reports, lacking a systematic synthesis of absorption, distribution, metabolism, and excretion absorption, distribution, metabolism, and excretion (ADME) rules and core bottlenecks. The disconnection between preparation research and pharmacokinetic research makes it difficult to optimize formulation development from a full-chain perspective [25,26].

As the first part of a two-part series review on MA, this paper focuses on the material basis and druggability of MA and achieves the following contributions: a. Constructs a full-chain evidence framework for MA spanning chemical fundamentals, biosynthetic production, green preparation, and pharmacokinetic characteristics, forming a logically closed structure from molecular basis to in vivo disposition and providing a complete material foundation for subsequent pharmacological and translational research. b. Systematically sorts out MA's structure–activity relationship rules and structural modification directions from a medicinal chemistry perspective and critically defines the core structural determinants of activity differentiation and the methodological limitations of current inferences. c. Comprehensively compares the technical characteristics and industrialization bottlenecks of four mainstream production systems and clarifies the core druggability bottleneck represented by extremely low oral bioavailability, providing clear problem orientation for subsequent formulation development and mechanism research.

https://doi.org/10.3390/biom16111663

2. Literature Search and Screening Methods

This paper is the first part of a systematic narrative review series on madecassoside. The evidence synthesis adopted a narrative approach due to the high heterogeneity of study designs across included studies.

This narrative review searched three mainstream academic databases: PubMed, Web of Science, and China National Knowledge Infrastructure (CNKI). The last literature search date was updated to 31 August 2026. Only peer-reviewed journal papers were included; preprints, conference abstracts, dissertations, and book chapters were excluded. For Chinese literature, the Peking University Core Journal Catalogue was used as a first-pass quality threshold for initial screening, given the extremely large volume of domestic publications and highly variable reporting quality. All finally included studies underwent further full-text methodological evaluation. This criterion served as a pragmatic initial filter rather than a definitive judgment of individual study quality; it may introduce publication bias toward positive results and potentially omit high-quality studies from non-core journals, which is acknowledged as an inherent methodological limitation. Before final exclusion, all 33 non-core records were manually screened at the title/abstract level, and no findings that would alter the core conclusions of this review were identified. Specifically, core evidence for MA biosynthetic pathways and key enzyme identification comes almost entirely from international English-language studies, and all relevant high-quality Chinese studies with original biosynthetic data have been included. For extraction technology and pharmacokinetics, the excluded records were predominantly small-scale process optimization reports with locally sourced raw materials; they do not alter the overall conclusions regarding technical maturity, typical yield ranges, or core ADME characteristics. Embase, Scopus, and Cochrane Library were not searched, which may lead to omission of some pharmacokinetic and safety studies. Additionally, the PubMed search was restricted to the title/abstract field, which carries an inherent risk of missing studies that investigate madecassoside as a secondary component or embed it within a broader experimental framework, and thus do not explicitly name the compound in the title or abstract. To mitigate this risk, supplementary backward snowball screening of reference lists from high-impact core reviews and landmark studies was performed for all core chapters (biosynthesis, pharmacokinetics, and extraction technology). Despite this mitigation, title/abstract-restricted retrieval remains an inherent methodological limitation of the current search design. The search strategies for each database were as follows: PubMed (“Madecassoside” [Title/Abstract] OR “Asiaticoside A” [Title/Abstract]); Web of Science (TS = (“Madecassoside” OR “Asiaticoside A”)); CNKI (SU= “羟基积雪草苷” OR “羟基积雪草甙”, two standard Chinese terms for madecassoside with variant Chinese characters for "glycoside"). During pilot optimization, additional compound synonyms and trade names were tested but not included in the final search string, as they did not retrieve unique relevant records beyond the core terms. Supplementary backward snowball screening of high-impact review references was performed for core chapters (biosynthesis and pharmacokinetics) to mitigate the risk of missing relevant studies.

A total of 906 records were retrieved from the initial search: 275 from PubMed, 433 from Web of Science, and 198 from CNKI. Identification stage: After removing 258 duplicate records and 41 non-journal documents (including 24 dissertations, 10 conference abstracts, 3 retracted papers, 1 book chapter, 2 correction notes, and 1 editorial), 607 records remained for title/abstract screening. Screening stage: 258 records were excluded after title and abstract evaluation, for reasons including irrelevance to MA research, unavailable full text, or non-original research. A total of 349 records remained for full-text eligibility assessment. Eligibility stage: 33 records were excluded after full-text review, all of which were Chinese-language publications not indexed in Peking University core journals. Inclusion stage: A final set of 316 eligible studies constituted the shared literature pool for

the entire two-part review series. Of these, 235 studies focusing on chemical basis, biosynthesis, green extraction/purification, and pharmacokinetic characteristics were selected for analysis in Part I; notably, a subset of these studies also covers pharmacological activity, safety evaluation, and other topics relevant to Part II, which are cited and analyzed in both parts as cross-thematic shared literature. The 235 unique studies in Part I are distributed across all eight sections as follows: Introduction (n = 26), Literature Search and Screening Methods (n = 0), Chemical Basis and Structure–Activity Relationship (n = 90), Biosynthesis and Metabolic Engineering Regulation (n =70), Green Extraction and Efficient Purification Technologies (n = 57), Pharmacokinetics and In Vivo Disposition (n = 47), Research Challenges and Future Perspectives (n = 9 additional unique studies), and Conclusions (n = 0). Owing to extensive cross-chapter citation of core research articles, the total number of section-level citations exceeds the count of unique studies. The complete literature screening process and record counts at each stage are shown in Figure 1.

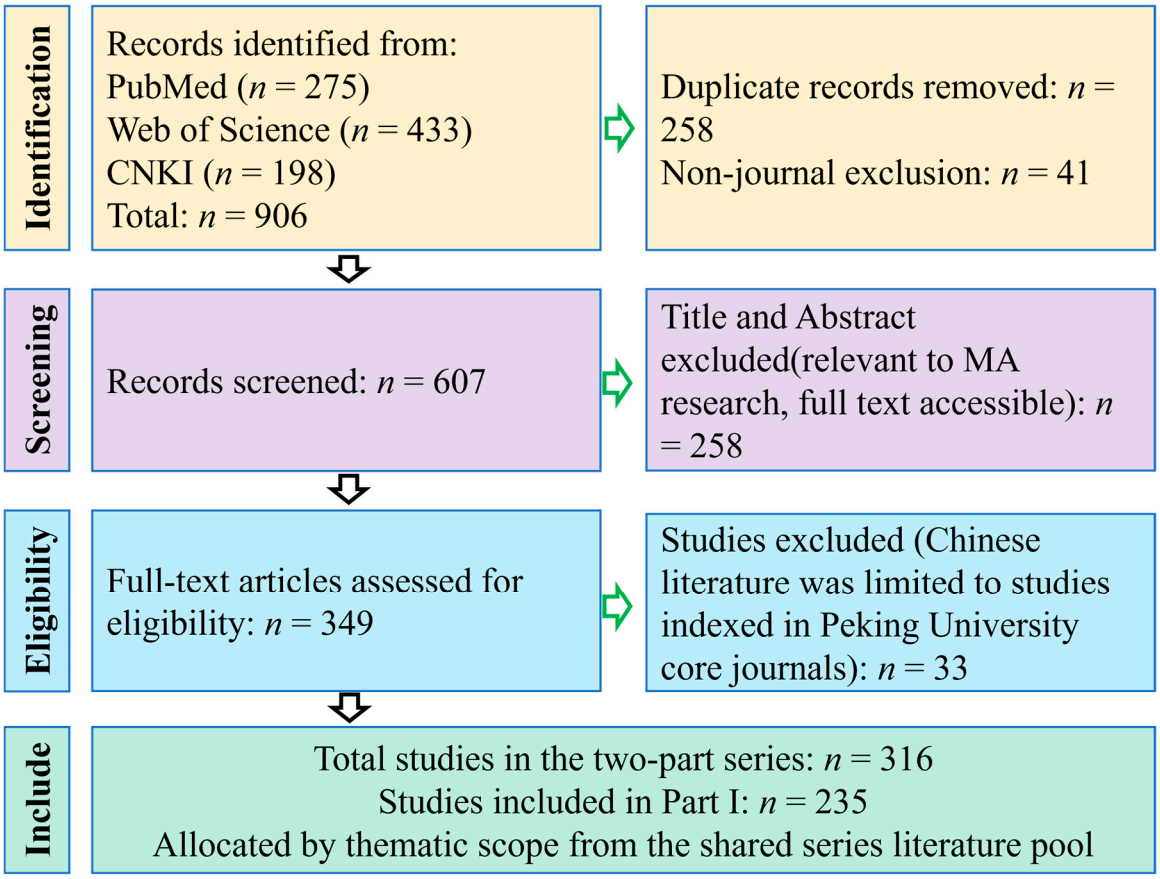


Figure 1. Literature screening flow diagram. The two parts of this review share an identical initial search strategy and a common pool of 318 eligible studies identified from three databases (PubMed, Web of Science, and CNKI). Studies were allocated to each part according to thematic scope: Part I covers chemical basis, biosynthesis, green extraction/purification, and pharmacokinetics; Part II covers pharmacological effects, drug delivery systems, clinical translation, safety evaluation, and paradoxical mechanisms.

All included studies were stratified into four evidence levels. Level A: Randomized controlled trials (RCTs) and clinical cohort studies; Level B: In vivo animal experiments and ex vivo tissue studies; Level C: In vitro cell culture experiments, enzyme activity assays, and physicochemical experiments; Level D: Molecular docking, molecular dynamics simulations, and theoretical predictions. This classification represents a study design-based evidence hierarchy rather than a systematic quality appraisal of individual studies.

No formal risk-of-bias assessment or quantitative quality scoring was performed for each included study, and dimensions such as replication adequacy, appropriateness of control groups, analytical method validation, and internal limitations of original studies were not systematically evaluated on a per-study basis. This constitutes an inherent methodological limitation of this narrative review. Conclusions were weighted by evidence level and replicability. Findings consistently supported by multiple independent studies and primarily backed by Level A or Level B evidence were presented as well-supported conclusions. Findings derived from single studies, supported exclusively by Level C or Level D evidence, or showing inconsistent results across the literature were treated as preliminary or tentative. Mechanistic conclusions derived from Level C/D evidence were explicitly labeled as working hypotheses.

Data extraction and study selection were first discussed between the two investigators to reach consensus based on predefined criteria; if consensus could not be achieved through discussion, a third reviewer was consulted for independent adjudication. Although prevention and control measures such as independent dual-person operation, evidence level stratification, and simultaneous presentation of positive and negative evidence were adopted during the screening stage, the design of the review framework, the condensation of core arguments, and the prioritization of future directions still reflect the authors' critical judgment of existing evidence. Readers should conduct independent evaluation in conjunction with the original literature.

3. Chemical Basis and Structure–Activity Relationship of MA

3.1. Chemical Structure and Physicochemical Properties of MA

MA belongs to the ursane-type pentacyclic triterpenoid saponins. Its chemical structure uses MAA as the aglycone, and a linear trisaccharide chain of β-D-glucose-(1→6)-β-D-glucose-(1→4)-α-L-rhamnose is linked to the carboxyl group at the C-28 position via an ester bond (from the aglycone end to the sugar chain end). The parent nucleus simultaneously has four hydroxyl substitutions at positions C-2 α, C-3 β, C-6 β, and C-23. This is the core difference from its structural analog AS (which has three hydroxyl groups at C-2 α, C-3 β, and C-23 on the aglycone) [2,27]. The molecular structure differences between the two are shown in Figure 2.

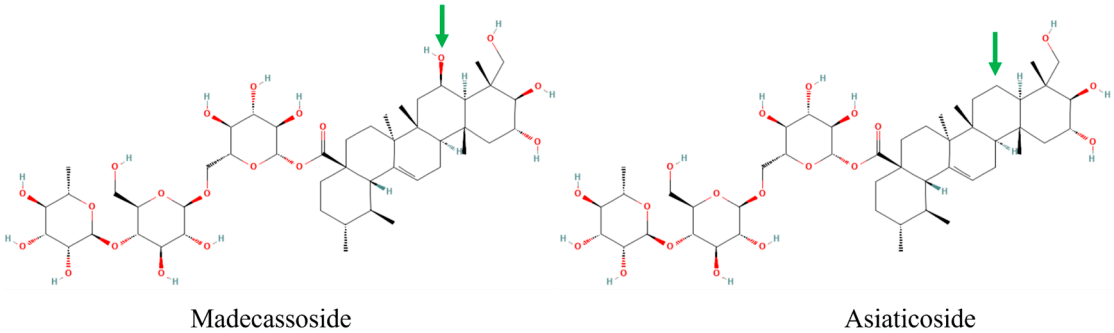


Figure 2. Comparative chemical structures of MA and AS. Both are ursane-type pentacyclic triterpenoid saponins sharing an identical linear trisaccharide chain [β-D-glucose-(1→6)-β-D-glucose-(1→4)-α-L-rhamnose] linked to the C-28 carboxyl group via an ester bond. As indicated by the arrow, the defining structural difference is the additional β-hydroxyl substitution at the C-6 position of the aglycone skeleton in MA, which is absent in the AS structure.

MA has a variety of structurally related derivatives. Among them, isomadecassoside is its double-bond position isomer: the double bond on the E ring migrates from position Δ^{12} to $\Delta^{20(21)}$, but it still retains anti-inflammatory activity comparable to the parent

compound [28]. It is a skeletal isomer of asiaticoside B (oleanane-type skeleton), with differences in the methyl substitution position on the E ring of the parent nucleus. Efficient separation of the two can be achieved by adding β-cyclodextrin to the mobile phase, with a resolution of up to 11.95 [29,30]. From a biosynthetic perspective, MA is generated from α-amyrin, catalyzed by CYP716A83 (C-28 oxidase) and CYP714E19 (C-23 oxidase), to form the aglycone, which then undergoes three-step glycosylation modifications at the C-28 position sequentially via glycosyltransferases such as UGT73AD1 and UGT73AH1 [31-33].

MA is a white amorphous powder or crystalline solid at room temperature, with typical physicochemical properties of triterpenoid saponins [34-36]: it is easily soluble in polar solvents such as methanol, ethanol, and water, and sparingly soluble in non-polar organic solvents such as chloroform, petroleum ether, and n-hexane. Due to one more hydroxyl group in the molecule and the strong polarity of the sugar chain, its overall polarity is slightly higher than that of AS. This difference results in weaker retention behavior during macroporous resin adsorption and reversed-phase chromatography separation, and the two can be enriched and separated by gradient elution [35,36].

Its chemical stability is significantly affected by pH and temperature. It is stable under neutral to weakly acidic (pH 4.0–7.0) conditions and at room temperature away from light but is prone to sugar chain hydrolysis to generate MAA or intramolecular isomerization under strongly acidic or strongly alkaline conditions or at high temperatures (>80 °C). In oil-in-water creams formulated with Centella asiatica extract and stored at 25 °C under sealed, light-protected conditions, MA retains over 90% of its initial content for at least 6 months; its degradation follows first-order kinetics, with sugar chain hydrolysis to MAA verified as the main degradation pathway [37]. For processed pennywort (*C. asiatica*) juice stored under refrigeration at 4 °C, MA content exhibits no statistically significant reduction over a 4-month observation period [38]. In both studies, MA was quantified using validated reversed-phase High-performance liquid chromatography (HPLC) methods with UV detection at 220 nm, whereas comprehensive structural characterization of all trace degradation products was not conducted.

The maximum ultraviolet absorption wavelength of MA is approximately 205 nm. It can be quantitatively detected using HPLC–UV, high-performance liquid chromatography coupled with evaporative light scattering detection (HPLC-ELSD), or liquid chromatography–tandem mass spectrometry (LC–MS/MS), with a limit of detection as low as 0.005 μg/mL [39,40]. It can form crystals in a methanol–water mixed solvent system, and its crystallization induction period is significantly longer than that of AS. Using this difference, monomers with a purity of more than 95% can be obtained through fractional crystallization, with a recovery rate of approximately 80% [36,41].

3.2. Structural Analogs and Isomers of MA in Centella asiatica

3.2.1. Structural Analogs

AS, MA, MAA, and AA all belong to ursane-type pentacyclic triterpenoids. The core structural differences lie in the hydroxylation status of the C-6 position on the parent nucleus and the degree of glycosylation at the C-28 position [22,42]. The specific structural differences are compared in Table 1. On the basis of structural differences, the pharmacological activity intensities of the four core triterpenoid components also show obvious differentiation (Table 2). It should be noted that all cross-compound activity comparisons in Table 2 are qualitatively summarized from independent studies with divergent experimental systems and are not intended to represent a standardized quantitative potency ranking. The grading is provided only as a quick reference for general activity trends. Readers should interpret the results in conjunction with the original experimental conditions and refer to the cited literature for detailed study designs and specific quantitative data.

Table 1. Structural differences among the four core triterpenoid constituents of *Centella asiatica* (L.) Urb.

Constituent	CAS Registry Number	C-6 Hydroxylation Status on Parent Nucleus	C-28 Glycosylation Modification	Reference
MA	34540-22-2	Hydroxyl present (C6-hydroxylated)	Linked to a linear trisaccharide chain of glucose-glucose-rhamnose	[9,27,29,30,42-45]
AS	16830-15-2	No hydroxyl group	Linked to a linear trisaccharide chain of glucose-glucose-rhamnose	[9,27,42-45]
MAA	18449-41-7	Hydroxyl present (C6-hydroxylated)	Free carboxyl group, no sugar chain	[42,43]
AA	464-92-6	No hydroxyl group	Free carboxyl group, no sugar chain	[42,43]

Table 2. Comparison of pharmacological activity intensities among the four core triterpenoid constituents of *Centella asiatica* (L.) Urb.

Constituent	Collagen Synthesis Promotion	Anti-Inflammatory Activity	Neuroprotection	Cardiovascular Protection	Pharmacokinetics (PK)/Blood–Brain Barrier (BBB) Profile	Reference
MA	+++ (type I collagen +25~30%; the only compound with significant type III collagen promotion)	++ (regulates NF-κB/NLRP3 pathways)	+++ (AChE binding energy −197.06 kJ/mol, superior to donepezil in molecular docking simulations)	+++ (alleviates myocardial is chemia–reperfusion injury; no cardiotoxicity at conventional doses)	Rat oral bioavailability <1%; In vitro BBB Papp = 53.31×10^{-6} cm/s; mainly metabolized to MAA after oral administration	[8,16,25,26,46-54]
AS	++ (type I collagen +25~30%; no effect on type III collagen)	++ (inhibits IL-6, TNF-α and other inflammatory cytokines)	+++ (highest BBB permeability among the four, Papp = 70.61×10^{-6} cm/s)	++ (no cardiotoxicity at conventional doses; limited research data)	Rat oral bioavailability <1%; BBB Papp = 70.61×10^{-6} cm/s; bidirectional interconversion with MA in vivo	[8,26,49,50,55-58]
MAA	− (no significant collagen synthesis promotion effect)	+++ (stronger anti-inflammatory activity in LPS-induced inflammation than glycosides)	++ (stronger in vitro AChE inhibition than glycosides; low BBB permeability)	− (cardiotoxic at high concentrations)	Mainly an intestinal microbiota metabolite of MA; lower BBB permeability than glycoside forms	[10,25,49,50,57,59,60]
AA	− (no significant collagen synthesis promotion effect)	+++ (anti-inflammatory activity comparable to MAA)	+++ (strongest in vitro AChE inhibitory activity)	− (cardiotoxic at high concentrations)	Mainly an intestinal microbiota metabolite of AS; BBB Papp = 50.94×10^{-6} cm/s	[25,49,50,57,59,60]

Note: Activity scores are qualitative assessments based on published peer-reviewed literature, not derived from head-to-head parallel comparisons under a unified experimental platform. Grading criteria: +++ (Strong activity): Consistently significant bioactivity across multiple independent studies, with well-documented dose–effect relationships; or significantly superior activity compared with other analogs in direct comparative studies. ++ (Moderate activity): Definite bioactivity reported in most studies, with partially verified dose dependency; overall intensity is generally lower than the +++ tier. + (Weak/limited activity): Bioactivity detected only in a subset of studies, or with weak intensity, or with a relatively limited evidence base. − (No significant activity/overt toxicity): No consistent significant bioactivity or verified cytotoxicity/adverse effect. Due to substantial heterogeneity in cell models, treatment concentrations, exposure durations, and outcome measures across original studies, this grading reflects only general activity trends and shall not be interpreted as a strict quantitative potency ranking.

3.2.2. Double-Bond Position Isomers

Isomadecassoside is a novel ursane-type triterpenoid glycoside double-bond isomer isolated and identified from the industrially purified MA-enriched fraction of *C. asiatica* leaves [28]. Researchers completed its full structural elucidation via high-resolution electrospray ionization mass spectrometry (HR-ESIMS) and two-dimensional nuclear magnetic resonance (NMR) techniques, including Proton nuclear magnetic resonance (^{1}H NMR), Carbon-13 nuclear magnetic resonance (^{13}C NMR), correlation spectroscopy (COSY), heteronuclear single quantum coherence (HSQC), and heteronuclear multiple bond correlation (HMBC). The compound has the exact same molecular formula as MA ($C_{48}H_{78}O_{20}$). The core structural difference is that the double bond on the E ring of its ursane parent nucleus migrates from the conventional $\Delta^{12(13)}$ to $\Delta^{20(21)}$. The corresponding aglycone is the novel 2*α*,3*β*,6*β*,23-tetrahydroxyurs-20-en-28-oic acid (isomadecassic acid). The sugar chain moiety still retains the same *α*-L-rhamnose-(1→4)-O-*β*-D-glucose-(1→6)-O-*β*-D-glucose trisaccharide structure as MA, linked to the C-28 carboxyl group via an ester bond [28].

In vitro anti-inflammatory activity evaluation showed that isomadecassoside, at non-cytotoxic concentrations of 2–50 μM, can dose-dependently inhibit the production of nitrite (a stable metabolite of nitric oxide) in J774A1 macrophages stimulated by lipopolysaccharide (LPS). At 50 μM, the inhibition rate reaches 19%, slightly better than MA and asiaticoside B (terminoloside) at the same concentration, with anti-inflammatory activity comparable to MA [28].

3.2.3. Skeletal Isomers

There are two types of triterpenoid saponins in *C. asiatica* with ursane and oleanane as the parent nuclei. Among them, asiaticoside B is a typical skeletal isomer of MA. The chemical structures of the two were first systematically elucidated in 1978: MA is the trisaccharide ester of 2*α*,3*β*,6*β*,23*α*-tetrahydroxyurs-12-en-28-oic acid, while asiaticoside B is the trisaccharide ester of the corresponding oleanane-type parent nucleus. The core difference lies in the substitution position of the methyl group on the E ring [61].

Separation and purification of asiaticoside B usually adopt preparative high-performance liquid chromatography (prep-HPLC) or the method of adding *β*-cyclodextrin as a mobile phase additive [29,30,45,62-67]. Researchers have successfully isolated this component from total AS and established a quantitative analysis method using the quantitative analysis of multi-components by single marker (QAMS) approach [68,69]. To date, approximately 40 such triterpenoid saponins (collectively called centelloids) with ursane and oleanane as parent nuclei have been identified from *C. asiatica*, most of which are trace secondary metabolites [70]. In addition, there are other oleanane-type triterpenoid oligosides such as asiaticosides B, C, and D [28,71,72].

3.2.4. Other Structurally Modified Derivatives

In addition to the above glycosylation and skeletal isomerization, there are various other types of structurally modified triterpenoid saponins in *C. asiatica*, covering acetylation, oxidation, methoxylation, and glycosylation variation.

Acetylated derivatives are the main modification type reported so far. 23-O-acetyl MA and 23-O-acetyl asiaticoside B have been reported [73]. Oxidized and methoxylated derivatives include 11-oxo-asiaticoside B, 11-oxo-MA, 11(*β*)-methoxy-asiaticoside B, and 11(*β*)-methoxy-MA [71], with carbonyl or methoxy groups introduced on the parent nucleus. Other novel triterpenoid glycosides include asiaticosides C, D, E, F, and G [71,72], as well as new polyacetylene glucosides such as centellosides A and B [74].

The structures of these novel triterpenoid glycosides are mostly determined usingy nuclear magnetic resonance, high-resolution mass spectrometry, and chemical methods.

Some compounds show neuroprotective, anti-inflammatory, and other biological activities, providing a new basis for the pharmacodynamic material foundation and quality control of *C. asiatica* [28,70,71,73,75].

3.3. Structure–Activity Relationship Studies of MA and Its Derivatives

Current understanding of MA's structure–activity relationships is predominantly derived from comparative studies of naturally occurring structural analogs (asiaticoside, madecassic acid, and asiatic acid) rather than site-directed chemically modified derivatives. Accordingly, the associations between structural motifs and bioactivity described in this section represent structural correlations based on existing literature, not definitively proven causal relationships. All conclusions should be interpreted as working hypotheses pending verification via controlled structural modification experiments. Structure–activity relationship research of MA covers three core dimensions: structural differentiation from analogs, activity modulation by sugar chain length, and functional switch between glycoside and aglycone forms. The core structural determinants and activity differentiation rules are schematically summarized in Figure 3. No systematic site-directed chemical modification study has been reported to date. Confounding factors such as differences in tissue distribution, metabolic stability, and physicochemical properties between analogs make it impossible to uniquely attribute activity differences to single functional groups. Therefore, all structure–activity rules summarized in this section should be regarded as working hypotheses (Level C evidence) rather than definitive conclusions.

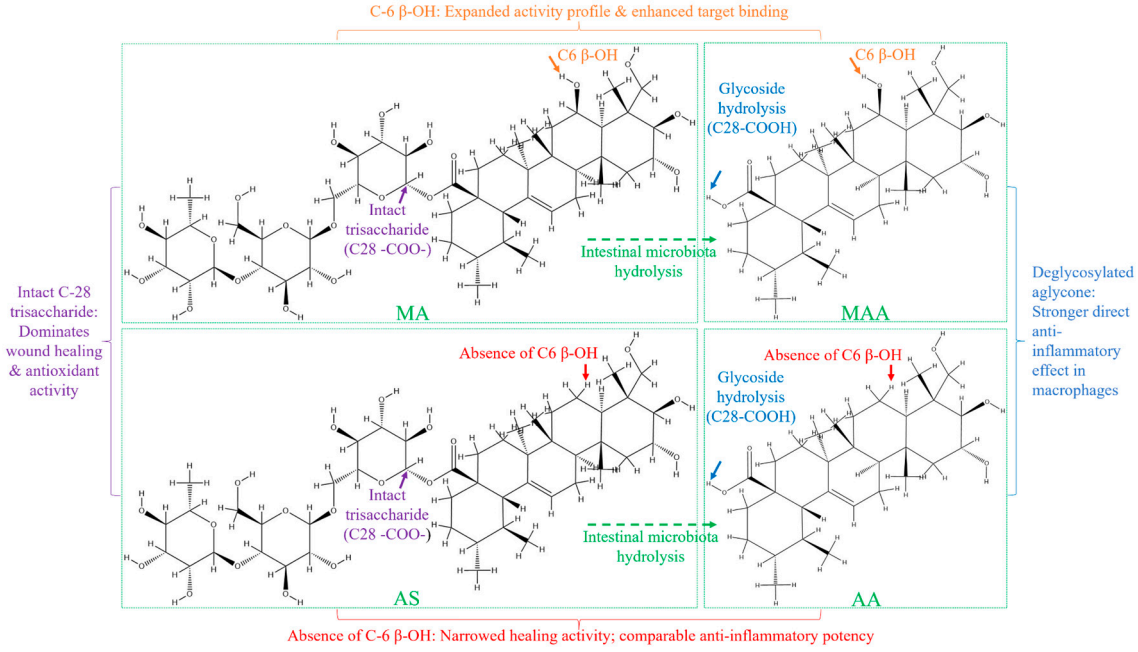


Figure 3. Schematic diagram of the structure–activity relationships of MA and its structural analogs. Arrows indicate the distinct structural motifs associated with corresponding bioactivity characteristics. The C-6 β-hydroxyl group on the ursane aglycone backbone and the intact linear trisaccharide chain at the C-28 carboxyl position are the two core structural determinants of the biological activity of these triterpenoids. The integrity of the C-28 trisaccharide chain defines the functional mode: intact glycoside forms [madecassoside (MA) and asiaticoside (AS)] dominate wound healing and antioxidant activities, and mediate anti-arthritis and anti-pulmonary fibrosis effects via intestinal-dependent mechanisms after oral administration. Aglycone metabolites [madecassic acid (MAA) and asiatic acid (AA)] produced by glycoside hydrolysis exert stronger direct anti-inflammatory effects in macrophages and function as the direct effector molecules in ulcerative colitis. The C-6 β-hydroxyl moiety broadens the activity profile and enhances target binding capacity, which

underlies the activity differentiation between MA and AS. Intestinal microbiota-mediated deglycosylation acts as the key metabolic switch between these two functional modes. All structure–activity inferences are working hypotheses derived from comparisons of naturally occurring analogs and remain to be verified using site-specific chemical modification studies.

3.3.1. Effects of Sugar Chain Length and Linkage Mode on Activity

The structure of the sugar chain has an important influence on the activity of asiatic triterpenoids. The degree of glycosylation and sugar chain composition can significantly change the physicochemical properties and biological effects of the compounds. For example, in promoting fibroblast proliferation and collagen synthesis, both AS and MA (both trisaccharides) show stronger biological activity than their corresponding aglycones, and this difference is only for type I collagen. MA has a higher comprehensive wound-healing activity score due to the additional type III collagen-promoting effect, suggesting that differences in sugar chain structure (MA has one more hydroxyl group at the C-6 position) affect its interaction with targets and activity intensity [7,76].

In studies on neurite outgrowth activity, parallel testing in the same Neuro-2a cell system revealed that AS and MA induce sustained Extracellular signal-regulated kinase (ERK) 1/2 phosphorylation and downstream cAMP response element-binding protein (CREB) activation, whereas their respective aglycones MAA and AA only elicit transient ERK1/2 activation, with corresponding differences in downstream biological effects [77]. This divergence in signaling kinetics is closely associated with the presence of the sugar chain but may also be jointly mediated by differences in physicochemical properties, cellular uptake rates, and intracellular metabolic kinetics between the two classes of compounds, suggesting that the intact sugar chain contributes to maintaining the sustained activation pattern of this signaling pathway.

In terms of anti-inflammatory activity, glycosides (AS and MA) directly extracted from *C. asiatica* are considered the main active ingredients for burn healing, rather than their aglycone metabolites [17].

In synthetic biology research, it has been found that the rhamnose at the end of the sugar chain and the middle glucose are sequentially added by two specific glycosyltransferases (UGT94M2 and UGT94BE1). UGT94M2 catalyzes the linkage of the second 1,6-linked glucose, and UGT94BE1 is responsible for the transfer of the terminal 1,4-linked rhamnose. The substrate specificity of the two determines the unique structure of trisaccharide saponins in *C. asiatica* [33,78].

Meanwhile, using molecularly imprinted polymer (MIP) technology, it was found that when enriching AS, the purity of AS increases by 3.01 times, while the purity of its homolog MA can increase by 6.51 times. This indirectly reflects the significant difference in their interaction with materials due to sugar chain differences [79].

3.3.2. Regulation of Pharmacological Activity by the Position and Number of Hydroxyl Substitutions on the Parent Nucleus

Structurally, the defining difference between the MA and AS aglycone backbones is the additional β-hydroxyl group at the C-6 position [27,41]. However, this single structural variation is accompanied by parallel differences in physicochemical properties, cellular exposure, and in vivo disposition, all of which may contribute to the observed activity gaps and confound causal attribution to the C-6 hydroxyl motif alone. Specifically, three categories of confounding factors should be acknowledged: Physicochemical properties: The extra C-6 β-hydroxyl group increases overall molecular polarity and aqueous solubility of MA, which may alter its dissolution behavior and passive transmembrane efficiency, leading to different intracellular exposure levels even at the same administered concentration [41,57]. Cellular biotransformation: MA and AS can undergo bidirectional

interconversion via C-6 hydroxylation/dehydroxylation in biological systems, resulting in divergent intracellular profiles of active forms (glycosides + aglycones) and further confounding direct comparison of intrinsic target potency [57]. In vivo pharmacokinetic behavior: The two compounds differ in tissue distribution, metabolic clearance, and enterohepatic circulation patterns. These disposition differences can widen or narrow the gap in in vivo efficacy independently of target-binding affinity [25,57]. That said, one lines of evidence provide relatively direct support for the structural contribution of the C-6 β-hydroxyl group, largely independent of solubility and metabolic confounding: Computational chemistry evidence (Level D): Molecular docking and quantum chemical calculations show that the C-6 β-hydroxyl group can directly form hydrogen bonds with key amino acid residues (e.g., Tyr124 and Arg296) in the acetylcholinesterase binding pocket, making a direct energetic contribution to binding affinity [80]. This reflects the intrinsic molecular interaction between the structural motif and the target, independent of solubility, absorption, or metabolism.

The activity performance of MA differs from that of AS in various models. In terms of antipyretic effect, both have cooling effects, but at specific time points (e.g., 5 h after LPS injection), the cooling effect of AS is better than that of MA [8]. In terms of stimulating collagen synthesis in fibroblasts, AS shows stronger biological activity than MA in certain dose ranges [7,81].

At the cellular level, the in vivo ratio of C6-hydroxylated products (such as MAA and MA) to non-hydroxylated products (AA and AS) is significantly higher (4.00 and 3.61 times, respectively), indicating that C6-hydroxylation is a major biotransformation step in vivo, but how this modification specifically regulates activity remains to be further studied [42].

Studies on other novel triterpenoid saponins in *C. asiatica* also reveal the importance of hydroxyl substitution. For example, 11-oxo-asiaticoside B (with a carbonyl group at the C-11 position) isolated from *C. asiatica* shows stronger neuroprotective effects than MA, with a cell survival rate as high as 91.75% at a concentration of 100 μM [72]. Similarly, isomadecassoside with $\Delta^{(20(21))}$ double bond migration also shows anti-inflammatory activity similar to MA [28].

However, the introduction of hydroxyl groups (such as MAA) shows a different trend in antimalarial activity: its activity is higher than the corresponding glycoside (MA) but lower than its non-hydroxylated aglycone (AA) [82].

3.3.3. Activity Differences and in Vivo Transformation Rules of Aglycone and Glycoside Forms

The activity differences and in vivo transformation rules between MA and its aglycone MAA are the key to structure–activity relationship research. After oral administration, MA is partially metabolized to MAA in vivo, but the biological activities of the parent drug and its metabolites differ.

Multiple studies have confirmed that MA exhibits stronger or more direct pharmacological effects than its aglycone MAA in anti-rheumatoid arthritis [83,84], anti-pulmonary fibrosis [85], and burn healing promotion [17], suggesting that in these models, the parent glycoside is the main active form.

For example, in the anti-rheumatoid arthritis effect, oral MA is effective, while its main metabolite MAA is ineffective. MA exerts its effect by regulating intestinal flora and inducing regulatory T cells (Treg), rather than through direct action after absorption into the blood [83,84]. In anti-colitis research, MA needs to be converted into its aglycone MAA by intestinal flora before it exerts a therapeutic effect of restoring Th17/Treg balance; that is, MAA is the true active form in vivo [86].

In vitro, it has also been found that MAA is more effective than MA in inhibiting the production of inflammatory factors in macrophages [10]. In contrast, intact glycosides exhibit superior wound-healing and collagen synthesis-promoting activity both in vitro and in vivo, as confirmed using head-to-head comparative studies of the four major triterpenoids [17]. Clinical evidence further verifies that *Centella asiatica* preparations rich in triterpenoid glycosides can accelerate acute wound healing in humans [87]. This indicates that the presence of glycosidic bonds can significantly change the pharmacokinetic properties of drugs (such as low oral bioavailability) and targeting (such as acting on the intestine), while aglycones may be more easily absorbed into the blood and exert direct systemic effects, but the specific strength of this effect depends on different pharmacological models and evaluation indicators [83-85]. In terms of chemical composition, free aglycones (AA and MAA) are present at very low levels in conventional n-butanol-enriched total triterpenoid saponin fractions [88]. Regarding antioxidant activity, consistent with their dominant content proportion, glycoside forms (MA and AS) are considered the main contributors to the total antioxidant capacity of the total saponin extract, with both compounds verified to exert direct antioxidant and cytoprotective effects via the Nrf2/HO-1 pathway [11,12]. Hydroxyl substitution on the parent nucleus and sugar chain structure are the key factors determining its pharmacological activity.

It should be emphasized that the above structure–activity rules are highly indication-dependent. The dominant active form (parent glycoside vs. aglycone metabolite) varies across different disease models and administration routes. For oral administration, Intact MA is regarded as the dominant functional form. Its anti-arthritis effect depends on intact gut microbiota, while the anti-pulmonary fibrosis effect is mediated via the intestinal tract [83-85]. This is directly supported by head-to-head comparison showing that oral administration of pure MAA alone fails to produce significant therapeutic efficacy in the arthritis model [84]. Ulcerative colitis: MAA is verified as the direct effector molecule that restores the Th17/Treg balance, whereas MA requires microbiota-mediated deglycosylation to exert efficacy [86]. Wound healing and skin repair: Intact glycoside forms (MA and AS) exhibit stronger collagen synthesis-promoting and wound-healing activity than their corresponding aglycones, as confirmed by parallel separate administration tests both in vitro and in vivo [17]. In vitro macrophage anti-inflammatory assay: At equal concentrations, MAA exerts significantly stronger direct inhibitory effects on NF-κB pathway activation and pro-inflammatory cytokine production than MA, based on direct cell-level comparative experiments [10].

Notably, the supporting evidence for mechanism attribution differs in strength. Directly verified findings: Activity differences between MA and MAA confirmed by separate administration [10,17,86]. After oral administration, prototype MA exhibits extremely low plasma exposure [25,26,89], and MAA accumulates as a major circulating metabolite upon repeated dosing, especially under inflammatory conditions [89]. Oral MA exerts therapeutic effects in an intestine-dependent manner in arthritis and colitis models; its anti-arthritis efficacy has been verified to depend on intact gut microbiota [84], while its anti-colitis effect requires intestinal deglycosylation to generate the active metabolite MAA [86]. In addition, measurable levels of MA prototype have been detected in target tissues including skin and brain after oral administration of standardized *C. asiatica* extract [26]. Evidence-based interpretations (working hypotheses): The generalized distinction that "MA acts mainly through local intestinal regulation rather than systemic exposure in oral arthritis and pulmonary fibrosis models". This inference is drawn from combined evidence of extremely low oral bioavailability, microbiota-dependent efficacy, and peripheral biomarker changes, but direct quantitative comparison of MA versus MAA concentrations at the target organ parenchyma level is still lacking across all disease models. Accordingly, the division of active forms and action modes across indications should be

interpreted as an evidence-based working model rather than an absolutely definitive conclusion. No single universal hierarchy of activity can be generalized across all indications.

3.3.4. Synergistic Effects of MA and AS

As the main active components in *C. asiatica*, MA and AS can produce pharmacological synergistic effects at specific ratios. In a model promoting HaCaT cell migration and wound healing, ECa 233 (a standardized *C. asiatica* extract with total triterpenes ≥ 85% and MA:AS ≈ 1.5:1) was confirmed to activate multiple signaling pathways such as focal adhesion kinase (FAK), Akt, and MAPK, and its comprehensive effect may stem from the synergistic action of various active components contained in it [90]. Clinically, compound preparations or skin care products containing MA and AS have been used to promote wound healing after laser surgery, improve skin wrinkles, and enhance the skin barrier. The realization of these composite effects also implies the synergistic potential among various active components [91-95].

To intuitively present the regulatory rules of different structural modifications on the pharmacological activity and druggability of MA, the effects of four types of modifications—sugar chain length, number of hydroxyl groups on the parent nucleus, double bond position, and acetylation—on wound healing promotion, anti-inflammation, transdermal penetration, and oral absorption are summarized in Table 3. Overall, sugar chain length is the core factor determining the mode of action (intestinal targeting vs. direct blood entry), the C6 hydroxyl group on the parent nucleus is the key site distinguishing its activity differentiation from AS, and modifications such as double bond migration and acetylation provide structural modification directions for targeted optimization of druggability.

Table 3. Structure–activity and druggability profiles corresponding to different structural modifications of MA.

Type of Structural Modification	Specific Modification Method	Wound Healing Activity	Anti-Inflammatory Activity	Transdermal Penetration Performance	Oral Absorption Characteristics	Reference
Sugar chain length	Intact trisaccharide chain (prototype: linear trisaccharide of glucose-glucose-rhamnose)	Strongest: can simultaneously promote type I and type III collagen synthesis, induce sustained ERK1/2 signal activation; main active form for burn wound healing	Moderate: exerts anti-inflammatory effects by inhibiting NF-κB, NLRP3 and other pathways	Weak: strong molecular polarity, low passive transdermal efficiency	Extremely low: absolute oral bioavailability of prototype <1% in rats; most are hydrolyzed to aglycone by intestinal flora in the intestine	[7,9,10,17,23,25,26,47,57,76,96,97]
	Sugar chain truncated to monosaccharide (MA2G, removal of 2 sugar groups)	Enhanced cell migration promotion effect, weaker collagen synthesis ability than trisaccharide prototype	Weaker than aglycone, stronger than trisaccharide prototype	Significantly improved: reduced polarity, better transdermal efficiency than parent MA	Theoretically improved intestinal passive permeability, but still easily metabolized and hydrolyzed by intestinal flora	[10,23,25]
	Complete deglycosylation (aglycone form: MAA)	Weakest: no significant collagen synthesis and wound healing effects	Strongest: significantly better inhibitory activity on macrophage inflammatory factors than glycoside forms	Optimal: high fat solubility, strong transmembrane penetration ability	Intestinal absorption is better than glycosides, but systemic exposure is still limited; there is a risk of cardiotoxicity at high concentrations	[7,10,17,23,25,60,86]

Parent nucleus hydroxyl groups	3 hydroxyl groups (control: AS, no C6 hydroxyl group)	Moderately strong: only promotes type I collagen synthesis, no significant effect on type III collagen	Moderate: inhibits the release of inflammatory factors such as IL-6 and TNF-α	Slightly better: slightly lower polarity, slightly stronger passive penetration ability than MA	Extremely low prototype bioavailability; can be converted to MA by C6 hydroxylation in vivo	[7-9,26,35,36,57,96]
	4 hydroxyl groups (prototype: new β-hydroxyl at C6 position)	Stronger: the only component in C. asiatica that can significantly promote type III collagen synthesis, with faster burn healing	Stronger: the strongest anti-acne-induced skin inflammation activity among the four core triterpenes	Slightly weaker: slightly higher polarity, slightly lower transdermal efficiency than AS	Pure product oral bioavailability is about 0.67%; when coexisting with AS, the in vivo residence time can be prolonged through bidirectional transformation	[7-9,17,35,36,57]
Double bond position	Double bond at $\Delta^{12(13)}$ position (prototype)	Baseline activity level	Baseline activity level	Baseline level	Baseline level	[2,27]
	Double bond at $\Delta^{20(21)}$ position (isomadecassoside)	No systematic comparative study, presumed to be equivalent to prototype	Equivalent to prototype: NO inhibition rate at 50 μM is slightly better than prototype	No significant difference in molecular polarity, presumed to be similar to prototype	Similar physicochemical properties, presumed in vivo disposition process is consistent with prototype	[28]
Acetylation	No acetylation (prototype)	Baseline activity level	Baseline activity level	Baseline level	Baseline level	[34,35]
	23-O-acetyl modification	Systematic activity evaluation has not been carried out	Activity has not been clearly verified	Theoretical improvement: enhanced fat solubility, expected to improve transdermal efficiency, no direct experimental data	Theoretical improvement: improved fat solubility can enhance intestinal passive permeability, no in vivo pharmacokinetic evidence	[71]

Note: All profiles are derived from comparative studies of natural analogs and enzymatic hydrolysis products. No systematic site-directed modification study has validated these structure–activity rules. Data should be interpreted as directional trends (working hypotheses), not definitive quantitative relationships.

3.3.5. Limitations of Structure–Activity Relationship Research

Current understanding of MA's structure–activity relationships is predominantly derived from comparative studies of naturally occurring analogs [7,10,17,28,76], with three key methodological limitations: ① A critical limitation is the complete lack of evidence from site-directed structural modification. All current Structure–activity relationship (SAR) inferences rely on comparisons between naturally occurring analogs with multiple concurrent differences in physicochemical and pharmacokinetic properties. No study has yet verified the causal role of the C-6 β-hydroxyl group via selective hydroxylation or dehydroxylation at this site under otherwise identical molecular backbones. Until such controlled modification evidence is available, all structure–activity rules regarding the C-6 hydroxyl group should be interpreted as working hypotheses rather than definitive causal conclusions. ② Confounding factors such as tissue distribution, metabolic stability, and physicochemical properties differ between analogs, which may contribute to observed activity differences independently of the target structural motif [17,41,57]. ③ Most inferences are assembled from data generated in different laboratories with divergent experimental systems, lacking standardized head-to-head parallel comparisons under a unified platform [7,77]. ④ A further limitation pertains to in vivo active form attribution. Although separate administration studies have verified distinct activity profiles of MA and its aglycone MAA across multiple disease models [10,17,83,86], direct quantitative

comparison of prototype versus metabolite concentrations at target organ parenchyma sites remains incomplete for most in vivo models [25,26]. The mechanistic division between local intestinal action and systemic effector function is largely inferred from combined pharmacokinetic and efficacy evidence, rather than from direct tissue-level concentration–effect correlation verification [83,86]. Accordingly, all structure–activity rules summarized in this section should be regarded as working hypotheses (Level C evidence) rather than definitive conclusions.

3.4. Structural Modification and Derivative Research of MA

The extremely low oral bioavailability of MA (<1% in rats) [26] and poor intestinal permeability [98] severely restrict its clinical translation. Covalent structural modification is one of the core strategies to break through this bottleneck. However, current research in this field is still in its infancy. Existing work mainly focuses on the isolation and identification of a few enzymatic conversion products and naturally derived derivatives, and there is a lack of systematic prodrug design, site-selective chemical modification, and quantitative structure–activity relationship research.

3.4.1. Core Modification Sites and General Synthetic Routes

MA belongs to ursane-type pentacyclic triterpenoid saponins, and its structural basis is the pentacyclic triterpene skeleton derived from α-amyrin [27,43]. From the perspective of structural modification, there are three types of potential modification sites in the MA molecule: (1) hydroxyl groups (C-2 α, C-3 β, C-6 β, and C-23 positions) and carboxyl groups (C-28 position) on the aglycone parent nucleus; (2) the linear trisaccharide chain of glucose–glucose–rhamnose linked at the C-28 position; (3) the Δ^{12} double bond in the ursane-type skeleton.

Among these three types of sites, the sugar chain moiety is the most concentrated area of current artificial modification research because it is exposed on the molecular surface and can be selectively hydrolyzed by glycosidases.

At the biosynthetic level, the MA aglycone MAA is generated from α-amyrin through three key oxidation reactions: C-28 carboxylation is catalyzed by CYP716A83, C-23 hydroxylation is catalyzed by CYP714E19 [31], and the C-2 α-hydroxylase remains to be identified. Thereafter, UDP-glycosyltransferases UGT73AD1 and UGT73AH1 catalyze the glucosylation of the C-28 carboxyl group to form monoglucoside [99,100]. UGT94M2 and UGT94BE1 sequentially add the second glucose molecule and the terminal rhamnose group to complete the trisaccharide chain assembly [33,78]. The substrate specificity of these glycosyltransferases provides molecular tools for engineering the sugar chain structure.

From the perspective of organic synthesis, the total chemical synthesis of MA is extremely challenging due to its complex structure, and there is currently no economically feasible total synthesis route reported. Existing structural modifications mainly focus on (1) directional hydrolysis modification of the sugar chain part of MA by enzymatic methods [23]; (2) structural identification of trace derivatives isolated from natural products [28,71,72]. This situation indicates that the research on MA derivatives is still dominated by biocatalysis and natural product chemistry, and there is a lack of systematic exploration of chemical synthesis methodology.

3.4.2. Reported Derivative Types and Modification Effects

Sugar Chain Enzymatic Hydrolysis Modified Derivatives

The only MA derivative prepared through artificial modification and with systematically reported biological activity is the sugar-chain-truncated product produced via enzymatic hydrolysis. Researchers used glycoside hydrolase to perform directed

deglycosylation of MA and prepared madecassoside monoglucoside (removing one glucose group) and madecassoside diglucoside (further removing the rhamnose group, i.e., monoglucoside) [23].

Enzymatic hydrolysis modification produces significant changes in activity and properties. In terms of transdermal performance, the transdermal permeability of MA2G is better than that of parent MA, suggesting that moderately reducing sugar chain polarity is an effective strategy to improve transdermal delivery efficiency [23]. In terms of biological activity, MA2G shows stronger reactive oxygen species (ROS)-scavenging activity (43.05~147.50% lower than MA) and cell migration-promoting effect (36.76~77.28% stronger than MA) [23].

These results indicate that sugar chain truncation modification—rather than the intact trisaccharide chain—may be a better direction for optimizing the transdermal administration performance of MA. However, the current modification strategy is still limited to the preparation and preliminary activity evaluation of enzymatic hydrolysis products and has not involved in vivo pharmacokinetic research or formulation development.

Parent Nucleus Derivatization and Complex Formation

Research on covalent chemical modification of the MA parent nucleus is extremely limited. Almost all reported derivatives come from isolation and identification of natural sources, rather than rational design and synthesis. 23-O-acetyl MA is a natural acetylated derivative isolated from *C. asiatica* [71]. Its structural identification proves that acetylation of hydroxyl groups on the parent nucleus can occur in nature, but systematic pharmacological activity evaluation of this compound has not been carried out. MA derivatives substituted with 11-oxo and 11β-methoxy groups have also been reported [72], all from plant natural extracts. There are currently no research reports on the selective introduction of acetyl, methyl, or other functional groups on the parent nucleus using chemical methods to systematically optimize the druggability of MA.

Esterification and Prodrug Derivatives: A Key Blank Area in Current Research

At present, to our knowledge, no peer-reviewed study has reported systematic covalent prodrug design and synthesis of MA. The C-28 carboxyl group of MA provides classic ester prodrug design sites (such as pivaloyloxymethyl ester, amino acid ester, and other strategies), and multiple hydroxyl groups on the parent nucleus also have the potential for phosphate ester prodrug modification, but no systematic prodrug design research has been reported so far. Amide derivatives of MA have also not been documented in the literature.

This gap is one of the fundamental bottlenecks restricting the development of MA oral preparations. Against the background of the extremely low oral bioavailability of MA (<1% in rats) [26,57], temporarily blocking polar groups through prodrug design to improve intestinal permeability, and then restoring activity through in vivo enzymatic hydrolysis is one of the most mature optimization strategies in the field of medicinal chemistry. This strategy has successful precedents in the derivatization research of similar triterpenoid saponins (such as glycyrrhizic acid and ginsenosides), but there is no exploration in the field of MA.

3.4.3. Existing Explorations of Druggability Optimization Strategies

Attempts to Improve Oral Bioavailability

There are currently no reports of successfully improving the oral bioavailability of MA through covalent structural modification. The structural root of poor oral absorption of MA lies in its high polarity (multiple hydroxyl groups and sugar groups) and large molecular weight (Mw ≈ 975), resulting in weak transmembrane passive diffusion ability.

The reported improvement strategies are all physical pharmaceutical means (liposomes, phospholipid complexes, nanoparticles, etc.) [101-103] or the use of bioenhancers such as piperine to inhibit efflux transporters and metabolic enzymes [104]. However, these are all non-covalent complexation or drug combination strategies and do not involve covalent bond modification of the MA molecule itself. Solving the problem of oral absorption at the molecular structure level—that is, reducing polarity and blocking hydrogen bond donors through covalent bond modification—is still a direction to be broken through.

Structural Modification Strategies for Optimizing Transdermal Performance

The high hydrophilicity of MA limits its transdermal penetration ability. It is worth noting that MA2G prepared via enzymatic hydrolysis has significantly better transdermal permeability than parent MA [23], which provides proof of concept for optimizing transdermal performance through enzymatic sugar chain truncation. However, the above strategies are all non-covalent physical complexation or enzymatic deglycosylation, and there is no research on systematically optimizing transdermal performance by introducing lipophilic groups at hydroxyl groups such as C-6 or C-23 through chemical modification.

Preliminary Exploration of Quantitative Structure–Activity Relationships and Computational Simulation

Current quantitative structure–activity relationship research on MA is extremely scarce. Existing knowledge mainly comes from activity comparisons of natural analogs (detailed in Section 3.3), and there is a lack of systematically designed artificial derivative structure–activity databases.

Molecular docking and molecular dynamics simulations have been used to study the binding mode of MA to acetylcholinesterase (AChE). Free energy calculations show that the binding affinity of MA (−197.06 kJ/mol) is better than that of the clinical drug donepezil (−133.51 kJ/mol) [80]. Quantum chemical calculations further confirmed that the key interactions between triterpenoids and AChE include hydrogen bonds with Tyr124, Arg296, Tyr337, and Tyr341, as well as H-π and van der Waals interactions, providing a structural basis for the neuroprotective activity of MA [80]. These computational studies provide a preliminary basis for the rational design of derivatives based on target structures but have not yet formed a closed loop with synthetic verification.

3.4.4. Existing Problems and Future Directions in Structural Modification Research

Based on the above analysis, there are four core problems in the field of MA structural modification: ① At present, to our knowledge, no peer-reviewed study has reported systematic covalent prodrug design and synthesis of MA: As of August 2026, no systematic prodrug design and synthesis of MA has been reported in published literature, and the fundamental problem of low oral bioavailability remains unsolved. ② Enzymatic sugar chain modification lacks systematicity: There are only preliminary studies on individual enzymatic deglycosylation products [23], and a systematic structure–activity map of the contribution weights of different sugar chain lengths (monoglycoside, diglycoside, and triglycoside) to transdermal and oral absorption, anti-inflammation, wound healing, and other activities has not been established. ③ Methodology for parent nucleus chemical modification is missing: The complex multi-hydroxyl and polycyclic structure of MA makes selective chemical modification very challenging. Currently, there is no efficient site-selective protection–deprotection strategy for site-directed introduction of functional groups. ④ Disconnection between computationally guided design and experimental verification: Molecular docking studies have identified the key binding mode of MA to targets [80] but have not yet guided the synthesis and evaluation of any new derivatives.

Future research directions should focus on ① developing covalent prodrug strategies: designing ester prodrugs (such as pivaloyloxymethyl ester and amino acid ester) for the C-28 carboxyl group to improve oral absorption or designing phosphate prodrugs for the C-6 hydroxyl group to improve water solubility. This is the highest-priority direction worth exploring to break through the bottleneck of MA oral bioavailability. ② Establishing a systematic sugar chain structure–activity relationship map: preparing a series of sugar chain truncated derivatives (monoglycoside and diglycoside) through systematic enzymatic hydrolysis, combined with multi-model parallel evaluation of transdermal, oral absorption, anti-inflammation, etc., to clarify the independent contribution and synergistic effect of each sugar group on activity [23,77]. ③ Developing green chemical modification methods: using enzymatic catalysis to achieve site-selective glycosylation/acylation [33,78], or exploring mild C-H bond functionalization strategies such as photocatalysis and electrochemistry, to provide methodological support for solving selective modification of the parent nucleus. ④ AI-driven rational design: integrating molecular docking, molecular dynamics simulation, and experimental activity data [80], combined with generative AI to design highly active derivatives and guide synthetic verification [105,106].

4. Biosynthesis and Metabolic Engineering Regulation of MA

4.1. Elucidation of the Biosynthetic Pathway of MA

The biosynthesis of MA is a complex multi-step, multi-enzyme process. Its proposed complete biosynthetic pathway and experimentally validated key enzymes are illustrated in Figure 4. Steps marked with dashed arrows represent proposed reactions for which the responsible enzymes have not been definitively identified.

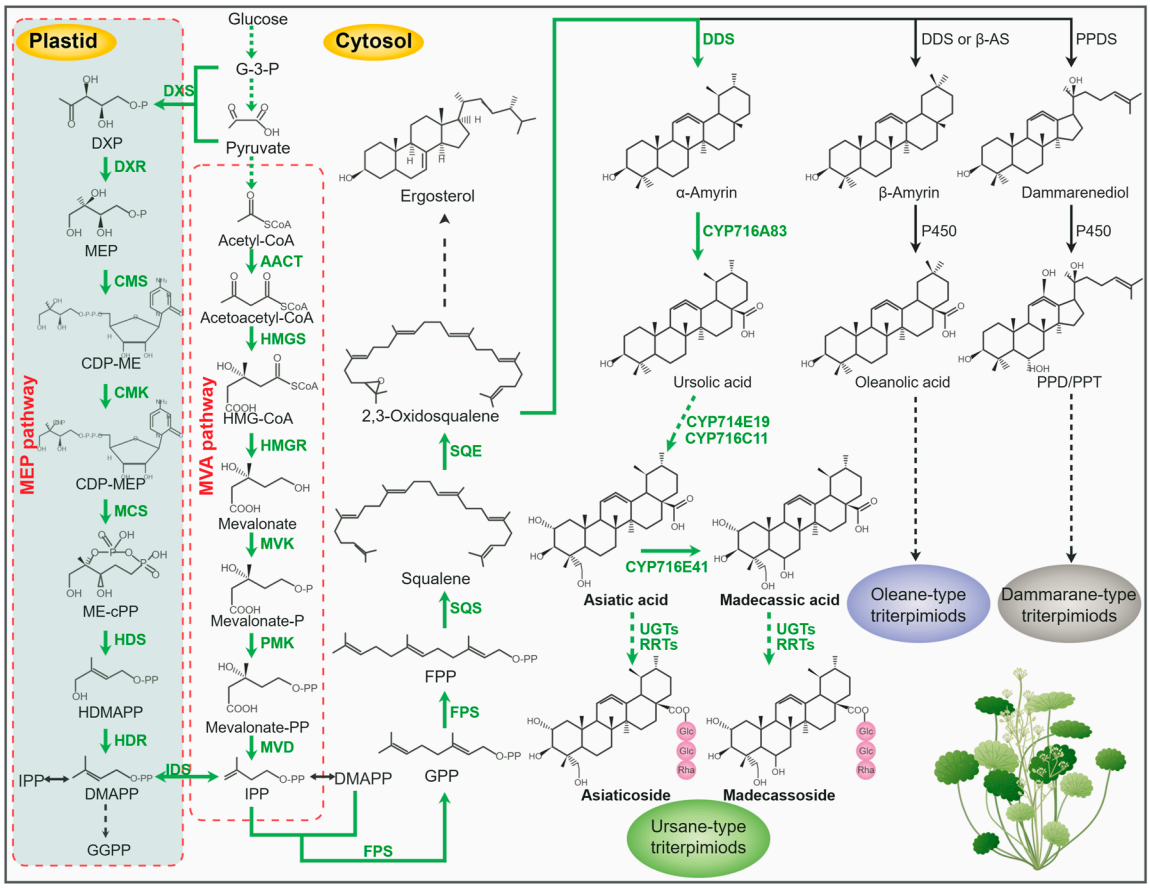


Figure 4. Complete biosynthetic pathway of MA in *Centella asiatica* (L.) Urb. Triterpenoid scaffolds originate from two parallel isoprenoid pathways: the cytosolic mevalonate (MVA) pathway and the

plastid-localized methylerythritol phosphate (MEP) pathway, both supplying the universal precursors isopentenyl diphosphate (IPP) and dimethylallyl diphosphate (DMAPP). Downstream modifications include sequential oxidation by cytochrome P450 monooxygenases (P450) and stepwise glycosylation by UDP-glycosyltransferases. The green line highlights the proposed centelloside-specific biosynthetic route. Reproduced from [24] with permission from Elsevier B.V. (License Number: 6286260156386).

4.1.1. Upstream MVA Pathway and Methylerythritol Phosphate (MEP) Pathway

As a pentacyclic triterpenoid saponin, MA is derived from two classic isoprenoid biosynthetic pathways in plants: the cytosolic MVA pathway and the plastid-localized methylerythritol phosphate (MEP) pathway, both of which generate the precursor isopentenyl diphosphate (IPP) and its isomer dimethylallyl diphosphate (DMAPP) [22,27]. In the MVA pathway, the rate-limiting enzyme 3-hydroxy-3-methylglutaryl coenzyme A reductase (HMGR) catalyzes the formation of MVA, while research on this enzyme in *Centella asiatica* remains limited. In contrast, downstream enzymes have been more extensively characterized. For example, farnesyl diphosphate synthase (FPS) catalyzes the production of farnesyl diphosphate (FPP). Overexpression of the *PgFPS* gene in *C. asiatica* hairy roots upregulates the expression of downstream key enzymes, indicating that FPS plays a regulatory role in triterpenoid biosynthesis [107]. The squalene synthase (SQS) gene *CaSQS* has also been cloned and identified from *C. asiatica*; this enzyme catalyzes the condensation of two FPP molecules to form squalene, representing another critical branch point in the triterpenoid biosynthetic pathway [108]. Research on the MEP pathway is relatively scarce, but it is known to act in concert with the MVA pathway to supply precursors for triterpenoid saponin synthesis [22]. The coordinated regulation of these two pathways lays the foundation for the downstream assembly of complex pentacyclic triterpenoid structures.

4.1.2. Midstream Biosynthesis of the Pentacyclic Triterpenoid Scaffold

After the linear precursor squalene is formed, it is oxidized to 2,3-oxidosqualene, which is then cyclized by oxidosqualene cyclase (OSC) to generate the pentacyclic triterpenoid scaffold. In *C. asiatica*, ursane-type and oleanane-type triterpenoid saponins share the common precursor 2,3-oxidosqualene. α-Amyrin (the direct precursor of the aglycones of MA and AS, ursane-type skeleton) is mainly catalyzed by CasiOSC03, while β-amyrin (oleanane-type skeleton) is generated by multiple distinct oxidosqualene cyclase isoforms including CasiOSC04, CasiOSC07, CasiOSC08 and CasiOSC09, as verified by heterologous expression in yeast [109]. Notably, the previously reported CabAS was initially presumed to be a β-amyrin synthase based on sequence homology, but its catalytic function was not confirmed by heterologous expression validation [110]. Methyl jasmonate (MeJA) treatment significantly upregulates CabAS expression, thereby promoting triterpenoid saponin biosynthesis [110-112]. Bioconversion experiments in cell suspension cultures of *C. asiatica* have demonstrated that exogenously supplied α-amyrin can be efficiently converted into MA and AS, further confirming that α-amyrin is the key direct precursor for the synthesis of these active saponins [113].

4.1.3. Downstream Hydroxylation Modifications

The generated β-amyrin scaffold undergoes multi-step hydroxylation and oxidation reactions catalyzed by P450 to form complex aglycones such as madecassic acid (MAA). Among these modifications, C-28 carboxylation is one of the critical steps for saponin formation. Studies have identified CYP716A83 as a multifunctional triterpenoid C-28 oxidase that can sequentially oxidize α-amyrin and β-amyrin to generate corresponding ursolic acid and oleanolic acid, respectively, by introducing a carboxyl group at the C-28 position

[31]. Specifically, α-amyrin is oxidized by CYP716A83 to ursolic acid, the direct precursor of MAA, while β-amyrin is oxidized to oleanolic acid, the precursor of oleanane-type triterpenoids.

C-23 hydroxylation is an essential modification for MAA biosynthesis, and this reaction is catalyzed by CYP714E19. This enzyme has been characterized as a multifunctional triterpenoid oxidase that catalyzes C-23 hydroxylation of both oleanolic acid and ursolic acid to generate hederagenin and 23-hydroxyursolic acid, respectively [31]. Yeast heterologous co-expression experiments have confirmed that three enzymes—CaDDS (oxidosqualene cyclase), CYP716A83, and CYP714E19—are sufficient to catalyze the consecutive reaction steps from 2,3-oxidosqualene to 23-hydroxyursolic acid [31]. In *C. asiatica*, CaCYP716C11p has been verified to catalyze the conversion of α-amyrin to ursolic acid. Among the above reactions, C-28 carboxylation catalyzed by CYP716A83 and C-23 hydroxylation catalyzed by CYP714E19 have been directly verified via heterologous expression in yeast [31]. CYP716C11, the candidate C-2 α-hydroxylase, has been identified at the genomic scale in *C. asiatica* [109], and its biochemical function has been characterized in previous phylogenetic and functional studies. In contrast, the specific enzyme responsible for C-6 β-hydroxylation remains uncharacterized. Within the full biosynthetic cascade, 23-hydroxyursolic acid represents a validated intermediate located downstream of C-28 carboxylation and C-23 hydroxylation, and upstream of the uncharacterized C-2 α- and C-6 β-hydroxylation steps. Two additional site-specific hydroxylation reactions are required to convert 23-hydroxyursolic acid into the final aglycone, madecassic acid. The precise sequential order of these two hydroxylation steps also remains to be experimentally determined [31]. Subsequent C-2 α- and C-6 β-hydroxylation steps leading to MAA remain putative (working hypothesis, Level D evidence); the specific enzymes responsible have not been definitively identified. The order of these hydroxylation modifications and the precise enzymatic functions require further investigation.

4.1.4. Glycosylation Steps

After the formation of aglycones such as MAA and AA, UDP-glycosyltransferases (UGTs) catalyze the attachment of sugar chains at specific positions to ultimately form trisaccharide saponins including MA and AS. Among these steps, glycosylation at the C-28 carboxyl group is the first and most crucial step. Through an integrated research strategy combining partial enzyme purification, proteomics, and transcriptomics, multiple UGTs involved in this step have been identified from *C. asiatica* [114]. UGT73AD1 (from the UGT73 family) has been confirmed as a triterpenoid carboxylic acid: UDP-glucose 28-O-glucosyltransferase that specifically transfers a glucosyl group from UDP-glucose to the C-28 carboxyl of AA and MAA to form monoglucosides [100]. An independent study identified UGT73AH1, which also catalyzes C-28 glycosylation of AA [99]. These two studies mutually corroborate that C-28 glycosylation is accomplished by the coordinated action of multiple UGTs [32].

After obtaining the C-28 monoglucoside, subsequent sugar chain elongation is catalyzed by additional glycosyltransferases. Studies have found that two glycoside glycosyltransferases, UGT94M2 and UGT94BE1 (from the UGT94 family), sequentially add the second glucose and the terminal rhamnose, ultimately forming the unique glucose–glucose–rhamnose (G–G–R) trisaccharide chain characteristic of AS and MA [33,78]. When the corresponding aglycones (asiatic acid and madecassic acid) are supplied exogenously, co-expression of the three glycosyltransferases (UGT73AD1, UGT94M2, and UGT94BE1) in *Nicotiana benthamiana* produces fully glycosylated asiaticoside and madecassoside, respectively. Both products were positively identified by matching retention times and characteristic MS fragmentation patterns against authentic reference standards [33,78]. Complete de novo synthesis of intact asiaticoside and madecassoside from simple isoprenoid

precursors has not yet been achieved in this plant system, as the specific enzymes responsible for C-2 α- and C-6 β-hydroxylation of the ursane scaffold remain to be definitively identified [24,31]. The three characterized UGTs exhibit high catalytic efficiency and strict regioselectivity, yielding predominantly fully glycosylated trisaccharide end products with minimal accumulation of incompletely glycosylated monoglucoside or diglucoside intermediates [33,78]. The upstream cytochrome P450-mediated hydroxylation steps, rather than glycosylation reactions, represent the main flux-limiting factor for overall triterpenoid saponin yield in the reconstituted pathway [24,31]. Reconstruction of the entire biosynthetic pathway in *Nicotiana benthamiana* has confirmed that these key enzymes (including CaDDS, CYP716A83, CYP714E19, UGT73AD1, UGT94M2, and UGT94BE1) are sufficient to achieve heterologous de novo synthesis of intact triterpenoid saponins from simple precursors [33,78].

4.2. Transcriptional Regulatory Network of MA Biosynthesis

4.2.1. Regulatory Effects of Elicitors Such as MeJA

MeJA is the most commonly used and thoroughly investigated elicitor for regulating the biosynthesis of triterpenoid saponins, including MA, in *C. asiatica*. It significantly promotes the expression of key enzyme genes and the accumulation of active ingredients. MeJA treatment upregulates the transcription levels of key genes such as β-AS and SQS in *C. asiatica* leaves and suspension cells, thereby increasing the contents of MA and AS [110-112]. Targeted metabolomic studies have further confirmed that treatment of cell suspensions with 0.2 mM MeJA for 2–6 days not only significantly increases the biosynthesis of target centelloids (including MA, AS, and their aglycones) but also triggers global metabolic reprogramming in cells. Principal component analysis can clearly distinguish control and treated samples, and the aforementioned triterpenoids have been identified as the most significantly differential biomarkers [115].

In hairy root culture systems, MeJA treatment can induce abundant AS production (7.12 mg/g dry weight) in hairy root lines that previously had undetectable AS levels [111], while appropriate concentrations of MeJA (e.g., 100–200 μM) can significantly increase total saponin yield in cell suspension cultures, with MA as the major product [112]. The synergistic effects of MeJA combined with other regulatory substances have also attracted considerable attention. For example, combined use with thidiazuron increases MA yield by 2.40-fold compared with MeJA alone [116], and co-administration with coronatine exerts a particularly prominent yield-enhancing effect on MA [117]. Silver ion ($AgNO_3$) treatment can also increase AS content by approximately 6-fold and substantially upregulate gene expression, making it an effective metabolic stimulant [118].

In addition to MeJA and silver ions, salicylic acid (SA) is another highly effective chemical elicitor. In *C. asiatica* cell suspension cultures, supplementation with 100 μM SA on day 10 after inoculation increased madecassoside monomer content to 114 ± 3.1 mg per gram of dry cell weight by day 24 of culture, representing an approximately 4-fold increase relative to the untreated control. Quantification was performed via reversed-phase HPLC–UV (254 nm) with at least three independent biological replicates [119]. This elicitation effect is significantly greater when SA is administered at the mid-exponential growth phase rather than during early culture stages [119]. MeJA is also involved in metabolic responses under drought stress; exogenous foliar spraying of MeJA can alleviate the negative impact of water deficit on MA content [120]. Gene expression regulation studies based on MeJA have also aided in the identification of multiple key enzymes involved in hydroxylation (e.g., CYP714E19) and glycosylation (e.g., UGTs) [31,121].

4.2.2. Effects of Environmental Factors Such as Light, Temperature, and Water on Biosynthesis

Environmental factors significantly regulate the accumulation of MA. Light is a key determinant: high light intensity generally promotes the synthesis of MA and AS in *C. asiatica*. Both saponins reach their highest contents under 0% shading (full sunlight), while low light causes a significant decline [122,123]. In controlled vertical farm environments, increasing light intensity from 100 to 300 $\mu mol \cdot m^{-2} \cdot s^{-1}$ elevates beneficial secondary metabolite levels [124]. Further studies have confirmed that an LED light intensity corresponding to photosynthetic photon flux density of 330 $\mu mol/m^2/s$ is optimal, simultaneously achieving the highest biomass, triterpenoid glycoside content, and antioxidant activity. Nutrient solution formulations also exert synergistic effects with light intensity; Resh's Tropical Dry Summer solution more effectively promotes active ingredient accumulation compared with Hoagland's solution [125]. In addition, specific light wavelengths exert effects: ultraviolet C irradiation for 8 h maximizes triterpenoid content [126], while far-red (FR) light selectively increases glycoside levels without affecting triterpenoid acids [127]. Different LED spectra exert markedly selective regulatory effects on secondary metabolites: specific LED treatments significantly increase levels of phenolic compounds such as dicaffeoylquinic acid and enhance neuroinflammatory and tyrosinase inhibitory activities, but globally reduce triterpenoid components including MA, AS, and their corresponding aglycones [128].

Regarding temperature, low temperatures (15 °C) significantly inhibit plant growth and reduce MA content, while 25 °C favors the highest biomass and total saponin yield [129]. Water conditions exert dual effects: moderate water stress (e.g., 50–75% pot water-holding capacity) increases MA content [130], while severe drought causes a substantial decline [131]. Exogenous MeJA spraying can alleviate the negative impact of drought on total triterpenoids [120]. For salt stress, moderate NaCl treatment (12.5–25 mM) significantly increases MA and total saponin yields, while high concentrations (50 mM) exert inhibitory effects [132].

In addition to field environmental factors, nutritional conditions in in vitro culture systems also significantly regulate MA accumulation. Carbon source type and concentration are key influencing factors: treatment with 7% xylose achieves an MA content of 43.02 ± 0.15 mg/g DW while increasing AS, AA, and MAA levels; 1.5% sucrose, 7% maltose, and 5% galactose also promote triterpenoid saponin synthesis to varying degrees [133]. Harvest season also affects content: Australian *C. asiatica* exhibits the highest total content of the four triterpenoids in summer (January–February) [134]. For drying methods, freeze drying maximally preserves active ingredients, including MA [135], while moderate dehydration (e.g., 12 h) increases their content [136,137]. These findings provide a theoretical basis for optimizing MA yield by regulating environmental conditions.

4.2.3. Plant–Microbe Interactions

Interactions between plants and beneficial microorganisms significantly affect the accumulation of secondary metabolites such as MA. A key study treated *C. asiatica* in the field with fermentation broth of the plant growth-promoting rhizobacterium *Priestia megaterium* HyangYak-01. The results showed that the strain's fermentation broth significantly increased the contents of medicinal ingredients such as AS and MA in leaves and altered the chemical composition ratio of extracts. Skin cell experiments demonstrated that *C. asiatica* extracts treated with this strain exert better skin barrier-improving effects and lower inflammatory responses [138].

Arbuscular mycorrhizal fungi maintain relatively high MA content (approximately 118.9 mg/g dry weight) and total saponin yield under moderate water deficit conditions, while un-inoculated plants exhibit a >37% decline in saponin content under severe water

shortage. This indicates that Arbuscular mycorrhizal fungi can alleviate the negative impact of drought stress on MA accumulation [131]. Other microbial-derived elicitors such as yeast extracts have also been reported to increase *C. asiatica* biomass and MA content [139], while endophytic fungus research focuses more on product fermentation. For example, the endophytic fungus *Colletotrichum gloeosporioides* isolated from *C. asiatica* can produce AS [140]. Lactic acid bacteria-mediated fermentation can also drive metabolic remodeling of *C. asiatica*, significantly enriching acidic triterpenoids (MAA and AA) and enhancing anti-neuroinflammatory activity, providing a biotransformation strategy for directional regulation of active ingredient composition [141]. These studies reveal the potential of regulating plant–microbe interactions to directionally increase MA yield, providing a new strategy for green and sustainable production.

4.2.4. Regulatory Network of Transcription Factors (MYB and bHLH) in Biosynthesis

In addition to environmental factors and elicitors, transcription factors play a central role in regulating MA biosynthesis. Multi-omics association analysis has revealed that MYB and bHLH transcription factors constitute the core network nodes regulating triterpenoid saponin biosynthesis. Transcriptome–metabolome association analysis of 26 wild *C. asiatica* germplasms found that expression levels of *C. asiatica oxidosqualene cyclase 5* and *C. asiatica oxidosqualene cyclase 7* (OSC genes) are significantly positively correlated with MA accumulation levels, suggesting that these two types of transcription factors may influence triterpenoid saponin biosynthetic flux by cooperatively regulating OSC expression [142]. This finding provides potential targets for molecular marker-assisted breeding and a theoretical basis for increasing MA yield by regulating transcription factor expression.

Current research in this direction remains at the omics association level; specific MYB/bHLH family members have not been identified, and direct functional verification evidence is lacking. Future studies should further identify specific transcription factors that regulate key enzyme genes (e.g., *CYP716A83*, *CYP714E19*, and *UGT73AD1*) and elucidate the upstream signal transduction mechanisms in response to elicitors such as MeJA.

4.2.5. Regulatory Effects of Physical Elicitors Such as Nanoparticles

As novel physical elicitors, nanoparticles can activate secondary metabolic pathways by triggering oxidative stress responses in plant cells, effectively promoting the accumulation of triterpenoid saponins, including MA, in *C. asiatica* hairy roots. Treatment with gold nanoparticles and zinc nanoparticles increases the fresh weight and total saponin yield of transgenic hairy roots carrying the Arabidopsis squalene synthase gene (*At-SQS1*). Among them, zinc nanoparticles (100 μg/mL) treatment yields the highest hairy root biomass, while gold nanoparticles (2 μg/mL) treatment achieves the highest total saponin content (predominantly MA) at 1.9 mg/g dry weight, a 2.71-fold increase compared with untreated controls [143]. Similar to chemical elicitors such as MeJA and SA, nanoparticle-induced MA accumulation is accompanied by upregulated expression of key enzyme genes (e.g., *CabAS* and *CaSQS*) [143], suggesting that its mechanism may be mediated by ROS-induced transcriptional activation. This technology provides a new approach for large-scale production of MA using nanobiotechnology, but its applicability in cell suspension culture systems and feasibility for large-scale application remain to be further verified.

4.3. Strategies for Efficient MA Production Based on Synthetic Biology

4.3.1. Establishment and Optimization of Transgenic Hairy Root Culture Systems

Transgenic hairy root culture systems mediated by *Agrobacterium rhizogenes* have been successfully established and serve as important platforms for producing triterpenoid saponins, including MA. As wild *C. asiatica* resources become increasingly depleted due to over-harvesting, and traditional cultivation suffers from low seed vigor and unstable secondary metabolite content, in vitro biotechnology has become a key approach to address the large-scale production of medicinal ingredients [144]. Multiple reviews have systematically evaluated various in vitro production strategies for *C. asiatica*, including hairy root culture, confirming that it represents one of the most industrially promising triterpenoid saponin production systems due to its genetic stability, rapid growth, and autonomous growth without exogenous hormones [144,145]. Studies have found that leaf explants exhibit higher transformation efficiency (approximately 27%) than petioles (approximately 12%), and petiole-derived hairy root lines (e.g., HP2) contain higher total triterpenoid content [146]. By optimizing co-culture conditions, the hairy root induction frequency can reach 36.1% [111].

To enhance target product yield, researchers have further combined multiple optimization strategies such as elicitor treatment and precursor feeding [145]. MeJA significantly induces *CabAS* gene expression in hairy roots, leading to abundant AS production (7.12 mg/g dry weight) in lines that previously had undetectable levels [111]. Coronatine, alone or in combination with MeJA, exerts a particularly prominent yield-increasing effect on MA [117]. Hairy root lines of different genotypes exhibit marked differences in saponin synthesis capacity; transformed roots of two Malaysian *C. asiatica* phenotypes show completely undetectable AS and MA, and undifferentiated callus also lacks accumulation of these two active ingredients [147], indicating that genotype selection is a critical prerequisite for successful hairy root systems. Precursor feeding (e.g., 2.5 mM squalene and 5 mM pyruvate) also effectively increases triterpenoid content in hairy roots [148]. Long-term culture (up to 8 weeks) and optimized batch culture systems can stably yield high-productivity hairy root lines, enabling potential industrial production [146,149].

In addition to hairy root systems, cell suspension culture, somatic embryogenesis, and synthetic seed technology are also used for rapid propagation and secondary metabolite production of *C. asiatica*, collectively constituting a complete in vitro biotechnological production system [144,145].

4.3.2. Overexpression of Key Enzyme Genes and Metabolic Flux Redirection

Redirecting metabolic flux by overexpressing key enzyme genes is a core strategy to increase MA yield. Transgenic hairy root lines (HRL3) of *C. asiatica* transformed with the *At-SQS* exhibit significantly higher total saponin yield (especially MA) than wild-type lines (2.67-fold) [149]. Similarly, hairy roots overexpressing the ginseng farnesyl diphosphate synthase gene (*PgFPS*) show a transient 1.15-fold increase in saponin content 14 days after MeJA induction, indicating that FPS not only participates in phytosterol synthesis but also plays a regulatory role in the triterpenoid pathway [107].

Genome analysis of *C. asiatica* itself reveals significant expansion of multiple gene families related to triterpenoid saponin biosynthesis (e.g., *CYP716*, *CYP714*, and *UGT73*). Among them, the *UGT73* gene cluster is located within the same topologically associating domain, which may be closely associated with enhanced saponin synthesis capacity [109]. Through co-expression strategies, the complete synthetic pathway from simple precursors to MA and asiaticoside B has been reconstructed in *N. benthamiana*, verifying the functions of multiple key genes [33,78].

4.3.3. Research Progress in Heterologous MA Synthesis Using Yeast Cell Factories

Currently, heterologous synthesis of intact MA using yeast cell factories has not been reported, but enzymes required for key catalytic steps have been successfully expressed and functionally characterized in yeast. For example, co-expression of *C. asiatica* OSC (CaDDS) with P450 enzymes CYP716A83 and CYP714E19 in *Saccharomyces cerevisiae* successfully generates 23-hydroxyursolic acid (a precursor of MAA), confirming the key role of CYP714E19 as a multifunctional C-23 oxidase [31].

In terms of heterologous synthesis yield, *S. cerevisiae* chassis cells have achieved de novo synthesis of AA (the aglycone of MA). By optimizing the pairing efficiency of P450 oxidase and reductase, reconstructing the galactose regulatory network (knocking out *GAL80*/*GAL1*), and enhancing the mevalonate pathway, AA yield reaches significant levels [150]. On this basis, heterologous expression of CaCYP716C11p in oleanolic acid-producing strains yields maslinic acid (C-2 α-hydroxylated product) at 8.9 mg/g dry cell weight [150], laying a yield foundation for subsequent heterologous synthesis of the complete MA trisaccharide chain via multi-enzyme cascade reactions.

UDP-glycosyltransferases (e.g., UGT73AD1 and UGT73AH1) have been expressed and characterized in prokaryotic systems and can catalyze C-28 glucosylation of AA and MAA [99,100]. Although the final assembly of the complete trisaccharide chain (requiring sequential catalysis by multiple glycosyltransferases) has been achieved in *N. benthamiana* [33,78], reconstructing the complete MA biosynthetic pathway in yeast remains a future research direction. Relevant reviews also emphasize the great potential of microbial cell factories in addressing raw material shortages [24,151].

4.3.4. Precursor Feeding Technology

Among synthetic biology-based efficient MA production strategies, precursor feeding technology effectively increases target triterpenoid saponin yield by adding specific precursor substances to plant cell or tissue cultures. Studies have found that adding α-amyrin to *C. asiatica* cell suspension cultures, supplemented with the permeabilizing agent Dimethyl sulfoxide (DMSO), results in nearly 84% of α-amyrin being converted into active ingredients such as MA and AS after 7 days, indicating that this precursor can be efficiently taken up by cells and converted into target products [113]. In hairy root culture systems, feeding squalene (2.5 mM) and pyruvic acid (5 mM) significantly enhances triterpenoid biosynthesis, achieving total triterpenoid contents of 57.53 mg/g DW and 29.13 mg/g DW, respectively, with squalene exerting a particularly prominent promoting effect [148]. These studies confirm that direct supplementation of key precursors in the terpenoid synthesis pathway can effectively break rate-limiting steps in the metabolic pathway and represents a feasible strategy for increasing MA yield [113,148].

4.4. Effects of Different Genetic Backgrounds and Germplasm Resources on MA Content

Variations in MA content among *C. asiatica* from different production areas are fundamentally determined by the genetic background of the germplasm, in addition to environmental regulation (detailed in Section 4.2.2). A survey of 60 germplasms from South India and the Andaman Islands showed that the highest MA content reaches 5.67% (dry weight), and differences in content among germplasms are primarily attributed to genetic background rather than altitude [152]. Cultivation experiments under uniform agronomic conditions in the Indo–Gangetic Plain further confirmed that germplasm M from southern India has the highest AS (52.1 mg/g DW) and MA (25.7 mg/g DW) contents, with 83–95% genetic divergence from northern, eastern, and northeastern germplasms [153].

Analysis of genetic diversity in 96 germplasms from 12 regions of China revealed that Guizhou populations exhibit the highest genetic diversity, and polymorphism at the EST-SSR54 locus encoding the key terpenoid synthesis enzyme 4-hydroxy-3-methylbut-

2-enyl-diphosphate synthase (HDS) is significantly correlated with differences in triterpenoid content [154]. Based on these germplasm resource surveys, researchers have screened multiple high-MA elite lines, such as CA-51 and CA-59 from southern India (total saponin content ≥ 4.0% industrial benchmark) [155,156], and the Nakhonpathom germplasm from Thailand (with further enhancement after SA induction) [157]. A germplasm evaluation of 24 accessions from Yunnan Province also identified significant phenotypic, genetic, and biochemical diversity, with total triterpenoid content ranging from 4.09 to 20.18 $mg \cdot g^{-1}$, providing elite germplasm resources for selective breeding [158].

Globally, *C. asiatica* mainly exists in two chemotypes: an AS-dominant chemotype and an MA-dominant chemotype [42,159,160]. Their differentiation originates from differences in C6 hydroxylation efficiency, providing a theoretical basis for molecular marker-assisted breeding to directionally select high-MA germplasm. It is noteworthy that *C. asiatica* is often morphologically confused with closely related species of the genus *Hydrocotyle* (e.g., *Hydrocotyle umbellata* and *Hydrocotyle brasiliensis*), which do not contain characteristic ursane-type triterpenoid saponins such as MA and AS. Combined morphological, chemical fingerprinting, and molecular marker identification is required to ensure accurate screening of high-content germplasms [161-164]. These germplasm resource surveys and genetic analyses provide foundational data for sustainable raw material supply and molecular breeding of MA.

4.5. Comprehensive Comparison of Different Production Systems and Industrialization Bottlenecks

To intuitively present the technical potential and industrialization gaps of each MA production route, Table 4 summarizes the yield levels, production cycles, techno-economic characteristics, and core industrialization bottlenecks of four mainstream systems: original plant cultivation, transgenic hairy roots, cell suspension culture, and yeast heterologous synthesis. It should be explicitly noted that yield units differ across systems to align with standard reporting conventions in each research field: plant-based systems (field cultivation, hairy roots, and cell suspensions) report yields as mg per gram dry weight (mg/g DW), while the yeast microbial cell factory system reports yields as mg per gram dry cell weight (mg/g DCW). Furthermore, product forms differ substantially across systems: all plant-based production systems accumulate fully glycosylated intact MA, whereas current yeast cell factory platforms only achieve the synthesis of aglycone pathway intermediates, and de novo synthesis of the complete trisaccharide glycoside has not yet been realized. Given the differences in cultivation matrices, product forms, and calculation units, direct cross-category comparison of absolute yield values should be interpreted with caution; the core purpose of this comparison is to systematically contrast technical characteristics, production cycles, and industrialization feasibility, with yield data serving as a reference indicator of production potential. Overall, original plant cultivation remains the main source of current industrial raw materials but has inherent drawbacks such as poor quality uniformity and limited wild resources; cell suspension culture and hairy root systems offer certain advantages in yield controllability, but large-scale scale-up processes remain immature. Microbial cell factories represent the future development direction due to their short cycle time and green sustainability, but the complete glycosylation synthesis pathway has not been fully established in microorganisms, leaving a considerable gap for large-scale industrial production.

Table 4. Techno-economic comparison of different production systems for MA.

Production System	MA Yield	Production Cycle	Core Advantages	Main Disadvantages	Core Industrialization Bottlenecks	References
Original plant cultivation (field/hydroponic)	Product: Intact MA (full trisaccharide glycoside) Elite germplasm: 10–56.7 mg/g DW Common cultivars: 10–20 mg/g DW Hydroponic leaves: ~11 mg/g DW	60–120 days after transplanting, regulated by local climate and harvest period	Low planting cost, low technical threshold, suitable for large-scale promotion; natural and complete component composition, consistent with traditional medication habits	Large content fluctuations, significantly affected by seasons, climate, pests and diseases; increasingly endangered wild resources; high land occupation and long growth cycle	Poor germplasm uniformity and unstable raw material quality; cumbersome harvesting and pretreatment processes, difficult to meet pharmaceutical-grade standardized raw material requirements	[134,152,165,166]
Transgenic hairy root culture	Product: Intact MA (full trisaccharide glycoside) Wild-type lines: trace to ~1 mg/g DW After elicitor optimization: 1–10 mg/g DW Total triterpenoids (including aglycones, with precursor feeding): up to 57.53 mg/g DW	4–8 weeks batch culture	The genetic traits are stable, and growth does not require exogenous hormones. Production can be directionally enhanced through elicitors or metabolic engineering, and it is not constrained by seasons or environmental conditions.	Strict sterile culture requirements, high investment in culture media and equipment; difficult scale-up culture, shear force and oxygen transfer limit growth; low basal saponin content in most lines	Difficulty in screening and preservation of high-yield hairy root lines; immature large-scale bioreactor culture processes, low volumetric productivity per unit volume	[111,143,148,149]
Cell suspension culture	Product: Intact MA (full trisaccharide glycoside) Untreated control: ~27 mg/g DW Optimized with 100 μM salicylic acid (added on day 10, harvested on day 24): up to 114 mg/g DW	10–14 days per generation, continuous subculture expansion	Short culture cycle and rapid proliferation; significant elicitor yield-enhancing effect, unit dry weight content can far exceed high-quality original plants; closed sterile production with strong quality controllability	Cell lines prone to browning and genetic degradation, poor long-term subculture stability; high culture medium cost; most products accumulate intracellularly, requiring multiple extraction and purification steps	Insufficient long-term preservation and passage stability of cell lines; prominent shear force damage issue in large-scale suspension culture; high downstream separation and purification costs	[112,119,133]
Yeast heterologous synthesis (microbial cell factory)	Product: Aglycone pathway intermediates (maslinic acid, 23-hydroxyursolic acid) Intact MA with full trisaccharide chain: not yet achieved Aglycone intermediate (maslinic acid): up to 8.9 mg/g DCW	3–7 days fermentation cycle	The fermentation cycle is extremely short, enabling continuous year-round production; it requires no arable land and is unaffected by natural environmental conditions; and its simple product spectrum ensures low downstream separation and purification costs.	Extremely low technical maturity, complete glycosylation pathway not yet established in microorganisms; current aglycone yield far lower than plant systems; high initial R&D investment	Poor substrate specificity of UGT enzymes, low multi-enzyme cascade catalytic efficiency; mismatched metabolic flux between triterpene scaffold synthesis and glycosylation modules; cytotoxicity and protein folding issues in heterologous expression	[31,33,150]

Note: Yield units are differentiated by production system: all plant-based systems use mg per gram dry weight (mg/g DW); the microbial heterologous system uses mg per gram dry cell weight (mg/g DCW). Direct cross-category comparison of absolute yield values (plant biomass vs. microbial cells) should be interpreted with caution due to different cultivation matrices and product forms. All yield values represent typical reported levels under optimized experimental conditions.

5. Green Extraction and Efficient Purification Technologies of MA

The full technical system of extraction, purification, and quality control for MA is systematically presented in Figure 5. In this review, the term "green extraction technology" is used to describe processes with verified advantages of shorter extraction time, lower energy consumption, and reduced organic solvent usage compared with conventional maceration and Soxhlet methods. It should be noted that most existing studies focused on extraction efficiency optimization, and systematic full life cycle environmental assessments covering solvent recovery, waste generation, and ecological toxicity remain limited. The comprehensive environmental benefits of these technologies still require further specialized verification. Each technical system is discussed and analyzed in detail in the following sections of this chapter.

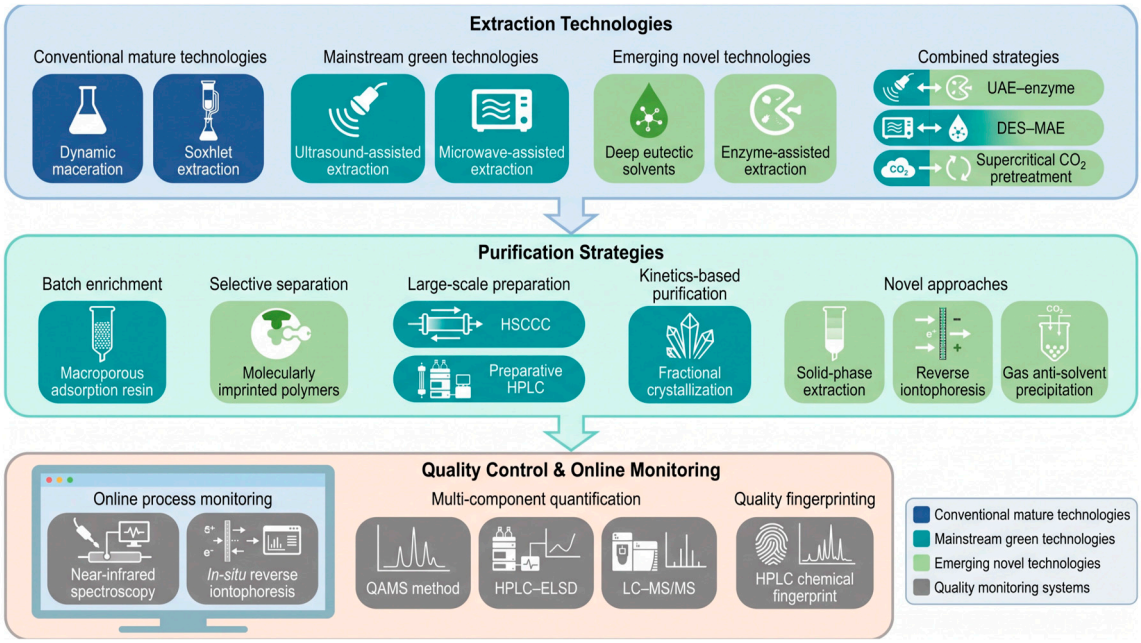


Figure 5. Green Extraction, Efficient Purification, and Quality Control Technologies for Madecassoside (MA). Created with Figdraw(https://www.figdraw.com/#/), Copyright Code: PPPAP4dd81). Technologies are classified into three tiers by process sequence: extraction technologies (conventional mature, mainstream green, emerging novel, and combined strategies), purification strategies (batch enrichment, selective separation, large-scale preparation, and kinetic-based and novel approaches), and quality control and online monitoring systems. Color coding indicates technology maturity.

5.1. Limitations of Traditional Extraction Methods and Development of Green Extraction Technologies

The industrial preparation of MA is a complete systematic engineering process covering raw material pretreatment, target component extraction, enrichment and purification, refinement and standardization, and terminal application. Razzaq et al. [167] systematically compared the advantages and disadvantages of traditional maceration, Soxhlet extraction, and green technologies such as ultrasound-assisted extraction (UAE), microwave-assisted extraction (MAE), and supercritical fluid extraction. They detailed downstream purification processes, including macroporous adsorption resin enrichment, molecular imprinting separation, preparative chromatography, and recrystallization, and constructed a full-chain transformation pathway from *C. asiatica* biomass to pharmaceutical, cosmetic, health product, and biomaterial fields.

Raw material pretreatment is a key prerequisite affecting extraction efficiency. Freeze drying and low-temperature drying at 40–50 °C can maximally preserve MA activity, while high-temperature drying or sun exposure causes sugar chain hydrolysis, reducing extraction rate and product activity [135,137].

5.1.1. Process Optimization of Ultrasound-Assisted Extraction (UAE) and MAE

Ultrasound-assisted extraction (UAE) and MAE are the most widely used green extraction technologies, and process optimization can significantly improve MA extraction efficiency. Solvent type is one of the core factors affecting extraction performance. Among the three extraction solvents—ethanol, methanol, and water—ethanol extracts exhibit the highest MA (18.66 mg/g) and AS (42.86 mg/g) contents, and significantly superior cyclooxygenase (COX)-1/COX-2 inhibitory activity and stronger inhibition of TPA-induced PGE_2 production than the methanol and water extracts. Ethanol is therefore the preferred solvent for extracting *C. asiatica* triterpenoid saponins [168].

One study optimized MAE to obtain optimal conditions: liquid-to-solid ratio 10 mL/g, 58% ethanol, 300 W, 3.4 min [169]. Using MAE combined with 80% ethanol and 100 W extraction for 7.5 min, the obtained extract dry powder achieves an MA content of 7.332% (extract purity) and an AS content of 4.560% [170], indicating that this process exerts good enrichment effects on target components. Based on the rapid extraction characteristics of MAE, researchers have established a supporting liquid chromatography with diode array detection-electrospray ionization tandem mass spectrometry quantitative analysis method that can simultaneously separate and determine MA, AS, and AA within 50 min. The method exhibits good linearity ($r^2 > 0.9992$), precision RSD < 3%, and recovery rates of 95.4–106.8%, suitable for rapid quality evaluation of *C. asiatica* samples from different origins [171].

For UAE, using methanol as the solvent, a solid-to-liquid ratio of 1:25, and extraction for 20 min achieves relatively high triterpenoid yield [172]; optimized UAE conditions (75% ethanol, 87.5 W, 30 min, 20 mL solvent) yield an MA extraction amount of 16.91 mg/g [173]. UAE combined with methanol extraction achieves an MA content of 8.21 mg/g [174]. As a comparison with traditional extraction methods, dynamic maceration extraction optimized via response surface methodology achieves the highest contents of all four major *C. asiatica* triterpenoids at 60 °C for 120 min [175], while the classic Soxhlet extraction method requires 8 h to achieve similar extraction efficiency [176].

Comparative analysis shows that MAE and UAE significantly outperform traditional maceration and Soxhlet extraction in extraction efficiency, with energy consumption reduced by 59% and 54%, respectively [170]. These optimization studies provide reliable parameters for industrial green extraction.

5.1.2. Deep Eutectic Solvent Extraction

As a novel green solvent, deep eutectic solvents (DESs) can achieve selective and efficient extraction of MA by adjusting the ratio of hydrogen bond donors (HBDs) to hydrogen bond acceptors (HBAs) and water content. Studies have found that, among the DESs prepared using choline chloride, acetylcholine chloride, or chlorocholine chloride as the HBA and ethylene glycol as the HBD, the chlorocholine chloride-based DES, containing 20% water content, achieves the highest MA extraction efficiency (17.38 μg/mg) due to weakened hydrogen bonding and lower viscosity. In contrast, acetylcholine chloride-based DES containing ester groups exhibits reduced extraction rates due to increased viscosity and limited diffusion [177].

Increasing the HBD/HBA ratio and adding appropriate amounts of water (≤30%) can improve extraction efficiency by reducing viscosity, but excessive water (>30%) disrupts the DES network structure [177,178]. Natural DESs prepared with acetylcholine chloride:malic acid:water (1:2:2) plus additional water (40:60) combined with MAE yield 21.7

mg/g dry weight of MA and 12.7 mg/g dry weight of AS, and the extract has a lighter color, suitable for cosmetic applications [179]. Another study showed that when DES is mixed with distilled water at a 3:7 ratio, extraction efficiency is approximately 1.4 times higher than pure methanol [180].

Therefore, the extraction performance of DES for MA can be directionally optimized by regulating HBA structure, HBD/HBA ratio, and water content. DES systems remain at the laboratory stage with limited industrial application due to high viscosity, difficulty in recovering target components, and challenges in controlling solvent residues.

5.1.3. Pulsed Electric Field (PEF) and Neutral Electrolyzed Water (NEW) Extraction Technologies

Pulsed electric field (PEF) is a non-thermal extraction technology conducive to preserving the natural structure of active ingredients. Studies have detected MA and confirmed its antioxidant activity in plant polyphenol extracts treated with PEF combined with ultrasound [181], providing indirect evidence for the application of this technology in *C. asiatica* extraction.

Neutral electrolyzed water (NEW) is mainly used for surface disinfection and virus inactivation of *C. asiatica*. An incidental finding revealed that soaking *C. asiatica* leaves in NEW containing 205 ppm available chlorine for 5 min significantly increases AS content from 29.96 mg/g dry weight to 37.82 mg/g [182]. Given the highly similar structure and metabolic pathways of MA and AS, it is speculated that NEW may exert similar retention effects on MA, but direct experimental verification is required. Combined treatment with acidic electrolyzed water and pulsed light can effectively preserve triterpenoid glycosides, including MA, in *C. asiatica* leaves during cold storage [183]. These non-thermal processing technologies provide potential technical support for mild and green extraction of MA, but overall research remains preliminary, and direct evidence needs to be enriched.

5.1.4. Enzyme-Assisted Extraction

Enzyme-assisted extraction (EAE) improves the dissolution efficiency of MA by enzymatically disrupting plant cell walls, and precise regulation of pH and time is the key to achieving selective release. One study found that cellulase (12 mg/g) enzymatic hydrolysis at 60 °C for 60 min, combined with ultrasonic extraction for 50 min, achieves a total asiaticoside extraction rate of 1.92% (calculated as the sum of asiaticoside and madecassoside contents) [184].

More in-depth research has revealed a two-stage pH regulation mechanism: Stage I (pH 4.0, 15 min) is dominated by proton-induced pectin relaxation and rapid glycoside release, with MA and AS extraction amounts reaching 18.20 and 8.51 mg/g, respectively; Stage II (pH 5.0–6.0, 60 min) is dominated by enzyme-mediated matrix disintegration and aglycone re-adsorption, at which point aglycone extraction is optimal. Under the optimized two-stage protocol, the extracted target saponins exist predominantly as intact glycosides, with no significant hydrolytic deglycosylation observed. All individual compound quantification was performed via validated HPLC–UV methods calibrated with authentic reference standards. However, prolonged treatment reduces aglycone content due to non-specific re-adsorption [185]. This finding indicates that sequential release and selective extraction of MA (glycoside) and corresponding aglycones can be achieved by precisely controlling enzymatic hydrolysis pH and time. This strategy provides a feasible framework for green, efficient, and low-cost separation of active ingredients from *C. asiatica*.

5.1.5. Combined Extraction Technologies

The combined use of multiple green extraction technologies often produces synergistic effects, further improving MA extraction efficiency and purity. Ultrasound–enzyme

combined treatment is the most common combination; for example, the aforementioned cellulase hydrolysis combined with ultrasonic extraction yields a stable and feasible process [184]. Microwave–ultrasound combined treatment has been used at pilot scale to prepare pentacyclic triterpenoid-enriched extracts. Using 4 kW microwave-assisted and 0.55 kW ultrasound-assisted extraction, the total pentacyclic triterpenoid content reaches 106.02 mg/g crude extract, and the purity of components, including MA, is significantly improved after macroporous resin purification [186].

DES–MAE combined treatment: using natural DESs as solvents combined with MAE not only increases MA yield but also produces extracts with lighter color and higher antioxidant activity [179]. PEF+US combined treatment, although mainly used for other plants, has identified MA as a target product, proving that this combination is suitable for extracting active ingredients from *C. asiatica* [181]. Supercritical CO_2 pretreatment combined with traditional ethanol extraction first removes pigments and then performs extraction, significantly enriching components such as MA and asiaticoside B and enhancing cell migration and angiogenesis activities [187].

In addition to the above physical–chemical technology combinations, the development of novel green solvent systems and research on traditional Chinese medicine compatibility effects provide new directions for optimizing MA extraction processes. Supramolecular solvents, a novel extraction medium composed of n-hexanol, tetrahydrofuran, and water, achieve efficient extraction of target components through dispersion and hydrogen bonding interactions. Extraction of MA, AS, and their aglycones takes only 5 min, with recovery rates of 91.6–99.9% combined with HPLC–MS/MS detection and relative standard deviations of 1.7–7.9%, exhibiting significant advantages of rapidity, greenness, and sensitivity [188]. These combined extraction strategies achieve efficient, environmentally friendly, and high-quality MA extraction by integrating the advantages of different technologies.

5.1.6. Comparison of Core Parameters of Different Extraction Technologies and Process Selection

To intuitively quantify the comprehensive performance of various extraction technologies and provide a comparable reference for process selection in different application scenarios, Table 5 horizontally summarizes the key parameters of traditional extraction methods and mainstream green extraction technologies, covering core dimensions such as extraction efficiency, time cost, solvent consumption, energy consumption level, and product characteristics. Natural product extraction technology systems can be divided into two categories: core extraction processes and auxiliary pretreatment processes, with significant differences in research depth, substrate adaptability, and industrialization maturity among different technologies. To ensure consistency of comparison dimensions and reference values, this comparison focuses only on mature extraction technologies that can serve as core processes. It should be noted that the absolute extraction efficiency values listed in Table 5 are typical levels reported under respective optimized conditions and specific raw materials. Due to differences in raw material attributes such as medicinal parts, origin, and harvest season among different studies, these values are not suitable for direct absolute efficiency ranking but are used to reflect the achievable yield range of each technology. In this context, the term "green extraction technologies" refers specifically to processes with verified advantages in extraction efficiency, energy consumption, and organic solvent usage relative to conventional maceration and Soxhlet extraction. It should be acknowledged that comprehensive environmental benefits—including full solvent recovery efficiency, net waste emission reduction, and total carbon footprint—have not been systematically evaluated in most optimization studies, and dedicated life cycle assessment studies at industrial scale are still warranted.

Table 5. Core performance parameters of different extraction technologies for MA.

Extraction Technology Type	MA Extraction Efficiency (mg/g Dry Weight)	Extraction Time	Relative Level of Solvent Consumption	Relative Level of Energy Consumption	Characteristics of Crude Extract	Core Advantages	Typical Application Scenarios	References
Traditional dynamic maceration	~12.5	~120 min (optimized conditions at 60 °C)	High (liquid-to-solid ratio usually ≥20:1)	Medium (low-temperature heating, but long duration leads to high total energy consumption)	Many types of impurities, low proportion of target components	Low equipment threshold, suitable for large-batch processing, minimal damage to ingredients	Raw material pretreatment, crude extraction processes, batch leaching of heat-sensitive ingredients	[175]
Soxhlet extraction	~13.2	~480 min (8 h)	Very high (solvent continuously refluxes)	High (long-term continuous heating and reflux)	Thorough extraction, but high co-dissolution of fat-soluble impurities	Sufficient extraction, no manual intervention, good result stability	Laboratory benchmark control method, full-component extraction of small samples	[170,176]
UAE	16.91 (optimized ethanol system conditions)	20–30 min	Medium-low (liquid-to-solid ratio ~20:1)	Low (54% lower energy consumption than traditional methods)	High dissolution efficiency of target components, fewer impurities than traditional methods	Simple operation, room-temperature extraction, friendly to heat-sensitive ingredients, high equipment popularity	Laboratory and small-to-medium scale production, extraction of heat-sensitive active ingredients such as triterpenoid saponins	[172-174]
MAE	Extraction rate based on raw material dry weight not reported	3.4–7.5 min	Low (liquid-to-solid ratio ~10:1)	Lowest (59% lower energy consumption than traditional methods)	Strong extraction selectivity, less dissolution of non-target impurities	Fastest extraction speed, least solvent consumption, high thermal efficiency	Industrial rapid batch extraction, large-scale production with stable raw material components	[169-171]
DES	17.38 (single solvent system); 21.7 (combined with MAE)	10–30 min; <10 min when combined with MAE	Low (solvent recyclable)	Low	Light-colored extract, few polar impurities, good cosmetic compatibility	Green degradable solvent, high selectivity, good product appearance	Cosmetic-grade high-value extract preparation, clean production process requirements	[177,179,180]
EAE	18.20 (pH staged regulation process)	60–75 min (including enzymatic hydrolysis process)	Low (aqueous phase system, very little organic solvent consumption)	Low (room-temperature enzymatic hydrolysis, mild conditions)	Directional release of glycosides or aglycones, high purity of target components	Mild conditions, controllable selectivity, directional enrichment of specific active components	Directional extraction of specific active components, clean production with low solvent residues	[184,185]

Note: All extraction efficiency values are expressed as mg of madecassoside (MA) monomer per gram of dry raw material (mg/g DW), not total triterpenoid content. Data were collected from independent studies with different raw material sources (whole herb vs. leaves), solvent systems, and analytical methods. Direct cross-technology comparison of absolute yield should be interpreted with caution, as extraction efficiency is highly dependent on raw material quality, medicinal part, particle size, origin, and harvest conditions. The core purpose of this table is to compare the techno-economic characteristics of different technologies, rather than to rank absolute extraction efficiency. Regarding environmental performance, the energy- and solvent-saving advantages of ultrasound-assisted extraction and microwave-assisted extraction have been quantitatively verified in head-to-head comparative studies [170]. The "green" attribute of DESs is predominantly inferred from their inherent low volatility and recyclability. Systematic life cycle assessment data covering solvent recovery rate, waste discharge, and total carbon footprint remain limited for all included extraction technologies.

5.2. Efficient Separation and Purification Technologies of MA

As the "purification core" link in the *C. asiatica* biorefining process, separation and purification are the key steps to obtain high-purity monomers from crude extracts, directly determining product quality and application value. Industrial downstream purification of MA generally follows a standardized four-step process: clarification and degreasing → preliminary enrichment via macroporous adsorption resin → refinement via preparative chromatography or recrystallization → drying and quality standardization [167]. The first step removes insoluble impurities and non-polar interferences such as waxes and pigments from crude extracts through filtration and non-polar solvent degreasing; the second step achieves batch enrichment of total triterpenoids using the polar selective adsorption of macroporous resins; the third step obtains high-purity monomers via preparative chromatography or fractional crystallization; finally, products meeting pharmaceutical or cosmetic grade requirements are obtained through drying and standardization.

5.2.1. Screening of Macroporous Adsorption Resins and Optimization of Dynamic Adsorption–Desorption Processes

Macroporous adsorption resin is an effective material for enriching and purifying MA from total asiaticosides. The key to process optimization lies in resin model selection and regulation of dynamic adsorption–desorption parameters. A study by Jia et al. showed that among resins such as HPD100, HPD300, X-5, AB-8, and D101, HPD100 exhibits higher adsorption and desorption capacities for MA and AS. After gradient elution, MA content increases from 3.9% to 39.7% with a recovery rate of 70.4% [35]. In the pretreatment of total asiaticoside liposome preparation, the macroporous resin process optimized via Box–Behnken response surface methodology achieves an MA encapsulation efficiency of 75.85% [101]. Using Diaion HP-20 macroporous resin combined with 50% and 75% ethanol gradient elution, high-purity pentacyclic triterpenoid-enriched fractions can be prepared with significantly increased MA content [186]. Monitoring the entire purification process via ultrahigh-performance liquid chromatography–quadrupole time-of-flight mass spectrometry achieves an MA product with 72.51% purity and a total recovery rate of 90.79% [189]. These studies provide mature technical parameters for industrial separation of MA using macroporous resins.

5.2.2. Preparation of MIP and Selective Separation

MIP technology provides a new strategy for highly selective separation of specific triterpenoid saponins (e.g., AS and MA) from *C. asiatica*. Researchers synthesized MIP via precipitation polymerization using AS as a template. Under optimized ratios of functional monomer, porogen, and cross-linking agent, the maximum adsorption capacity reaches 19.16 mg/g with an imprinting factor of 2.86. When the MIP is used for molecularly imprinted solid-phase extraction of *C. asiatica* crude extracts, MA purity increases by 6.51-fold, while AS purity increases by only 3.01-fold, indicating that MIP exerts a more significant enrichment effect on MA [79]. Although the study used AS as the template, the prepared MIP exhibits good cross-recognition ability for structurally similar MA, indirectly achieving efficient separation of MA. This method offers advantages of low cost, high selectivity, and reusability, providing a new approach for targeted separation of MA from complex mixtures.

5.2.3. Large-Scale Preparation via High-Speed Counter-Current Chromatography and Preparative HPLC

High-speed counter-current chromatography (HSCCC) and prep-HPLC are important technologies for large-scale preparation of MA. HSCCC uses the solvent system n-hexane–n-butanol–0.05 M NaOH (5:1:6). Through a gradient elution mode with gradually increasing elution strength, 75 mg of MA and 140 mg of AS are isolated in one run from 600 mg of polar *C. asiatica* extract. Product purities are confirmed via electrospray ionization tandem mass spectrometry and nuclear magnetic resonance [190]. HSCCC can also be directly coupled with thin-layer chromatography (TLC) for online monitoring of column effluents, successfully applied to the separation of AS and MA [191].

For preparative HPLC, multiple studies have established mature large-scale preparation processes: using a C18 column (50 mm × 200 mm, 5 μm) with methanol–water (60:40) as the mobile phase, a flow rate of 100 mL/min, an injection volume of 1.5 mL (40 mg/mL), and a diode array detector at 220 nm, both AS and MA with >98% purity can be obtained within 20 min [192,193]. Another study adopts a two-step preparation method: first separating AS (98.8% purity) using a YMC ODS-AC18 column (methanol/water), then further separating MA (76.2% purity) and asiaticoside B (82.3% purity) via a semi-preparative column (water/acetonitrile) [62]. Adding *β*-cyclodextrin to the mobile phase can effectively resolve the isomer pairs MA/asiaticoside B and MAA/terminolic acid, achieving baseline separation within 25 min [64,66,67]. These technologies provide reliable platforms for reference substance preparation and industrial production of MA.

5.2.4. Mechanistic Study of MA and AS Separation via Crystallization

Crystallization achieves efficient separation of MA and AS by utilizing their significant differences in crystallization behavior in specific solvent systems. Studies have found that in methanol–water systems, despite similar solubility, MA exhibits an induction period at least 10 times longer than AS, mainly attributed to the sole molecular structural difference between the two: an additional hydroxyl group at the C-6 position of MA [41].

Based on this difference, fractional crystallization can preferentially precipitate AS (short crystallization induction period) from total triterpenoid saponins of *C. asiatica*, with a yield of approximately 80% and purity of 95% [36]. After further optimization, crystallization yields 60% AS with 70% purity from total saponins; after recrystallization, the yield reaches 76% with 91% purity [36]. Due to its significantly longer crystallization induction period, MA is difficult to precipitate under the same conditions and mainly remains in the mother liquor. It requires further purification via chromatographic methods such as preparative HPLC or HSCCC to obtain high-purity monomers.

The essence of this crystallization strategy is to achieve selective enrichment of AS by utilizing the fundamental difference in crystallization kinetics between the two saponins, rather than directly preparing MA. It reveals the molecular structure dependence of their crystallization behavior, providing a theoretical basis for the design of subsequent separation processes based on crystallization principles.

5.2.5. Novel Large-Scale Purification Technologies

In addition to traditional chromatography and crystallization methods, multiple novel large-scale purification technologies have been applied to MA separation. Solid-phase extraction: anion-exchange solid-phase extraction can remove interfering compounds that co-elute with MA, solving interference issues in simple HPLC detection [194]. Supercritical CO_2 pretreatment: first removing pigments via supercritical CO_2 fluid extraction, then performing ethanol extraction, significantly enriches triterpenoids such as MA and improves the wound-healing activity of extracts [187]. Reverse iontophoresis sampling: at a current density of 0.5 mA/cm^2, MA can be extracted in situ and non-

destructively from fresh *C. asiatica* leaves, with an extraction amount of approximately 0.03 mg/100 mg biomass, providing a rapid detection method for harvest timing judgment [195]. Gas anti-solvent precipitation: using CO_2 as an anti-solvent under low-temperature and low-ethanol concentration conditions, active ingredients including MA can be efficiently precipitated, and the product exhibits high antioxidant activity [196]. These novel technologies each have unique characteristics, providing diversified options for green, efficient, and large-scale purification of MA.

5.3. Online Monitoring and Quality Control Technologies During Extraction and Purification

5.3.1. Near-Infrared Spectroscopy Online Detection Technology

Near-infrared spectroscopy technology provides a rapid, non-destructive online monitoring method for the column chromatography separation and purification process of MA and AS. Researchers collect 50% ethanol eluates, acquire their NIR spectra, and establish partial least squares calibration models between spectral data and HPLC-determined contents. To further improve model robustness and prediction accuracy, researchers systematically compared the performance of wavelength interval selection methods such as interval partial least squares, backward interval partial least squares, and synergy interval partial least squares with single-wavelength selection methods such as competitive adaptive reweighted sampling. The results showed that wavelength interval selection methods significantly outperform full-spectrum modeling and single-wavelength selection methods. Among them, the AS model constructed by the interval partial least squares method achieves a residual predictive deviation value of 7.5, and the MA model constructed by the backward interval partial least squares method achieves a residual predictive deviation value of 2.9, effectively reducing computational load and improving model prediction accuracy [197].

After optimization via the above variable selection methods, the optimal wavenumber ranges for MA and AS are 12,000.8–7499.8 cm^{-1} and 12,000.8–9750.3 cm^{-1}, respectively. The model correlation coefficients (R^2) reach 96.44% and 96.07%, and the root mean square errors of cross-validation are 0.08480 and 0.00099, respectively. The model is used for real-time prediction of the contents of the two components during the column separation and purification process, with satisfactory results. This method is rapid, convenient, and accurate, and can be used for online monitoring and quality control of MA and AS production processes [198].

5.3.2. Non-Destructive in Situ Detection via RI

RI technology achieves non-destructive, in situ sampling of active ingredients such as MA from plant materials, providing a green and efficient strategy for harvest timing determination. In a lateral diffusion cell, at a current density of 0.5 mA/cm^2 under specific pH conditions and a predetermined time, MA can be directly extracted from fresh *C. asiatica* leaves, with an extraction amount of approximately 0.03 mg/100 mg biomass. This method does not damage plant tissues and exhibits a good linear relationship ($r^2 = 0.73$) with component contents determined using conventional methods. Reverse iontophoresis technology, as a convenient on-site analytical tool, can rapidly assess target component levels without damaging plant materials, thereby guiding the determination of optimal harvest periods [195].

5.3.3. Application of QAMS in Simultaneous Quantification of Multiple Components

Quantitative analysis of multicomponents by single marker (QAMS) enables simultaneous determination of multiple indicator components by establishing relative correction factors between one component and multiple others, significantly improving the efficiency and reliability of quality control for *C. asiatica* and its preparations. It is currently

one of the mainstream methods for multi-component quality evaluation of traditional Chinese medicines.

Researchers established a QAMS method for simultaneous determination of asiaticoside B, MA, and AS in total asiaticosides, asiaticoside tablets, and asiaticoside ointments, using MA as the internal standard, an Eclipse XDB-C18 column, acetonitrile–2 mmol/L hydroxypropyl-β-cyclodextrin (24:76) as the mobile phase, and a detection wavelength of 205 nm. The results showed that all three components exhibit good linearity within their respective ranges ($r \geq 0.9998$), with average spiked recoveries of 97.93–102.05%. The results obtained via QAMS are close to those of the external standard method, indicating that the method is stable and reliable, suitable for quality control of total asiaticosides and their preparations [68].

In addition to QAMS, various chromatographic and immunoassay technologies collectively construct a multi-dimensional quality control system for *C. asiatica*. High-performance liquid chromatography (HPLC) remains the most commonly used quantitative method. Multiple studies have optimized chromatographic conditions to achieve simultaneous separation of more components: using a Phenomenex Aqua C18 column and trifluoroacetic acid gradient elution system, six active triterpenoids—MA, AS, MAA, AA, terminolic acid, and asiaticoside B—can be simultaneously separated within 50 min, with detection limits as low as 0.01 μg/mL [199]. For industrial quality control of raw herbal and cosmetic materials, HPLC-ELSD provides a robust, calibration-free alternative, with validated linear ranges of 100–702 mg/L for AS and 105–738 mg/L for MA, average recoveries of 98.30–101.20%, and RSD values below 3% [200]. Multiple classic HPLC methods have established simultaneous quantitative systems for the four major triterpenoids (MA, AS, and their aglycones), suitable for routine quality testing of medicinal materials, extracts, and various preparations [201,202].

LC–MS/MS further enhances quantitative sensitivity and throughput: an LC–MRM–MS method based on multiple reaction monitoring mode can simultaneously accurately quantify 12 bioactive components, including 4 triterpenoids and 8 caffeoylquinic acids. It has been successfully applied to quality calibration of standardized *C. asiatica* products for Phase I clinical trials and animal feed for preclinical research [203]. The UHPLC–ESI-MS/MS–MRM method significantly shortens analysis time, suitable for rapid screening of chemotype variations in *C. asiatica* under different geographical and climatic conditions [204].

TLC technology, with its advantages of simplicity and rapidity, is suitable for on-site rapid detection. The established high-performance thin-layer chromatography–densitometry method does not require derivatization or heating and can directly determine the four major triterpenoids at 202 nm, with validation parameters meeting analytical requirements [205]. TLC–densitometry with anisaldehyde–sulfuric acid coloration is also widely used for semi-quantitative screening of triterpenoids [206].

Immunoassay technology provides a new approach for high-throughput rapid detection: prepared MA polyclonal antibodies can simultaneously recognize MA and AS. The established enzyme-linked immunosorbent assay (ELISA) method has a detection range of 0.39–50 μg/mL, and the immunoblotting method has a detection limit as low as 31.25 ng [207]. The monoclonal antibody 2B4 against AS exhibits high specificity, with only 7.08% cross-reactivity with MA. The established ELISA method shows a correlation coefficient of 0.999 with HPLC measurement results, suitable for rapid screening of large batches of samples [208].

The principle of QAMS is often combined with characteristic fingerprint technology to achieve comprehensive quality evaluation of *C. asiatica* medicinal materials and preparations: an established HPLC fingerprint containing 15 common peaks identifies six major components, including MA, AS, MAA, and AA, via LC–ESI-MS^n, which can effectively

distinguish *C. asiatica* samples from different origins [209]. Multiple studies have combined multi-component quantification with fingerprint similarity analysis to construct a more comprehensive quality evaluation system for *C. asiatica* [69,210].

6. Pharmacokinetics and in Vivo Disposition of MA

The overall in vivo disposition process and core druggability bottlenecks of oral MA are visually summarized in Figure 6, and each process will be discussed and analyzed in detail in the following sections of this chapter.

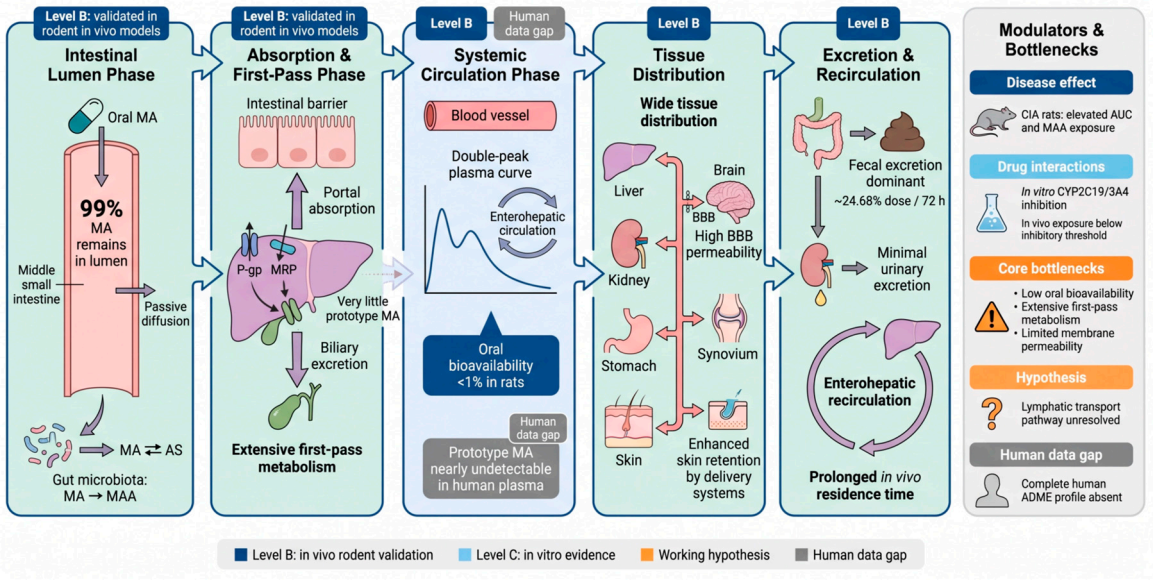


Figure 6. The diagram traces the full journey of oral MA from the intestinal lumen to systemic circulation, tissue distribution, and excretion. Created with Figdraw (https://www.figdraw.com/#/), Copyright Code: PORAO0afba. Key modules include luminal phase, intestinal absorption and first-pass metabolism, systemic circulation, tissue distribution, excretion, and enterohepatic circulation. Modulating factors and core druggability bottlenecks are annotated. Color coding indicates evidence status: dark blue = validated in rodent in vivo models (Level B); light blue = in vitro evidence (Level C); orange = working hypothesis; gray = human data gap.

6.1. Absorption Process and Oral Bioavailability

6.1.1. Intestinal Absorption Mechanism and Role of Transporters

To systematically elucidate the in vivo pharmacokinetic characteristics of MA, researchers have established multiple quantitative analytical methods for MA in biological samples. Among them, an HPLC–UV detection method using solid-phase extraction for plasma sample purification and cucurbitacin B as an internal standard exhibits good linearity in the range of 5 μg/mL to 1.5 mg/mL ($r = 0.9998$), with method recoveries of 90.21–95.65% and intra- and inter-day precision RSD < 3.1%. It meets the requirements for biological sample analysis and provides reliable technical support for studies on intestinal absorption, tissue distribution, and excretion processes [211].

Intestinal absorption of MA mainly occurs in the middle small intestine, with passive diffusion as the main absorption mechanism. In situ rat intestinal perfusion experiments show that MA absorption in the small intestine is stronger than in the large intestine, with absorption rates in each intestinal segment ranked as ileum > jejunum ≥ duodenum > colon. Ileal absorption rates show no significant difference across different drug concentrations, consistent with the characteristics of passive diffusion [98]. The nonionic surfactant polysorbate 80 can significantly promote ileal absorption of MA [98].

Biliary excretion of MA involves transporters P-glycoprotein (P-gp) and multidrug resistance-associated protein (MRP). Co-administration of the P-gp inhibitor digoxin or the MRP inhibitor probenecid significantly reduces biliary excretion of the prototype drug, indicating that these efflux transporters participate in the enterohepatic circulation process, which may also be a factor affecting oral absorption [25].

6.1.2. Molecular Mechanism of Low Oral Bioavailability of the Prototype Drug

The oral bioavailability of prototype MA is extremely low (less than 1%), mainly attributed to poor intestinal absorption, difficulty in entering the bloodstream, and rapid metabolic transformation in vivo. To accurately determine trace concentrations of MA in biological matrices, researchers have established a rapid and sensitive liquid chromatography–electrospray ionization mass spectrometry (LC–ESI-MS) quantitative method. This bioanalytical workflow was first fully validated in rat plasma in early pharmacokinetic studies, yielding a linear range of 11–5500 ng/mL ($r^2 = 0.9995$), a lower limit of quantification of 11 ng/mL, and extraction recoveries exceeding 92% [212]. Using paeoniflorin as an internal standard, plasma samples are processed via simple liquid–liquid extraction, chromatographic separation is completed within 6 min on a Shim-pack CLC-ODS column with acetonitrile–water (60:40) containing 0.1% formic acid as the mobile phase, and detection is performed in negative-ion selected ion monitoring mode. The linear range reaches 11–5500 ng/mL, with a lower limit of quantification as low as 11 ng/mL, intra- and inter-day precision RSD < 9.1%, and recovery > 92%. It fully meets the requirements for pharmacokinetic studies of low-exposure drugs [212].

Pharmacokinetic studies in rats based on this highly sensitive method show that the oral bioavailability of pure MA prototype is less than 1% in rats [26,57]. This value refers specifically to unchanged madecassoside monomer, calculated using intravenous administration as the reference for absolute bioavailability. In human studies using oral standardized C. asiatica extracts, prototype MA is almost undetectable in plasma due to extremely low systemic exposure, and only the aglycone metabolite madecassic acid can be reliably quantified [213-215]. The absolute oral bioavailability of prototype MA in humans therefore cannot be accurately determined, and rat data cannot be directly extrapolated to human populations. In Phase I clinical trials conducted in healthy subjects and elderly patients with mild dementia, after oral administration of standardized *C. asiatica* extracts (ECa 233 or CAP), MA prototype is almost undetectable in plasma, and only its metabolite MAA can be detected [213-215]. It should be emphasized that all human data come from oral administration trials of standardized extracts, not pure MA monomer. There are currently no systematic human pharmacokinetic studies on single oral administration of pure MA, so the ADME characteristics of pure MA in humans remain to be further clarified. Rat pharmacokinetic data cannot be directly extrapolated to humans.

6.1.3. Absorption-Enhancing Effects of Bioenhancers (Piperine and Curcumin)

Piperine is an effective bioavailability enhancer that can be combined with MA to increase its systemic exposure. In a beagle dog pharmacokinetic study, when the water-soluble *C. asiatica* extract Centell-S (a water-soluble standardized extract with triterpenoid glycoside content exceeding 80% (*w*/*w*) and MA:AS ratio of 1.5–2.0:1) was administered alone, oral absorption of MA and AS was low. However, when combined with piperine, the maximum plasma concentration (C_{max}) and area under the concentration–time curve (AUC) values of MA increased significantly by approximately 1.5–3.0-fold on day 1, and the exposure of the active metabolite AA also significantly increased on day 7 [104]. Another study also confirmed that the combination of Centell-S and piperine increases plasma levels of MA and AS by approximately 2-fold compared with an equal dose of ECa 233 [216]. In contrast, the addition of curcumin does not significantly improve the

pharmacokinetic parameters of MA [104]. Therefore, piperine can serve as an effective bioenhancer to improve the oral bioavailability of MA by inhibiting drug efflux or metabolism, providing a new strategy for its formulation development.

6.1.4. Pharmacokinetic Differences Between Pure MA and Standardized Extracts

Direct head-to-head comparisons confirm that systemic exposure of MA is markedly higher when delivered as part of a standardized *C. asiatica* extract than as an isolated pure compound, for both intravenous and oral routes. In a well-controlled rat study, intravenous administration of the standardized extract ECa 233 yielded a 2.32-fold higher MA $AUC_{0-\infty}$ compared with an equivalent dose of pure MA, accompanied by reduced apparent clearance and prolonged elimination half-life ($t_{1/2}$). After oral dosing, MA absolute bioavailability nearly doubled in the extract group (1.26% vs. 0.67% for pure MA), with a similarly extended half-life [57].

The primary contributor to this exposure difference is bidirectional interconversion between MA and its structural analog AS in vivo. The conversion efficiency of AS to MA reaches 58.95% (intravenous) and 84.22% (oral), which is higher than the reverse conversion rate [57]. This mutual transformation may form a circulating precursor pool that sustains MA plasma concentrations and extends its in vivo residence time. In addition, other phytochemicals in the extract may further modulate MA disposition, potentially via mild inhibition of intestinal efflux transporters and hepatic metabolic enzymes—a commonly proposed mechanism for altered pharmacokinetics of bioactive compounds in complex botanical extracts—but this remains to be directly verified. Current evidence shows that MA can distribute to target tissues including the brain, stomach, and skin after extract administration [26,57], but whether the extract enhances tissue distribution of MA relative to the pure compound requires further investigation.

This pharmacokinetic discrepancy carries important translational implications. First, pure-compound pharmacokinetic parameters cannot be directly extrapolated to predict MA exposure from standardized extracts, which is a common source of dose-design bias in preclinical-to-clinical translation. Second, the prolonged systemic exposure may partially explain why whole extracts often exhibit greater in vivo efficacy than equivalent doses of isolated monomers in disease models. Clinically, all currently available human pharmacokinetic data are derived from standardized extract formulations [213,215], and no pure-MA human pharmacokinetic data exist to date, representing a notable knowledge gap for monomer-based drug development.

Head-to-head comparative studies between the standardized *C. asiatica* extract ECa 233 and equal doses of pure MA show that plasma exposure of MA in the extract group is significantly higher than in the pure product group, whether administered intravenously or orally. After intravenous injection of 10 mg/kg ECa 233, the area under the concentration–time curve $(AUC)_{0-\infty}$ of MA reaches 77,154.66 ± 42,227.64 μg·h/L, which is 2.32 times that of the equal-dose pure product (5.1 mg/kg, 33,301.72 ± 11,073.39 μg·h/L). Apparent clearance decreases from 0.17 L/h/kg for the pure product to 0.08 L/h/kg, and $t_{1/2}$ extends from 4.99 ± 2.29 h to 6.45 ± 1.38 h [57].

After oral administration of 100 mg/kg ECa 233 (MA content in ECa 233 is approximately 51%, equivalent to approximately 51 mg/kg MA), the C_{max} of MA increases from 1227.47 ± 1283.74 μg/L for the pure product (at an equivalent MA dose, i.e., 51 mg/kg pure MA) to 3013.27 ± 1993.01 μg/L, and $AUC_{0-\infty}$ increases from 2241.44 ± 1104.43 μg·h/L to 4210.00 ± 2240.27 μg·h/L. Absolute bioavailability increases from 0.67% for the pure product to 1.26%, and $t_{1/2}$ extends from 4.33 ± 0.74 h to 7.68 ± 1.96 h ($p < 0.05$) [57].

The core mechanism underlying the improved pharmacokinetic parameters in the extract group is the bidirectional transformation between MA and AS in vivo: AS can be converted to MA via C6 hydroxylation, and the conversion efficiency (58.95% intravenous,

84.22% oral) is significantly higher than the reverse conversion of MA to AS (23.53% intravenous, 68.65% oral). The coexistence of the two saponins in the extract continuously supplements prototype drug concentrations through mutual transformation, prolonging in vivo residence time [57]. In addition, tissue distribution concentrations of MA in target organs such as the brain, stomach, and skin are higher after extract administration than after pure product administration, further enhancing the material basis for its pharmacological activity [57].

6.2. Tissue Distribution and Target Organ Accumulation

6.2.1. Systemic Tissue Distribution Characteristics

After oral or intravenous administration, MA is widely distributed in multiple organs in rats, with relatively high concentrations in tissues such as the liver, kidneys, stomach, and skin. After intragastric administration of MA (100 mg/kg) to rats, the drug is widely distributed in the heart, liver, spleen, lungs, and kidneys, with higher levels in the liver and kidneys than in other tissues [25]. Another study using the standardized extract ECa 233 found that MA is also widely distributed in the brain, stomach, and skin, reaching these tissues 1 h after administration and maintaining for at least 4 h [26]. In beagle dogs, oral administration of Centell-S also shows extensive tissue distribution characteristics of MA and AS [216]. MA is also distributed in synovial tissue, which is related to its anti-arthritis effect [20,217]. This multi-organ distribution characteristic provides a material basis for its pharmacological effects in cardiovascular, neurological, skin, and other systems.

6.2.2. Blood–Brain Barrier Penetration

MA exhibits strong blood–brain barrier (BBB) penetration ability, providing a key material basis for its central nervous system (CNS) effects such as neuroprotection, antidepressant activity, and cognitive improvement. In vitro BBB model studies using primary porcine brain microvascular endothelial cells found that the apparent permeability coefficient (Papp) of MA is 53.31 ± 12.55 × 10^{-6} cm/s. Along with AS (70.61 ± 6.60 × 10^{-6} cm/s) and AA (50.94 ± 10.94 × 10^{-6} cm/s), it is classified as a high BBB permeability compound, with penetration capacity comparable to CNS drugs. Meanwhile, the compound does not produce cytotoxicity or disrupt intercellular tight junctions [50].

Animal experiments further confirm that after oral administration of ECa 233 to rats, MA is rapidly absorbed and distributed to brain tissue, reaching peak levels 15 min after administration [26]. MA can effectively penetrate the BBB and improve neurological function in various neurological disease models such as traumatic brain injury, ischemia–reperfusion injury, Alzheimer's disease, and Parkinson's disease [13,14,218-220].

6.2.3. Skin Tissue Penetration and Retention Patterns

The hydrophilicity of MA limits its transdermal penetration ability, but novel drug delivery systems such as liposomes, transfersomes, and nanoemulsions can significantly increase its skin retention and transdermal efficiency, achieving sustained release effects. For total asiaticoside liposomes prepared via the reverse-phase evaporation method, the skin retention of MA reaches 76.0 μg/cm^2, a 1.56-fold increase compared with the raw material solution, with obvious sustained release effects [101]. MA liposomes prepared by the double emulsion method (average particle size 151 nm) not only exhibit excellent transdermal performance but also significantly promote burn wound healing [103]. When transfersomes are used as carriers, the skin permeability of MA is further improved compared with ordinary liposomes and ethosomes, with an encapsulation efficiency exceeding 68% [47].

Film-forming polymer dispersions allow approximately 5% of MA to accumulate in the skin within 12 h [221]. Smart delivery systems such as pH-responsive chitosan nanogels and temperature-sensitive PEG–PCL–PEG modified liposomes also significantly enhance skin adhesion and retention effects [222,223]. Microemulsion carriers can further improve the topical delivery efficiency of MA; the optimized formulation achieves a 43.2-fold increase in 24 h cumulative skin permeation compared with the control solution, with good skin biocompatibility [224]. These studies provide a pharmaceutical basis for the application of MA in local treatments such as wound repair, scar prevention, and skin anti-inflammation.

6.3. Metabolic Transformation and Major Metabolites

6.3.1. Hepatic Phase I and Phase II Metabolism

MA undergoes extensive metabolism in rats, mainly via phase I metabolic reactions. After oral administration, MA is extensively metabolized before entering the bloodstream: after intragastric administration to rats, MAA, the main metabolite, is predominant in plasma, while prototype drug concentrations are extremely low [25,89]. Fecal analysis shows that MA is mainly excreted in the form of metabolites rather than the prototype [25,26]. In vitro liver microsome experiments indicate that MA exerts non-competitive inhibition on CYP2C19 and CYP3A4 and can act as a mechanism-based inhibitor of these two enzymes, participating in hepatic metabolism [225]. Although no phase II conjugated products of MA have been found in humans or rats, its aglycone MAA can undergo further oxidative transformations in vivo [89].

6.3.2. Gut Microbiota-Mediated Metabolism

The gut microbiota plays a key bidirectional role in the metabolic transformation and pharmacological activity of MA. On the one hand, gut microbiota hydrolyze MA into MAA via glycoside hydrolases, and the latter has been confirmed as the true active form that restores Th17/Treg balance in ulcerative colitis models [86]. A similar microbiota-dependent activation mechanism has also been verified for AS, which is hydrolyzed to asiatic acid by gut microbes and accumulates in colonic tissues to suppress IL-17 signaling and restore intestinal homeostasis [226]. In alcoholic liver disease models, MA intervention can also reverse gut microbiota dysbiosis, increase the abundance of beneficial bacteria such as *Duncaniella* and *Muribaculum*, and reduce pathogenic bacteria such as *Escherichia* and *Klebsiella*, forming a bidirectional interaction between MA and gut microbiota [227]. On the other hand, MA itself can directly regulate intestinal microecological composition. In collagen-induced arthritis (CIA) models, oral MA enriches butyrate-producing bacteria such as Lachnospiraceae, *Butyricicoccus*, and *Faecalibacterium*, increases intestinal butyric acid levels, and thereby induces Treg cell differentiation and promotes IL-10 expression, exerting anti-arthritis effects [84]. This effect depends on intact gut microbiota, and broad-spectrum antibiotics can significantly attenuate its efficacy [84].

It is noteworthy that MA and AS undergo bidirectional transformation in vivo [57], and oral bioavailability is extremely low (less than 1%) [25,26]. This means that after oral administration, MA maintains a high concentration locally in the intestine, while very little prototype drug enters the systemic circulation. Currently, the specific bacterial genera (e.g., *Bacteroides*, *Bifidobacterium*, *Lactobacillus*) and specific glycosidases involved in MA deglycosylation metabolism have not been directly identified, and further clarification through anaerobic isolation and culture, metagenomic screening, and enzymatic characterization is urgently needed [23,78,228].

Piperine, as a bioenhancer, can increase the systemic exposure of MA and its metabolites by inhibiting drug efflux or metabolic enzymes [104], suggesting that combination medication strategies can improve its oral absorption. These metabolic transformation

characteristics constitute an important prerequisite for understanding the "low exposure-high efficacy" pharmacological paradox of MA. The complete downstream effect mechanism of this paradox—how MA exerts pharmacological effects on distal target organs via the gut-host axis—will be systematically discussed in Section 7.1.

6.3.3. In Vivo Bidirectional Transformation Between MA and AS

MA and AS exhibit bidirectional transformation in vivo. After oral administration of the standard extract ECa 233 to rats, plasma concentrations of both are higher than after administration of equal amounts of the pure compounds alone, and two metabolites, MAA and AA, are detected, suggesting that the two prototype compounds may undergo mutual transformation via reactions such as deglycosylation–glycosylation in vivo [57]. In an in vitro liver microsome system, both AS and MA can inhibit CYP2C19 and CYP3A4, indicating similar interaction characteristics with hepatic metabolic enzymes [225].

In a rat model of CIA, after repeated oral administration of MA, differences in pharmacokinetic parameters between arthritic and normal rats gradually decrease, while exposure to the metabolite MAA significantly increases. This suggests that metabolic transformation (including bidirectional transformation) of MA may change under disease conditions [89]. This bidirectional transformation mechanism makes the pharmacodynamic material basis of the two compounds more complex in vivo, which may exert synergistic or additive effects on overall pharmacological activity.

6.3.4. Effects of Disease States on MA Pharmacokinetics

Pharmacokinetic studies in a CIA rat model confirm that inflammatory states significantly alter the in vivo disposition process of MA: after a single oral dose of 40 mg/kg MA, the area under the plasma concentration–time curve ($AUC_{0-\infty}$) in CIA rats is significantly higher than in normal rats, time to peak concentration is prolonged, and apparent clearance is reduced, indicating increased drug absorption and slowed metabolism under inflammatory conditions [89].

After 14 days of repeated administration, differences in pharmacokinetic parameters between CIA and normal rats gradually narrow, but plasma exposure to the main metabolite MAA is significantly higher in CIA rats than in normal rats, suggesting that long-term inflammatory states may upregulate intestinal glycosidase activity and promote the conversion of MA to active aglycones [89]. This finding explains why MA exerts significant therapeutic effects in arthritis models despite extremely low oral bioavailability: pharmacokinetic changes under inflammatory conditions adaptively increase local and systemic exposure of active metabolites, thereby enhancing anti-inflammatory therapeutic effects [89]. Currently, there are no systematic studies on the effects of other disease states such as diabetes, liver fibrosis, and renal insufficiency on MA pharmacokinetics.

6.4. Excretion Pathways and Enterohepatic Circulation

6.4.1. Biliary Excretion

The biliary excretion process of MA is significantly regulated by efflux transporters, among which P-gp and MRP play key roles. After intragastric administration of MA to rats, prototype MA excretion in bile accounts for 7.16% of the administered dose within 0–12 h. When co-administered with the P-gp inhibitor digoxin or the MRP inhibitor probenecid, biliary excretion of prototype MA is significantly reduced, indicating that both transporters participate in the hepatobiliary efflux process of the drug [25]. It should be noted that this conclusion is based on functional inhibition studies; direct transporter assays such as membrane vesicle transport or transfected cell line verification are still lacking, and the specific MRP isoform involved has not been identified. The involvement of P-gp and MRPs should therefore be regarded as a functionally supported inference rather

than definitive confirmation. This finding reveals that MA may be actively transported into bile in the liver, thereby affecting its in vivo clearance rate and oral bioavailability.

6.4.2. Fecal and Urinary Excretion Characteristics

MA and its metabolites are mainly excreted via the fecal route, with urinary excretion accounting for a relatively low proportion. After intragastric administration of MA to rats, prototype MA excretion in bile accounts for 7.16% of the administered dose within 0–12 h [25]. Cumulative excretion of prototype MA in feces reaches 24.68% of the dose within 54 h, after which no prototype MA can be detected. Three stepwise deglycosylated metabolites have been qualitatively identified in feces but have not been quantitatively determined. The fecal fraction includes both unabsorbed drug and biliary-excreted material reentering the intestine via enterohepatic circulation, both of which are metabolized by gut microbiota. Prototype MA excreted via urine accounts for only 0.25% of the dose within 72 h, indicating that fecal excretion is the main clearance pathway [25]. It should be noted that the total recovery of detectable prototype drug is approximately 32% of the administered dose. Due to unquantified metabolites, tissue retention, and incomplete excretion within the observation window, these data cannot support a strict quantitative mass-balance conclusion and only reflect the distribution pattern of major excretion pathways. After administration of the standardized *C. asiatica* extract (ECa 233), MA and AS also mainly exist in feces in the form of corresponding triterpenoid acid metabolites (MAA and AA), further confirming the dominance of fecal excretion [26,57].

6.4.3. Effects of Enterohepatic Circulation on Pharmacokinetic Behavior

MA exhibits obvious enterohepatic circulation, which is one of the important mechanisms explaining its "low bioavailability but long-acting" pharmacological characteristics. After intragastric administration to rats, the plasma prototype drug concentration–time curve shows a typical double-peak feature, which usually suggests that the drug may be secreted into bile and then reabsorbed into the blood circulation. The double-peak pattern alone is not sufficient for definitive confirmation, as biphasic gastrointestinal absorption may also produce a similar profile. The existence of enterohepatic circulation has been directly verified by bile duct cannulation and linked rat model experiments [25], and the double-peak phenomenon serves only as a supportive phenotypic observation.

Enterohepatic circulation can significantly prolong the residence time of drugs in vivo, allowing them to exert continuous effects at low plasma concentrations. This provides an important pharmacokinetic basis for why MA, despite extremely low oral bioavailability (<1% in rats) [26,57], still exerts durable pharmacological effects.

6.5. Key Gaps in Current Pharmacokinetic Research

6.5.1. Systematic Deficiency of Core Pharmacokinetic Parameters for Intravenous Administration

Most intravenous MA studies focus on the overall pharmacokinetic characteristics of standardized *C. asiatica* extracts (e.g., ECa 233 [26,57,229] and Centell-S [216]), and systematic intravenous pharmacokinetic data for pure MA are severely insufficient [25]. Although studies have reported that after intravenous injection of 1.0 mg/kg Centell-S, MA plasma concentrations in beagle dogs range from 1 to 10,000 μg/L [216], and MA can be widely distributed in target organs such as the brain, stomach, and skin and maintained for at least 4 h after intravenous administration in rats [26], there is a lack of linear kinetic verification of pure MA at different doses, as well as accurate determination of core parameters such as volume of distribution, total clearance (CL), $t_{1/2}$, and plasma protein binding rate.

Meanwhile, the metabolic transformation pattern of MA after intravenous administration has not been fully elucidated. The formation rate, $t_{1/2}$, and tissue distribution characteristics of its main metabolite MAA have only been sporadically reported in extract administration studies [57,89], and quantitative metabolic data after pure product administration are lacking. In addition, interspecies differences in intravenous pharmacokinetic parameters among different species (rats, beagle dogs, and non-human primates) are almost unknown, which cannot provide a reliable basis for dose extrapolation in human clinical trials [215]. Furthermore, the exposure–response relationship of MA in target organs (e.g., synovium, retina, and CNS) has not been established [26], limiting its clinical translation in indications such as rheumatoid arthritis and neurodegenerative diseases.

6.5.2. Research Gap in Head-to-Head Comparison of Bioavailability via Different Administration Routes

Bioavailability data for MA via different administration routes are extremely scattered, and there is a lack of head-to-head comparative studies of intravenous, oral, transdermal, local injection, and other routes under the same experimental system [25]. Existing studies show that oral bioavailability of MA is extremely low, and absolute bioavailability of MA after oral administration of ECa 233 in rats is less than 1% [26,229], mainly eliminated via feces in prototype form or metabolized to MAA [25]. However, these data only come from a single extract formulation, and there is no unified standard comparison of the oral bioavailability of pure MA and the degree of improvement by different dosage forms (e.g., solid dispersions and phospholipid complexes) [230].

Although novel drug delivery systems such as transdermal administration [101], microneedle administration [231,232], and nanocarrier delivery [47] have been extensively studied to improve skin exposure of MA, the vast majority of studies only report in vitro transdermal rate or local tissue drug concentration, without calculating absolute bioavailability or synchronously comparing systemic and local exposure with oral and intravenous administration. In addition, studies on the bioavailability of administration routes targeting specific indications, such as intra-articular injection and nasal administration, are almost blank [98], and the metabolite profiles, tissue distribution preferences, and pharmacodynamic correlations of MA under different administration routes remain unclear, which cannot provide a scientific basis for clinical administration route selection [83,84].

6.5.3. Intestinal Lymphatic Transport Pathway Remains Unclear

Currently, no study has systematically elucidated whether oral MA enters the systemic circulation via the intestinal lymphatic system. Existing pharmacokinetic studies only focus on portal vein absorption and hepatic first-pass metabolism pathways, ignoring the intestinal lymphatic transport pathway as a potentially important absorption route for macromolecular amphiphilic saponins. MA has a molecular weight of 975 Da, and its structure combines a hydrophilic sugar chain with a hydrophobic aglycone, exhibiting typical amphiphilic characteristics that meet the physicochemical prerequisites for transport via the intestinal lymphatic system.

Theoretically, the compound may be taken up by intestinal epithelial cells, assembled into chylomicrons, and then absorbed into the systemic circulation via the intestinal lymphatic system, thereby bypassing hepatic first-pass metabolism. This mechanism may partially explain the paradox of extremely low prototype plasma drug concentration after oral administration but still exerting pharmacological effects on distal target organs. However, the above hypothesis remains to be verified (working hypothesis, Level D evidence); no direct in vivo experimental evidence from lymph fluid drug concentration monitoring or lymphatic cannulation models is available to date. Clarifying its lymphatic transport

mechanism has important guiding significance for in-depth understanding of the "low exposure-high efficacy" pharmacological characteristics of this compound and optimizing the design of oral delivery systems (e.g., lipid formulations and lymph-targeting preparations).

6.5.4. Systematic Research Gap in Pharmacokinetic Changes Under Different Disease States

Existing studies have only initially revealed pharmacokinetic changes of MA in a CIA model [89], but the effects of common clinical disease states such as diabetes, liver fibrosis, renal insufficiency, and heart failure on its ADME processes have not been reported. Changes in gut microbiota composition, hepatic drug-metabolizing enzyme activity, transporter expression, and tissue perfusion under different disease states may significantly alter the in vivo disposition process of MA, thereby affecting its efficacy and safety. The lack of pharmacokinetic data under different disease states cannot provide a scientific basis for the formulation of clinical individualized dosage regimens.

6.5.5. Lack of Human Systemic Pharmacokinetic Data

Current pharmacokinetic evidence for MA mainly comes from animal models, and human systemic ADME data remain blank. Completed human Phase I clinical trials all use oral administration of standardized *C. asiatica* extracts (e.g., ECa 233 and CAP). Limited by extremely low oral bioavailability, only aglycone metabolites such as MAA can be detected in the plasma of subjects, and prototype MA has never been detected. Given that prototype MA is almost undetectable in human plasma after oral administration, the absolute oral bioavailability of MA in humans cannot be accurately quantified with current analytical methods, and the <1% value derived from rat studies cannot be directly extrapolated to humans. Therefore, core pharmacokinetic parameters such as human absorption rate, apparent volume of distribution, systemic clearance, and $t_{1/2}$ of the prototype drug remain unreported [213-215]. This is a major knowledge gap that limits clinical dose optimization and translation.

Meanwhile, existing clinical studies have not conducted multi-dose gradient pharmacokinetic investigations, lacking verification of human linear kinetics of MA and its active metabolites at different administration doses. It is impossible to clarify the dose–exposure relationship, nor is it easy to support precise formulation of clinical administration frequency and dose. It should be particularly emphasized that the conclusion that "oral efficacy is mainly mediated by the gut–host axis" has clear limitations. The main evidence for this mechanism comes from models such as rheumatoid arthritis [83,84], pulmonary fibrosis [85], ulcerative colitis [86], and renal fibrosis [233].

However, in the field of neuroprotection, MA can effectively penetrate the BBB [26,50], and intravenous administration also produces significant therapeutic effects in models of cerebral ischemia–reperfusion [218,219], Parkinson's disease [13], and Alzheimer's disease [51]. In cardiovascular indications such as myocardial ischemia–reperfusion injury [16,54] and vascular endothelial protection [234], the direct protective effect of intravenous administration has been fully verified. Therefore, the pharmacodynamic mechanism of MA presents two parallel modes: "intestinal indirect regulation" and "prototype direct action", whose weights vary with indications, administration routes, and metabolic characteristics under disease states, and it is inappropriate to generalize all pharmacological effects with a single mechanism. In addition, key ADME information such as human target organ tissue distribution characteristics, drug-metabolizing enzyme action phenotypes, and excretion ratios in bile/urine/feces remains blank, becoming a core bottleneck restricting the clinical translation and dose optimization of oral MA preparations.

6.6. Drug-Metabolizing Enzyme-Mediated Drug Interactions

6.6.1. Cytochrome P450 (CYP) Enzyme-Mediated Metabolic Interactions

MA exerts in vitro inhibitory effects on some cytochrome P450 enzymes but based on its extremely low in vivo exposure level, the risk of metabolic drug interactions at conventional oral doses is extremely low. In terms of drug interactions, in vitro recombinant enzyme experiments show that MA exerts non-competitive inhibitory effects on CYP2C19 and CYP3A4, with Half maximal inhibitory concentration (IC_{50}) values of 539.04 ± 14.18 μM and 453.32 ± 39.33 μM and Ki values of 109.62 ± 6.14 μM and 456.84 ± 16.43 μM, respectively. It belongs to the mechanism-based inhibitors of CYP2C19 and CYP3A4 [225].

However, the peak plasma concentration (C_{max}) of pure MA (100 mg/kg) after oral administration in rats is only about 1.3 μM, and the C_{max} of the standardized extract ECa 233 is about 3.1 μM [57], both far lower than the above IC_{50} values (a difference of approximately 150–400 times). After oral administration in humans, prototype MA is almost undetectable in plasma [213-215], and the actual exposure level is even lower. Therefore, based on the huge gap between in vitro inhibitory concentrations and actual in vivo plasma exposure levels, the concentration of MA in the systemic circulation at conventional oral doses is far from reaching the threshold required to inhibit CYP2C19 and CYP3A4. This conclusion is limited to oral administration of MA at conventional pharmacological doses. The clinical risk of CYP-mediated metabolic drug interactions appears extremely low based on preclinical data, but no clinical drug–drug interaction (DDI) study has been conducted to confirm this.

Current understanding of structure–activity relationships is mainly based on the comparison of a limited number of natural analogs, lacking systematic site-directed chemical modification and quantitative structure–activity relationship verification. In particular, research on covalent prodrug design for improving oral bioavailability is completely lacking, and there is no effective structural modification strategy to break through the bottleneck of poor oral absorption [24,76]. This makes it impossible to optimize the druggability of MA at the molecular structure level. *C. asiatica* water extract (CAW-R61J) only exerts weak reversible inhibition on CYP1A2, CYP2B6, CYP2C8, CYP2C9, CYP2C19, CYP2D6, and CYP3A4/5 in human liver microsomes (IC_{50} for CYP2C9 is 330 μg/mL), with no time-dependent inhibition and no induction of CYP1A2, CYP2B6, and CYP3A4, suggesting that the overall extract also has a low risk of P450-mediated drug interactions [235].

6.6.2. Transporter-Mediated Drug Interactions

In addition to CYP enzyme-mediated metabolic interactions, as a substrate of P-gp and MRP, the in vivo disposition process of MA may also be affected by transporter inhibitors or substrates, leading to changes in pharmacokinetic properties. As described in Section 6.4.1, after intragastric administration of MA to rats, prototype excretion in bile accounts for 7.16% of the administered dose (0–12 h); when co-administered with the P-gp inhibitor digoxin or the MRP inhibitor probenecid, biliary excretion of prototype MA is significantly reduced, indicating that both efflux transporters participate in the hepatobiliary efflux process of MA [25].

From the perspective of clinical risk of transporter interactions, biliary excretion of MA depends on the functional integrity of P-gp and MRP. Therefore, when MA is combined with the following two types of drugs, transporter-mediated interactions may theoretically occur: (1) P-gp/MRP inhibitors (e.g., digoxin, verapamil, cyclosporine A, and probenecid)—these drugs may competitively inhibit biliary efflux of MA, leading to accumulation of MA and its metabolites in hepatocytes or increased plasma exposure; (2) P-gp/MRP substrates (e.g., digoxin, paclitaxel, and vincristine)—MA may competitively occupy efflux transporters, thereby affecting the in vivo clearance of these substrate drugs.

However, it should be emphasized that the above interaction risks are currently only based on indirect inference from rat biliary excretion experiments [25], and there is no direct clinical research evidence. In the human body, considering that prototype MA is almost undetectable in plasma after oral administration [213,214], the degree of competition between MA and P-gp/MRP substrates in the systemic circulation may be limited; but locally in intestinal epithelial cells and hepatocytes, the concentration of MA may be sufficient to affect the transport function of P-gp/MRP, especially when MA is administered orally at relatively high concentrations.

There are the following key research gaps in this field: (1) whether MA is a substrate of human P-gp and MRP2 (ABCC2) remains to be directly verified—existing evidence comes from rat models [25], and the substrate specificity of human transporters differs from that of rats, which needs to be confirmed via in vitro vesicle experiments with human transporter overexpression or Caco-2 cell bidirectional transport experiments; (2) the substrate characteristics or inhibitory effects of MA on other efflux transporters (e.g., breast cancer resistance protein and bile salt export pump) and uptake transporters (e.g., organic anion transporting polypeptide and organic cation transporter) have not been systematically evaluated; (3) clinical studies have not monitored pharmacokinetic changes when MA is combined with commonly used P-gp substrates/inhibitors (e.g., digoxin and statins).

In summary, at conventional oral doses, MA has an extremely low risk of CYP enzyme-mediated metabolic drug interactions based on its extremely low systemic exposure level [57,225]; however, considering that MA is an efflux substrate of P-gp and MRP [25], there is a theoretical risk of transporter-mediated interactions when combined with P-gp/MRP inhibitors or substrates, which may have clinical significance, especially locally in the intestine and liver. It is recommended that subsequent clinical development of MA formulations (1) include a combination medication cohort with transporter substrates/inhibitors in early clinical studies to monitor changes in blood concentrations of MA and its metabolites; (2) clearly label MA as a P-gp/MRP substrate in the drug insert, warning of potential risks when combined with potent transporter inhibitors; (3) conduct in vitro substrate identification studies on human transporters to clarify the complete transporter interaction profile of MA, providing a basis for clinical medication guidance.

7. Research Challenges and Future Perspectives

On the basis of the full-chain systematic analysis of MA's chemical fundamentals, biosynthetic pathways, green preparation technologies, and pharmacokinetic profiles presented in Chapters 3–6, this chapter identifies four core research bottlenecks limiting the clinical translation of MA and maps out corresponding priority future research directions. This four-dimensional analytical framework of core bottlenecks and corresponding priority directions is schematically illustrated in Figure 7, and each dimension will be discussed and analyzed in detail in the following sections of this chapter.

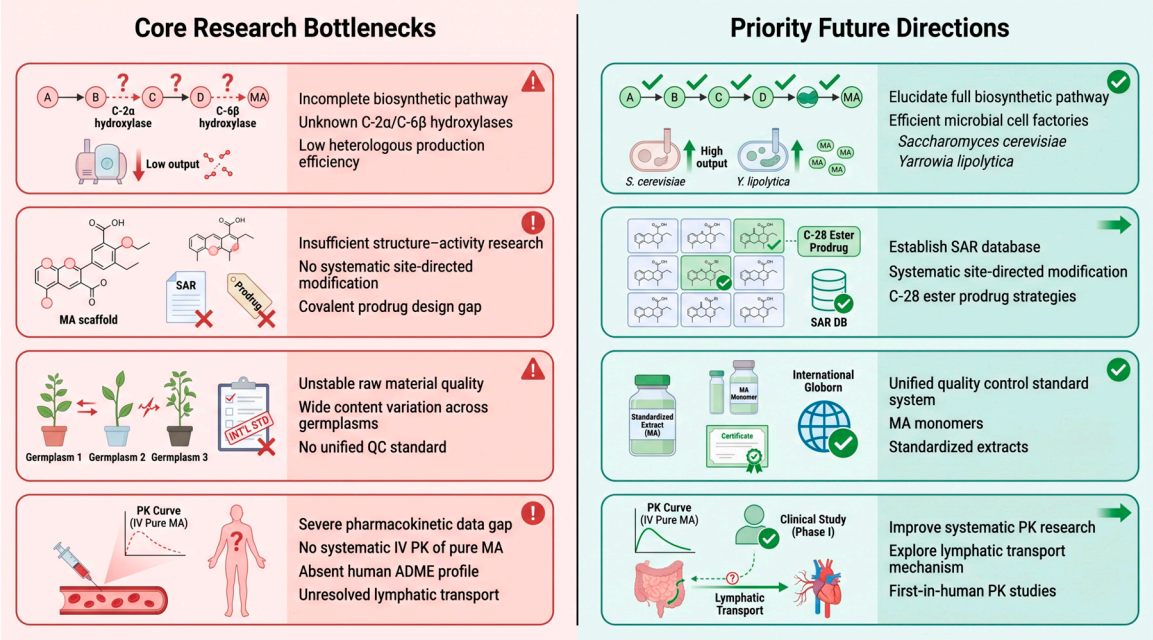


Figure 7. Research challenges and future perspectives for madecassoside (MA): bottlenecks and priority directions. Created with Figdraw(https://www.figdraw.com/#/), Copyright Code: YOPSIccff2. The left panel summarizes four core research bottlenecks in the material basis and druggability field of MA; the right panel presents corresponding priority future research directions.

7.1. Key Challenges in Material Basis and Druggability Research

From the perspective of promoting MA clinical translation, the research on material basis and druggability still faces four core bottlenecks.

7.1.1. Incomplete Biosynthetic Pathway and Restricted Heterologous Production Efficiency

Although the core biosynthetic pathway of MA has been largely elucidated, the enzymes responsible for C-2 α- and C-6 β-hydroxylation remain to be fully identified, and the substrate promiscuity of UDP-glycosyltransferases leads to abundant byproducts in heterologous synthesis. The yield of current microbial cell factories is far from economically viable levels, and plant cell and tissue culture systems also face problems such as high cost and difficulty in scale-up [24,153]. This lag in basic research directly restricts the stable and controllable supply of high-quality MA raw materials.

7.1.2. Insufficient Systematic Structure–Activity Relationship Research and Blank Prodrug Design

Current understanding of structure–activity relationships is mainly based on the comparison of a limited number of natural analogs, lacking systematic site-directed chemical modification and quantitative structure–activity relationship verification. In particular, research on covalent prodrug design for improving oral bioavailability remains largely unexplored, and there is no effective structural modification strategy to break through the bottleneck of poor oral absorption [23,76]. This makes it impossible to optimize the druggability of MA at the molecular structure level based on definitive structure–activity rules.

7.1.3. Unstable Raw Material Quality and Imperfect Quality Control System

MA content in *C. asiatica* from different origins varies widely (0.01–5.67% dry weight), and chemotype diversity is prominent. Even if large-scale cultivation is achieved, batch-to-batch consistency of raw materials remains difficult to guarantee. No internationally

universal quality evaluation system or reference standard has been established, and the quality control indicators are still limited to single component content, lacking indicators related to efficacy and safety such as component ratio and free aglycone impurity limit [152,159]. This brings great uncertainty to the consistency of subsequent pharmacological research and clinical efficacy.

7.1.4. Severe Lack of Systematic Pharmacokinetic Data

Most existing pharmacokinetic studies focus on standardized extracts, and systematic pharmacokinetic data for pure MA are severely insufficient. Core parameters such as volume of distribution, total clearance, and plasma protein binding rate after intravenous administration remain unclear. The intestinal lymphatic transport pathway, pharmacokinetic changes under different disease states, and human systemic ADME data are all lacking [25,26]. These gaps not only restrict the understanding of the in vivo action mode of MA but also cannot provide a reliable basis for clinical dose design.

7.2. Future Research Directions

To address the above challenges, future research in the material basis field should focus on the following priority directions.

7.2.1. Elucidate the Complete Biosynthetic Pathway and Construct Efficient Microbial Cell Factories

Identify the remaining key modifying enzymes (C-2 α-hydroxylase and C-6 β-hydroxylase) through multi-omics mining (transcriptome-metabolome correlation analysis and co-expression network analysis) and protein engineering (directed evolution of P450 enzymes) and clarify the precise regulatory mechanism of sequential glycosylation. On this basis, modularly assemble and optimize the complete biosynthetic pathway in a microbial chassis. Prioritize *Saccharomyces cerevisiae* and *Yarrowia lipolytica* as chassis microorganisms, given their superior native capacity for terpenoid precursor synthesis and well-established genetic manipulation tools. Improve precursor supply and conversion efficiency by overexpressing the rate-limiting enzyme HMGR in the mevalonate pathway and screening highly active enzyme mutants with enhanced substrate specificity. If successfully constructed, robust microbial cell factories could fundamentally solve the problem of unstable raw material supply and achieve controllable production of single components [24,150].

7.2.2. Carry Out Systematic Structure–Activity Relationship Research and Develop Prodrug Modification Strategies

Prepare a series of site-directed modified derivatives through enzymatic catalysis and semi-synthetic chemical methods, establish a quantitative structure–activity relationship (QSAR) database, and clarify the independent contribution of each structural unit to activity and druggability. Focus on developing covalent prodrug strategies for the C-28 carboxyl group and C-6 β-hydroxyl group. Ester prodrugs (pivaloyloxymethyl ester and amino acid ester) at the C-28 position to mask the polar carboxyl group and improve intestinal passive permeability; phosphate prodrugs at the C-6 hydroxyl group to improve aqueous solubility for parenteral formulations. This is the highest-priority direction to break through the bottleneck of MA oral bioavailability from the molecular level [23,76].

7.2.3. Establish an Internationally Unified Quality Control Standard System

Jointly establish an official reference standard collaborative calibration network for MA monomer and representative standardized extracts with multinational drug regulatory authorities. Incorporate the following key indicators into the quality control system

to upgrade from single content compliance to comprehensive evaluation: MA/AS mass ratio and batch-to-batch variation coefficient; free aglycone (MAA, AA) impurity limits and cytotoxicity threshold verification; in vitro simulated bidirectional conversion rate between MA and AS. This will provide institutional guarantees for batch release in large-scale confirmatory clinical trials.

7.2.4. Improve the Systematic Pharmacokinetic Research System

Supplement systematic intravenous pharmacokinetic studies of pure MA across multiple dose levels in rats and beagle dogs to clarify core parameters such as volume of distribution (Vd), total clearance, plasma protein binding rate, and $t_{1/2}$. Explore the intestinal lymphatic transport pathway using lymphatic cannulation rat models and chylomicron uptake assays. Clarify pharmacokinetic changes under different disease states (diabetes, liver fibrosis, and renal insufficiency) and their underlying mechanisms. Carry out first-in-human pharmacokinetic studies using ultra-sensitive LC–MS/MS detection methods and establish the exposure-response relationship of target organs. These studies will provide a necessary pharmacokinetic basis for elucidating the mechanism of action and optimizing clinical dosage regimens.

8. Conclusions

Since its first isolation and structural identification in 1981, research on MA has gradually deepened from basic phytochemical characterization to multi-dimensional fields such as biosynthetic pathway elucidation and preparation technology optimization. Based on the systematic integration of high-quality studies published as of 31 August 2026, this review systematically summarizes the full research chain of MA, covering chemical fundamentals, biosynthesis, green preparation, and pharmacokinetics, providing a complete material-basis framework for subsequent pharmacological and translational research. The following core conclusions can be drawn from this comprehensive analysis:

a. Current evidence supports that the C-6 β-hydroxyl group on the ursane-type aglycone skeleton and the intact linear trisaccharide chain attached at position C-28 are major structural correlates of MA's unique activity profile and functional differentiation from its structural analog AS. This remains a working hypothesis pending validation by site-directed chemical modification studies.
b. Although the core biosynthetic pathway has been largely elucidated, the enzymes responsible for C-2 α- and C-6 β-hydroxylation and the precise regulatory logic of sequential glycosylation remain to be fully resolved—this is the main bottleneck restricting efficient heterologous production.
c. Green extraction technologies represented by UAE, MAE, and DES have been relatively mature, and multiple purification strategies such as macroporous resin, preparative chromatography, and crystallization can meet the preparation needs of different purity grades. However, the quality uniformity of raw materials and the standardization degree of production processes still need to be improved.
d. In rats, the oral absolute bioavailability of prototype MA is less than 1%, with extensive intestinal microbiota metabolism and significant enterohepatic circulation. This extremely low systemic exposure of the parent compound is the core druggability bottleneck and an important prerequisite for understanding its unique in vivo pharmacological mode. Human pharmacokinetic data remain very limited, and rat values cannot be directly extrapolated to clinical populations.

As illustrated in Figure 8, this review systematically sorts out the full-chain evidence of MA from molecular structure to in vivo disposition for the first time and clarifies the core bottlenecks in the fields of biosynthesis, preparation, and druggability. These

material foundations are essential prerequisites for in-depth elucidation of pharmacological mechanisms, optimization of delivery systems, and promotion of clinical translation. In the second part of this series review, we will further focus on the pharmacological effects, clinical translation, and the "low-exposure, high-efficacy" paradox of MA, and systematically elaborate its mechanism of action and translational prospects on the basis of the material basis clarified in this paper.

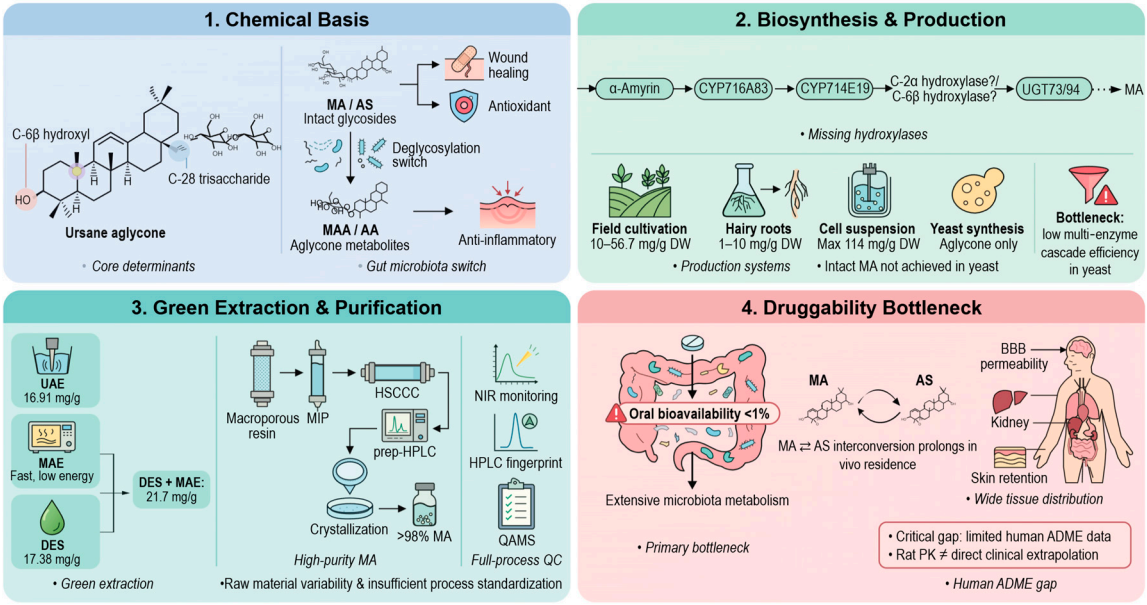


Figure 8. Schematic overview of the full-chain material basis framework for madecassoside (MA) spanning from molecular structure to in vivo disposition.Created with FigDraw (https://www.figdraw.com/#/), Copyright Code: APATWf1d48.

Author Contributions: Writing—Original draft, Y.L. (Yuping Li) and L.Z.; Methodology, Y.L. (Yuping Li); Conceptualization, Y.L. (Yuping Li), L.Z. and S.L.; Writing—Review and editing, M.X., L.Z. and Y.Y.; Data curation, M.X.; Investigation, M.X.; Formal analysis, Y.L. (Yucui Lu); Supervision, L.Z. and X.L.; Funding acquisition, L.Z. All authors have read and agreed to the published version of the manuscript.

Funding: This work was supported by the Doctoral Startup Fund Project of Guizhou University of Traditional Chinese Medicine (2025-01), the Guizhou Provincial Science and Technology Innovation Leading Talents Workstation for Elemental Chinese Materia Medica Innovation and High-Efficiency Utilization (Qian Ke He Ping Tai No. KXJZ [2025]045), the Guizhou Provincial Basic Research Program (QKHJC-MS[2025]163), the Guizhou University of Traditional Chinese Medicine Postgraduate Education Innovation Program Project (YCXKYB2025029), and the Guizhou Provincial Administration of Traditional Chinese Medicine Project (QZYY-2027-031).

Institutional Review Board Statement: Not applicable.

Informed Consent Statement: Not applicable.

Data Availability Statement: No new data were created or analyzed in this study. Data sharing is not applicable to this article.

Acknowledgments: The authors sincerely thank Lichun Zhao for her academic guidance and critical oversight throughout the development of this review. Financial support for this research work is also gratefully acknowledged.

Conflicts of Interest: The authors declare that they have no known competing financial interests or personal relationships that could have appeared to influence the work reported in this paper.

Abbreviations

The following abbreviations are used in this manuscript:

^{1}H NMR	Proton nuclear magnetic resonance
^{13}C NMR	Carbon-13 nuclear magnetic resonance
AA	Asiatic acid
AChE	Acetylcholinesterase
ADME	Absorption, distribution, metabolism and excretion
AS	Asiaticoside
AUC	Area under the concentration-time curve
BBB	Blood–brain barrier
CL	Total clearance
CIA	Collagen-induced arthritis
COSY	Correlation spectroscopy
COX	Cyclooxygenase
CREB	cAMP response element-binding protein
Cmax	Maximum plasma concentration
CYP	Cytochrome P450
DESs	Deep eutectic solvents
DMAPP	Dimethylallyl diphosphate
DMSO	Dimethyl sulfoxide
EAE	Enzyme-assisted extraction
ECa 233	Standardized Centella asiatica extract 233
ERK	Extracellular signal-regulated kinase
FAK	Focal adhesion kinase
FPP	Farnesyl diphosphate
FPS	Farnesyl diphosphate synthase
HDS	4-hydroxy-3-methylbut-2-enyl-diphosphate synthase
HMBC	Heteronuclear multiple bond correlation
HMGR	3-hydroxy-3-methylglutaryl-CoA reductase
HO-1	Heme oxygenase-1
HPLC	High-performance liquid chromatography
HPLC-ELSD	High-performance liquid chromatography coupled with evaporative light scattering detection
HSCCC	High-speed counter-current chromatography
HSQC	Heteronuclear single quantum coherence
HR-ESIMS	High-resolution electrospray ionization mass spectrometry
IC_{50}	Half maximal inhibitory concentration
IPP	Isopentenyl diphosphate
LC–ESI-MS	Liquid chromatography–electrospray ionization mass spectrometry
LC–MS/MS	Liquid chromatography-tandem mass spectrometry
MA	Madecassoside
MAA	Madecassic acid
MAE	Microwave-assisted extraction
MAPK	Mitogen-activated protein kinase
MEP	Methylerythritol phosphate
MeJA	Methyl jasmonate
MIP	Molecularly imprinted polymer
MRP	Multidrug resistance-associated protein
MVA	Mevalonate
NEW	Neutral electrolyzed water
NF-κB	Nuclear factor-κB
NMR	Nuclear magnetic resonance
Nrf2	Nuclear factor erythroid 2-related factor 2

OSC	Oxidosqualene cyclase
P450	Cytochrome P450 monooxygenase
Papp	Apparent permeability coefficient
PEF	Pulsed electric field
P-gp	P-glycoprotein
PK	Pharmacokinetics
prep-HPLC	Preparative high-performance liquid chromatography
QAMS	Quantitative analysis of multicomponents by single marker
RCT	Randomized controlled trial
ROS	Reactive oxygen species
SA	Salicylic acid
SAR	Structure–activity relationship
SQS	Squalene synthase
$t_{1/2}$	Elimination half-life
TLC	Thin-layer chromatography
Treg	Regulatory T cell
UAE	Ultrasound-assisted extraction
UGTs	UDP-glycosyltransferases
Vd	Volume of distribution

References

1. Park, K.S. Pharmacological Effects of *Centella asiatica* on Skin Diseases: Evidence and Possible Mechanisms. *Evid. Based Complement. Alternat. Med.* **2021**, *2021*, 5462633. https://doi.org/10.1155/2021/5462633.
2. Bandopadhyay, S.; Mandal, S.; Ghorai, M.; Jha, N.K.; Kumar, M.; Radha; Ghosh, A.; Proćków, J.; Pérez de la Lastra, J.M.; Dey, A. Therapeutic properties and pharmacological activities of asiaticoside and madecassoside: A review. *J. Cell Mol. Med.* **2023**, *27*, 593–608. https://doi.org/10.1111/jcmm.17635.
3. Tripathy, S.; Verma, D.K.; Thakur, M.; Chakravorty, N.; Singh, S.; Srivastav, P.P. Recent trends in extraction, identification and quantification methods of Centella asiatica phytochemicals with potential applications in food industry and therapeutic relevance: A review. *Food Biosci.* **2022**, *49*, 101864. https://doi.org/10.1016/j.fbio.2022.101864.
4. Bahramsoltani, R.; Farzaei, M.H.; Rahimi, R. Medicinal plants and their natural components as future drugs for the treatment of burn wounds: An integrative review. *Arch. Dermatol. Res.* **2014**, *306*, 601–617. https://doi.org/10.1007/s00403-014-1474-6.
5. Jorge, O.A.; Jorge, A.D. Hepatotoxicity associated with the ingestion of Centella asiatica. *Rev. Esp. Enferm. Dig.* **2005**, *97*, 115–124. https://doi.org/10.4321/s1130-01082005000200006.
6. Luo, S.; Jin, H. Isolation and Identification of Madecassoside from Centella asiatica. *Chin. Tradit. Herb. Drugs* **1981**, *12*, 5–6.
7. Qing-guo, Z.; ZHAOShi-fang. Effects of Asiaticoside and Madecassoside on Cells Proliferation and Synthesis of Collagen Type I and TypeI in Cultured Human SkinFibroblast. *Chin. J. Integr. Tradit. West. Med.* **2003**, *23*, 213–216.
8. Bonté, F.; Dumas, M.; Chaudagne, C.; Meybeck, A. [Comparative activity of asiaticoside and madecassoside on type I and III collagen synthesis by cultured human fibroblasts]. *Ann. Pharm. Fr.* **1995**, *53*, 38–42.
9. Zhai, L.; Meng, X.; Zhang, Y.; Li, L. Action mechanism of madecassoside in anti-inflammatory effects and skin barrier repair. *Fine Chem.* **2026**, *43*, 2294–2302. https://doi.org/10.13550/j.jxhg.20250659.
10. Won, J.H.; Shin, J.S.; Park, H.J.; Jung, H.J.; Koh, D.J.; Jo, B.G.; Lee, J.Y.; Yun, K.; Lee, K.T. Anti-inflammatory effects of madecassic acid via the suppression of NF-kappaB pathway in LPS-induced RAW 264.7 macrophage cells. *Planta Med.* **2010**, *76*, 251–257. https://doi.org/10.1055/s-0029-1186142.
11. Wang, D.; Yu, S.; Wang, Y.; Li, J.; Liu, C.; Lv, G. Madecassoside exerts anti-aging and skin repair effects by activating Nrf2-HO-1 pathway. *China Surfactant Deterg. Cosmet.* **2024**, *54*, 683–690. https://doi.org/10.3969/j.issn.2097-2806.2024.06.009.
12. Liu, L.; Niu, P.; Xiao, B.; Ma, H.; Cui, Y.; Ma, X.; Pei, X.; Liu, Q.; Shan, N.; Xu, T.; et al. Madecassoside attenuated UVB irradiation-induced skin ferroptosis by targeting POR. *Phytomedicine* **2026**, *150*, 157478. https://doi.org/10.1016/j.phymed.2025.157478.
13. Xu, C.L.; Qu, R.; Zhang, J.; Li, L.F.; Ma, S.P. Neuroprotective effects of madecassoside in early stage of Parkinson's disease induced by MPTP in rats. *Fitoterapia* **2013**, *90*, 112–118. https://doi.org/10.1016/j.fitote.2013.07.009.
14. Teerapattarakan, N.; Kamsrijai, U.; Janyou, A.; Hankittichai, P.; Anukanon, S.; Hawiset, T.; Issara, U. Preclinical neuropharmacological effects of Centella asiatica-derived asiaticoside and madecassoside in Alzheimer's disease. *S. Afr. J. Bot.* **2025**, *180*, 171–184. https://doi.org/10.1016/j.sajb.2025.03.014.

15. Liu, M.-R.; Han, T.; Chen, Y.; Qin, L.-P.; Zheng, H.-C.; Rui, Y.-C. Effect of madecassoside on depression behavior of mice and activities of MAO in different brain regions of rats. *J. Integr. Med.* **2004**, *2*, 440–444.
16. Li, G.G.; Bian, G.X.; Ren, J.P.; Wen, L.Q.; Zhang, M.; Lü, Q.J. [Protective effect of madecassoside against reperfusion injury after regional ischemia in rabbit heart in vivo]. *Yao xue xue bao = Acta Pharm. Sin.* **2007**, *42*, 475–480.
17. Wu, F.; Bian, D.; Xia, Y.; Gong, Z.; Tan, Q.; Chen, J.; Dai, Y. Identification of Major Active Ingredients Responsible for Burn Wound Healing of Centella asiatica Herbs. *Evid. Based Complement. Alternat Med.* **2012**, *2012*, 848093. https://doi.org/10.1155/2012/848093.
18. Song, J.; Dai, Y.; Bian, D.F.; Zhang, H.F.; Xu, X.X.; Xia, Y.F.; Gong, Z.N. Madecassoside Induces Apoptosis of Keloid Fibroblasts Via a Mitochondrial-Dependent Pathway. *Drug Dev. Res.* **2011**, *72*, 315–322. https://doi.org/10.1002/ddr.20432.
19. Wu, Z.H.; Li, H.Y.; Li, F.; Jing, M.S.; Ping, H.; Li, L.; Yun, D.Z. Studies on the synergistic anti-inflammatory effects of Ectoin and Madecassoside. *China Surfactant Deterg. Cosmet.* **2021**, *51*, 535–538+545. https://doi.org/10.3969/j.issn.1001-1803.2021.06.010.
20. Yu, W.G.; Shen, Y.; Wu, J.Z.; Gao, Y.B.; Zhang, L.X. Madecassoside impedes invasion of rheumatoid fibroblast-like synoviocyte from adjuvant arthritis rats via inhibition of NF-κB-mediated matrix metalloproteinase-13 expression. *Chin. J. Nat. Med.* **2018**, *16*, 330–338. https://doi.org/10.1016/s1875-5364(18)30064-5.
21. Tan, S.C.; Bhattamisra, S.K.; Chellappan, D.K.; Candasamy, M. Actions and Therapeutic Potential of Madecassoside and Other Major Constituents of Centella asiatica: A Review. *Appl. Sci.* **2021**, *11*, 8475. https://doi.org/10.3390/app11188475.
22. Min, D.H.; Yu, Y.B.; Kim, T.H.; Kim, H.; Lee, S. Pharmacological effects of pentacyclic triterpenoids isolated from Centella asiatica. *Hortic. Environ. Biotechnol.* **2024**, *65*, 189–197. https://doi.org/10.1007/s13580-023-00561-8.
23. Liu, J.; Li, Y.; Yang, C.; Zhao, B. Unraveling the Mechanisms of Madecassoside Derivatives in Wound Healing: Network Pharmacology and Experimental Validation. *Pharmaceuticals* **2025**, *18*, 1292. https://doi.org/10.3390/ph18091292.
24. Zeng, W.; Li, H.; Liu, S.; Luo, Z.; Chen, J.; Zhou, J. Biosynthesis and bioactivities of triterpenoids from Centella asiatica: Challenges and opportunities. *Biotechnol. Adv.* **2025**, *80*, 108541. https://doi.org/10.1016/j.biotechadv.2025.108541.
25. Leng, D.D.; Han, W.J.; Rui, Y.; Dai, Y.; Xia, Y.F. In vivo disposition and metabolism of madecassoside, a major bioactive constituent in *Centella asiatica* (L.) Urb. *J. Ethnopharmacol.* **2013**, *150*, 601–608. https://doi.org/10.1016/j.jep.2013.09.004.
26. Anukunwithaya, T.; Tantisira, M.H.; Tantisira, B.; Khemawoot, P. Pharmacokinetics of a Standardized Extract of Centella asiatica ECa 233 in Rats. *Planta Med.* **2017**, *83*, 710–717. https://doi.org/10.1055/s-0042-122344.
27. James, J.T.; Dubery, I.A. Pentacyclic triterpenoids from the medicinal herb, *Centella asiatica* (L.) Urban. *Molecules* **2009**, *14*, 3922–3941. https://doi.org/10.3390/molecules14103922.
28. Chianese, G.; Masi, F.; Cicia, D.; Ciceri, D.; Arpini, S.; Falzoni, M.; Pagano, E.; Taglialatela-Scafati, O. Isomadecassoside, a New Ursane-Type Triterpene Glycoside from Centella asiatica Leaves, Reduces Nitrite Levels in LPS-Stimulated Macrophages. *Biomolecules* **2021**, *11*, 494. https://doi.org/10.3390/biom11040494.
29. Kai, G.Q.; Pan, J.; Yuan, C.X.; Yuan, Y. Separation of madecassoside and madecassic acid isomers by high performance liquid chromatography using β-cyclodextrin as mobile phase additive. *Bull. Korean Chem. Soc.* **2008**, *29*, 551–554.
30. Kai, G.; Liu, L.; Wang, H. Separation mechanism of oleanane and ursane pentacyclic triterpenoid isomers by coordination chromatography. *Se Pu* **2014**, *32*, 235–241. https://doi.org/10.3724/sp.j.1123.2013.09015.
31. Kim, O.T.; Um, Y.; Jin, M.L.; Kim, J.U.; Hegebarth, D.; Busta, L.; Racovita, R.C.; Jetter, R. A Novel Multifunctional C-23 Oxidase, CYP714E19, is Involved in Asiaticoside Biosynthesis. *Plant Cell Physiol.* **2018**, *59*, 1200–1213. https://doi.org/10.1093/pcp/pcy055.
32. Han, X.Y.; Zhao, J.Y.; Chang, X.C.; Li, Q.Y.; Deng, Z.X.; Yu, Y. Revisiting the transcriptome data of Centella asiatica identified an ester-forming triterpenoid: UDP-glucose 28-O-glucosyltransferase. *Tetrahedron* **2022**, *129*, 133136. https://doi.org/10.1016/j.tet.2022.133136.
33. Han, X.; Zhao, J.; Zhou, H.; Zhou, X.; Deng, Z.; Liu, Z.; Yu, Y. The biosynthesis of asiaticoside and madecassoside reveals tandem duplication-directed evolution of glycoside glycosyltransferases in the Apiales. *Plant Commun.* **2024**, *5*, 101005. https://doi.org/10.1016/j.xplc.2024.101005.
34. Krzyzostan, M.; Nowak, I. Triterpenoid saponins derived from *Centella asiatica* L. *Przem. Chem.* **2024**, *103*, 128. https://doi.org/10.15199/62.2024.4.3.
35. Jia, G.; Lu, X. Enrichment and purification of madecassoside and asiaticoside from Centella asiatica extracts with macroporous resins. *J. Chromatogr. A* **2008**, *1193*, 136–141. https://doi.org/10.1016/j.chroma.2008.04.024.
36. Fu, J.; Zheng, X.F.; Lu, X.Y. Crystallization of Asiaticoside from Total Triterpenoid Saponins of Centella Asiatica in a Methanol plus Water System. *Ind. Eng. Chem. Res.* **2014**, *53*, 14022–14027. https://doi.org/10.1021/ie502657h.
37. Inamdar, P.K.; Yeole, R.D.; Srivastava, M.M.; deSouza, N.J. Stability study of the active constituents in the Centella asiatica extract formulations. *Drug Dev. Ind. Pharm.* **1996**, *22*, 211–216. https://doi.org/10.3109/03639049609058563.

38. Apichartsrangkoon, A.; Chattong, U.; Chunthanom, P. Comparison of bioactive components in fresh, pressurized, pasteurized and sterilized pennywort (*Centella asiatica* L.) juices. *High Press. Res.* **2012**, *32*, 309–315. https://doi.org/10.1080/08957959.2012.665051.
39. Kwon, H.J.; Park, J.H.; Kim, G.T.; Park, Y.D. Determination of madecassoside and asiaticoside contents of C. asiatica leaf and C. asiatica-containing ointment and dentifrice by HPLC-coupled pulsed amperometric detection. *Microchem. J.* **2011**, *98*, 115–120. https://doi.org/10.1016/j.microc.2010.12.008.
40. Gajbhiye, N.A.; Makasana, J.; Saha, A.; Patel, I.; Jat, R.S. LC-ESI-MS/MS Method for Simultaneous Determination of Triterpenoid Glycosides and Aglycones in *Centella asiatica* L. *Chromatographia* **2016**, *79*, 727–739. https://doi.org/10.1007/s10337-016-3089-x.
41. Zheng, X.F.; Fu, J.; Lu, X.Y. Solubility and Induction Period Study of Asiaticoside and Madecassoside in a Methanol plus Water Mixture. *J. Chem. Eng. Data* **2012**, *57*, 3258–3263. https://doi.org/10.1021/je300883a.
42. Kunjumon, R.; Johnson, A.J.; Remadevi, R.K.S.; Baby, S. Assessment of major centelloside ratios in Centella asiatica accessions grown under identical ecological conditions, bioconversion clues and identification of elite lines. *Sci. Rep.* **2022**, *12*, 8177. https://doi.org/10.1038/s41598-022-12077-9.
43. Zhan, X.-Y.; Zhang, Y.-L.; Zhang, J.-Y.; Tan, P.; Ji, J.-J.; Dong, J.; Liu, Y.-G. Fragmentation Pathways and Patterns of Asiaticoside and MadecassosideinESI-MS. *J. Chin. Mass Spectrom. Soc.* **2015**, *36*, 289–295. https://doi.org/10.7538/zpxb.youxian.2015.0015.
44. Xing, H.B.; Su, B.G.; Wang, Y.Y.; Yang, Y.W.; Ren, Q.L.; Xiao, W.G.; Lu, X.Y. Separation and Determination of Asiaticoside, Asiaticoside-B and Madecassoside in Centella asiatica Total Triterpenoid Saponins by HPLC. *J. Liq. Chromatogr. Relat. Technol.* **2009**, *32*, 1891–1900. https://doi.org/10.1080/10826070903091597.
45. Wang, C.; Zhao, Y.; Yang, R.; Liu, H. Simultaneous analysis of five triterpenes in Centella asiatica by high performance liquid chromatography with cyclodextrins as the mobile phase additives. *Sci. Rep.* **2020**, *10*, 18577. https://doi.org/10.1038/s41598-020-75554-z.
46. Bai, J.H.; Zhao, R.H.; Lv, Q.J.; Ren, J.P.; Ma, X.M. Studythe antihypertensive effect and the characteristics ofm adecassoside. *Pharmacol. Clin. Chin. Mater. Medica* **2010**, *26*, 18–21. https://doi.org/10.13412/j.cnki.zyyl.2010.01.031.
47. Lapmanee, S.; Bunwatcharaphansakun, P.; Phongsupa, W.; Namdee, K.; Suttisintong, K.; Asawapirom, U.; Ruktanonchai, U.; Wongchitrat, P.; Bhubhanil, S.; Maitarad, P.; et al. Transfersomal delivery of Centella asiatica promotes efficient excision wound healing in rats. *Drug Deliv.* **2025**, *32*, 2563649. https://doi.org/10.1080/10717544.2025.2563649.
48. Jung, E.; Lee, J.A.; Shin, S.; Roh, K.B.; Kim, J.H.; Park, D. Madecassoside inhibits melanin synthesis by blocking ultraviolet-induced inflammation. *Molecules* **2013**, *18*, 15724–15736. https://doi.org/10.3390/molecules181215724.
49. Hossain, M.L.; Rahman, M.A.; Siddika, A.; Adnan, M.H.; Rahman, H.; Diba, F.; Hasan, M.Z.; Asaduzzaman, S.M. Burn and Wound Healing Using Radiation Sterilized Human Amniotic Membrane andCentella asiaticaDerived Gel: A Review. *Regen. Eng. Transl. Med.* **2020**, *6*, 347–357. https://doi.org/10.1007/s40883-019-00122-5.
50. Hanapi, N.A.; Mohamad Arshad, A.S.; Abdullah, J.M.; Tengku Muhammad, T.S.; Yusof, S.R. Blood-Brain Barrier Permeability of Asiaticoside, Madecassoside and Asiatic Acid in Porcine Brain Endothelial Cell Model. *J. Pharm. Sci.* **2021**, *110*, 698–706. https://doi.org/10.1016/j.xphs.2020.09.015.
51. Du, B.; Zhang, Z.; Li, N. Madecassoside prevents Aβ(25-35)-induced inflammatory responses and autophagy in neuronal cells through the class III PI3K/Beclin-1/Bcl-2 pathway. *Int. Immunopharmacol.* **2014**, *20*, 221–228. https://doi.org/10.1016/j.intimp.2014.02.036.
52. Chen, W.; Zhao, Y.; Hu, L.; Dong, D.; Zeng, Y.; Su, T.; Shen, Y.; Liu, Y.; Zhao, Q.; Jiang, C.; et al. Madecassoside alleviates Clostridioides difficile infection by targeting ASC to inhibit inflammasome activation. *Int. Immunopharmacol.* **2025**, *165*, 115440. https://doi.org/10.1016/j.intimp.2025.115440.
53. Cao, W.; Li, X.Q.; Zhang, X.N.; Hou, Y.; Zeng, A.G.; Xie, Y.H.; Wang, S.W. Madecassoside suppresses LPS-induced TNF-alpha production in cardiomyocytes through inhibition of ERK, p38, and NF-kappaB activity. *Int. Immunopharmacol.* **2010**, *10*, 723–729. https://doi.org/10.1016/j.intimp.2010.03.015.
54. Bian, G.X.; Li, G.G.; Yang, Y.; Liu, R.T.; Ren, J.P.; Wen, L.Q.; Guo, S.M.; Lu, Q.J. Madecassoside reduces ischemia-reperfusion injury on regional ischemia induced heart infarction in rat. *Biol. Pharm. Bull.* **2008**, *31*, 458–463. https://doi.org/10.1248/bpb.31.458.
55. Lee, Y.; Choi, H.K.; N'Deh K, P.U.; Choi, Y.J.; Fan, M.; Kim, E.K.; Chung, K.H.; An, A.J.H. Inhibitory Effect of Centella asiatica Extract on DNCB-Induced Atopic Dermatitis in HaCaT Cells and BALB/c Mice. *Nutrients* **2020**, *12*, 411. https://doi.org/10.3390/nu12020411.
56. Jaisi, A.; Prema; Madla, S.; Lee, Y.E.; Septama, A.; Morita, H. Investigation of HIV-1 Viral Protein R Inhibitory Activities of Twelve Thai Medicinal Plants and Their Commercially Available Major Constituents. *Chem. Biodivers.* **2021**, *18*, e2100540. https://doi.org/10.1002/cbdv.202100540.

57. Hengjumrut, P.; Anukunwithaya, T.; Tantisira, M.H.; Tantisira, B.; Khemawoot, P. Comparative pharmacokinetics between madecassoside and asiaticoside presented in a standardised extract of Centella asiatica, ECa 233 and their respective pure compound given separately in rats. *Xenobiotica Fate Foreign Compd. Biol. Syst.* **2018**, *48*, 18–27. https://doi.org/10.1080/00498254.2016.1273562.
58. Hafiz, Z.Z.; Amin, M.M.; Johari James, R.M.; Teh, L.K.; Salleh, M.Z.; Adenan, M.I. Inhibitory Effects of Raw-Extract Centella asiatica (RECA) on Acetylcholinesterase, Inflammations, and Oxidative Stress Activities via In Vitro and In Vivo. *Molecules* **2020**, *25*, 892. https://doi.org/10.3390/molecules25040892.
59. Jusril, N.A.; Muhamad Juhari, A.N.N.; Abu Bakar, S.I.; Md Saad, W.M.; Adenan, M.I. Combining In Silico and In Vitro Studies to Evaluate the Acetylcholinesterase Inhibitory Profile of Different Accessions and the Biomarker Triterpenes of Centella asiatica. *Molecules* **2020**, *25*, 3353. https://doi.org/10.3390/molecules25153353.
60. Guo, Q.; Li, Q.; Liang, W.; Zhang, Y.; Jiang, C.; Zhang, Y.; Tan, J.; Zhao, H. Asiatic acid and madecassic acid cause cardiotoxicity via inflammation and production of excessive reactive oxygen species in zebrafish. *J. Appl. Toxicol. JAT* **2024**, *44*, 1028–1039. https://doi.org/10.1002/jat.4602.
61. Sahu, N.P.; Roy, S.K.; Mahato, S.B. Spectroscopic determination of structures of triterpenoid trisaccharides from centella-asiatica. *Phytochemistry* **1989**, *28*, 2852–2854. https://doi.org/10.1016/s0031-9422(00)98106-8.
62. Wang, Y.Y.; Xiao, W.G.; Xing, H.B.; Yang, Y.W.; Ren, Q.L.; Lv, X.Y. Separation and Preparation of Asiaticoside, Madecassoside, and Asiaticoside-B. *J. Chem. Eng. Chin. Univ.* **2010**, *24*, 376–381.
63. Wang, C.H.; Yang, R.M.; Zhang, B.H.; Qiao, R.X.; Liu, H.J. The apparent formation constants of asiatic acid and its derivatives existing inCentella asiaticawith cyclodextrins by HPLC. *J. Incl. Phenom. Macrocycl. Chem.* **2020**, *98*, 261–270. https://doi.org/10.1007/s10847-020-01026-6.
64. Pan, J.; Kai, G.Q.; Yuan, C.X.; Jin, R.S. Separation and determination of the structural isomers of madecassoside by HPLC using β-Cyclodextrin as mobile phase additive. *Chromatographia* **2007**, *66*, 121–123. https://doi.org/10.1365/s10337-007-0243-5.
65. Kai, G.Q.; Chen, Y.; Wang, Y.; Yan, Q.H. Separation Rule of Oleanane and Ursane Pentacyclic Triterpenoids Isomers from Nature Plants by Coordination Chromatography. *J. Chromatogr. Sci.* **2014**, *52*, 532–538. https://doi.org/10.1093/chromsci/bmt132.
66. Reuk-Ngam, P.; Chimnoi, N.; Maliwong, J.; Reuk-Ngam, N.; Patnin, S.; Limsiriwong, M.; Techasakul, S.; Kanchanapoom, T. Enhanced selectivity in RP-HPLC-UV separation of structurally similar pentacyclic triterpenes in Centella asiatica using β-cyclodextrin as a mobile-phase additive. *J. Pharm. Biomed. Anal.* **2027**, *282*, 117722. https://doi.org/10.1016/j.jpba.2026.117722.
67. Suntivich, R.; Malaphong, C.; Chaiyen, P.; Leartsakulpanich, U.; Maenpuen, S. Validated HPLC Method for Simultaneous Quantification of Six Triterpenes with Isomer Separation in Commercial Centella asiatica Products. *ACS Omega* **2026**, *11*, 44336–44350. https://doi.org/10.1021/acsomega.6c04697.
68. Chen, M.; Liu, W.Q.; Miao, S.; Zhou, H.; Lan, L.; Li, W.T.; Ji, S. Simultaneous determination of three constituents in Centella asiatica total glucosides and their two preparations by QAMS. *Chin. Tradit. Pat. Med.* **2020**, *42*, 2280–2284. https://doi.org/10.3969/j.issn.1001-1528.2020.09.007.
69. Duan, Y.; Guo, Z.J.; Zhao, Z.M.; Yang, D.P.; Xu, X.J. Establishment of chemical fingerprint and determination of main active ingredients in Centellae Herba by HPLC combined with multivariate chemometrics analysis. *Sep. Sci. Plus* **2024**, *7*, 12. https://doi.org/10.1002/sscp.202400021.
70. Azerad, R. Chemical structures, production and enzymatic transformations of sapogenins and saponins from *Centella asiatica* (L.) Urban. *Fitoterapia* **2016**, *114*, 168–187. https://doi.org/10.1016/j.fitote.2016.07.011.
71. Matsuda, H.; Morikawa, T.; Ueda, H.; Yoshikawa, M. Medicinal foodstuffs. XXVII. Saponin constituents of gotu kola (2): Structures of new ursane- and oleanane-type triterpene oligoglycosides, centellasaponins B, C, and D, from Centella asiatica cultivated in Sri Lanka. *Chem. Pharm. Bull.* **2001**, *49*, 1368–1371. https://doi.org/10.1248/cpb.49.1368.
72. Maliwong, J.; Reuk-ngam, P.; Chimnoi, N.; Srisuk, P.; Techasakul, S.; Ruchirawat, S.; Kanchanapoom, T. Phytochemical profiling of Thai Centella asiatica: Identification of new polyacetylene glucosides and analytical considerations in HPLC-UV analysis of triterpenoids. *J. Nat. Med.* **2026**, *80*, 404–417. https://doi.org/10.1007/s11418-025-01972-w.
73. Rumalla, C.S.; Ali, Z.; Weerasooriya, A.D.; Smillie, T.J.; Khan, I.A. Two new triterpene glycosides from Centella asiatica. *Planta Med.* **2010**, *76*, 1018–1021. https://doi.org/10.1055/s-0029-1240864.
74. Wu, Z.W.; Li, W.B.; Zhou, J.; Liu, X.; Wang, L.; Chen, B.; Wang, M.K.; Ji, L.; Hu, W.C.; Li, F. Oleanane- and Ursane-Type Triterpene Saponins from Centella asiatica Exhibit Neuroprotective Effects. *J. Agric. Food Chem.* **2020**, *68*, 6977–6986. https://doi.org/10.1021/acs.jafc.0c01476.
75. Jiang, Z.Y.; Zhang, X.M.; Zhou, J.; Chen, J.J. New triterpenoid glycosides from Centella asiatica. *Helv. Chim. Acta* **2005**, *88*, 297–303. https://doi.org/10.1002/hlca.200590011.

76. Lv, L.; Wei, S.M.; Lin, H.F.; Ma, L.J.; Ying, K.; Mao, Y.M. Effects of asiaticoside and madecassiside on synthesis of collagen in cultured human skin fibroblast. *China Surfactant Deterg. Cosmet.* **2002**, *36*, 23–25. https://doi.org/10.13218/j.cnki.csdc.2002.06.007.
77. Nalinratana, N.; Meksuriyen, D.; Ongpipattanakul, B. Differences in Neuritogenic Activity and Signaling Activation of Madecassoside, Asiaticoside, and Their Aglycones in Neuro-2a cells. *Planta Med.* **2018**, *84*, 1165–1173. https://doi.org/10.1055/a-0619-5710.
78. Zhou, P.; Yang, P.; Zhang, K.; Guo, H.; Du, J.; Huang, L.; Jin, D.; Alolga, R.N.; Wang, H.; Li, J.; et al. Discovery and engineering of the asiaticoside, madecassoside and asiaticoside B biosynthetic pathway. *Plant Physiol. Biochem.* **2025**, *223*, 109864. https://doi.org/10.1016/j.plaphy.2025.109864.
79. Fan, Y.; Chen, R.; Tang, L.; Fu, P.; Zhou, J.; Chen, X. Synthesis and Characterization of Molecularly Imprinted Polymers for the Selective Extraction of Triterpenoid Saponin From Centella asiatica Crude Extracts. *J. Sep. Sci.* **2025**, *48*, e70128. https://doi.org/10.1002/jssc.70128.
80. Chockchowwat, W.; Hannongbua, S.; Saparpakorn, P. Role of triterpenoid derivatives from Centella asiatica as quantum chemical calculations. *J. Biomol. Struct. Dyn.* **2026**, *44*, 5279–5295. https://doi.org/10.1080/07391102.2025.2578225.
81. Qi, L.Y.; Zhang, B.L. Effects of Asiaticoside and Madecassoside on Proliferation of Human Embryonic Skin Fibroblasts in vitro. *Natl. Med. Front. China* **2011**, *6*, 1–2.
82. Ramos-Morales, E.; Lyons, L.; de la Fuente, G.; Braganca, R.; Newbold, C.J. Not all saponins have a greater antiprotozoal activity than their related sapogenins. *FEMS Microbiol. Lett.* **2019**, *366*, fnz144. https://doi.org/10.1093/femsle/fnz144.
83. Wang, T.; Wei, Z.; Dou, Y.; Yang, Y.; Leng, D.; Kong, L.; Dai, Y.; Xia, Y. Intestinal interleukin-10 mobilization as a contributor to the anti-arthritis effect of orally administered madecassoside: A unique action mode of saponin compounds with poor bioavailability. *Biochem. Pharmacol.* **2015**, *94*, 30–38. https://doi.org/10.1016/j.bcp.2015.01.004.
84. Qiao, S.; Lian, X.; Yue, M.; Zhang, Q.; Wei, Z.; Chen, L.; Xia, Y.; Dai, Y. Regulation of gut microbiota substantially contributes to the induction of intestinal Treg cells and consequent anti-arthritis effect of madecassoside. *Int. Immunopharmacol.* **2020**, *89*, 107047. https://doi.org/10.1016/j.intimp.2020.107047.
85. Xia, Y.; Xia, Y.F.; Lv, Q.; Yue, M.F.; Qiao, S.M.; Yang, Y.; Wei, Z.F.; Dai, Y. Madecassoside ameliorates bleomycin-induced pulmonary fibrosis in mice through promoting the generation of hepatocyte growth factor via PPAR-γ in colon. *Br. J. Pharmacol.* **2016**, *173*, 1219–1235. https://doi.org/10.1111/bph.13421.
86. Xu, X.; Wang, Y.; Wei, Z.; Wei, W.; Zhao, P.; Tong, B.; Xia, Y.; Dai, Y. Madecassic acid, the contributor to the anti-colitis effect of madecassoside, enhances the shift of Th17 toward Treg cells via the PPARγ/AMPK/ACC1 pathway. *Cell Death Dis.* **2017**, *8*, e2723. https://doi.org/10.1038/cddis.2017.150.
87. Changsan, N.; Srichana, T.; Atipairin, A.; Sawatdee, S. Wound healing efficacy of a polymeric spray film solution containing Centella asiatica leaf extract on acute wounds. *J. Wound Care* **2023**, *32*, S22–S32. https://doi.org/10.12968/jowc.2023.32.Sup12.S22.
88. Qian, S.; Yu, L.S.; Zhou, H.; Zeng, S. Simultaneous determination of madecassoside,asiaticoside and their aglycones in *Centella asiatica* (L.) urban extracts by RP-HPLC. *J. Zhejiang Univ. (Med. Sci.)* **2014**, *43*, 135–140. https://doi.org/10.3785/j.issn.1008-9292.2014.03.002.
89. Wang, T.; Leng, D.D.; Gao, F.F.; Jiang, C.J.; Xia, Y.F.; Dai, Y. A LC-ESI-MS method for the simultaneous determination of madecassoside and its metabolite madecassic acid in rat plasma: Comparison pharmacokinetics in normal and collagen-induced arthritic rats. *Chin. J. Nat. Med.* **2014**, *12*, 943–951. https://doi.org/10.1016/s1875-5364(14)60138-2.
90. Singkhorn, S.; Tantisira, M.H.; Tanasawet, S.; Hutamekalin, P.; Wongtawatchai, T.; Sukketsiri, W. Induction of keratinocyte migration by ECa 233 is mediated through FAK/Akt, ERK, and p38 MAPK signaling. *Phytother. Res.* **2018**, *32*, 1397–1403. https://doi.org/10.1002/ptr.6075.
91. Li, W.; Yu, Q.; Shen, Z.; Zhang, Z.; Li, C.; Li, C.; Wu, Z.; Zhang, W. Effects of a cream containing madecassoside, 5% panthenol, and copper-zinc-manganese on improving postlaser resurfacing wound healing: A split-face, randomized trial. *Dermatol. Ther.* **2020**, *33*, e13533. https://doi.org/10.1111/dth.13533.
92. Gregoriou, S.; Vakirlis, E.; Zafiriou, E. Efficacy and tolerance of a prebiotic, panthenol-containing repair balm in patients diagnosed with skin lesions requiring regenerative care. *Eur. J. Dermatol. EJD* **2025**, *35*, 118–126. https://doi.org/10.1684/ejd.2025.4855.
93. Gao, M.; Gao, N.; Wang, L.; Yao, T.; Jing, H.; Liu, H.; Gao, L. Evaluation of the Efficacy and Safety of a Panthenol-Enriched Mask for Skin Barrier Recovery After Facial Laser Treatment: Results of a Double-Blind Randomized Controlled Study. *J. Cosmet. Dermatol.* **2025**, *24*, e70223. https://doi.org/10.1111/jocd.70223.

94. Chotritthirong, Y.; Chulikhit, Y.; Daodee, S.; Boonyarat, C.; Maneenet, J.; Khamphukdee, C.; Kwankhao, P.; Pitiporn, S.; Monthakantirat, O. Possible Mechanisms for the Prevention of Anxiety and Depressive-Like Behavior in a Chronic Mild Stress Mouse Model by the Thai Herbal Medicine with Nelumbo nucifera, Centella asiatica, and Piper nigrum. *Rev. Bras. Farmacogn.-Braz. J. Pharmacogn.* **2023**, *33*, 756–767. https://doi.org/10.1007/s43450-023-00401-x.
95. Chan, L.P.; Liang, C.H. Natural Plant-Based Rejuvenating Compositions: Human Study on Astragalus membranaceus and Centella asiatica Saponins for Skin Health. *Cosmetics* **2025**, *12*, 131. https://doi.org/10.3390/cosmetics12040131.
96. Zhang, S.S.; Cai, J.H.; Wan, J.Y.; Liu, H.L.; Liu, Y.J. Inhibitory effect of madecassoside on LPS-stimulated microglia. *Chin. J. Pathophysiol.* **2015**, *31*, 428–434. https://doi.org/10.3969/j.issn.1000-4718.2015.03.008.
97. Moqbel, S.A.A.; He, Y.; Xu, L.; Ma, C.; Ran, J.; Xu, K.; Wu, L. Rat Chondrocyte Inflammation and Osteoarthritis Are Ameliorated by Madecassoside. *Oxid. Med. Cell Longev.* **2020**, *2020*, 7540197. https://doi.org/10.1155/2020/7540197.
98. Xia, L.W.; Dong, P.L. Absorption mechanism of madecassoside in intestinal of rats. *Drug Eval. Res.* **2011**, *34*, 22–25.
99. Kim, O.T.; Jin, M.L.; Lee, D.Y.; Jetter, R. Characterization of the Asiatic Acid Glucosyltransferase, UGT73AH1, Involved in Asiaticoside Biosynthesis in *Centella asiatica* (L.) Urban. *Int. J. Mol. Sci.* **2017**, *18*, 2630. https://doi.org/10.3390/ijms18122630.
100. de Costa, F.; Barber, C.J.S.; Kim, Y.B.; Reed, D.W.; Zhang, H.; Fett-Neto, A.G.; Covello, P.S. Molecular cloning of an ester-forming triterpenoid: UDP-glucose 28-O-glucosyltransferase involved in saponin biosynthesis from the medicinal plant Centella asiatica. *Plant Sci. Int. J. Exp. Plant Biol.* **2017**, *262*, 9–17. https://doi.org/10.1016/j.plantsci.2017.05.009.
101. Yan, D.; Jiang, M.Y.; Wang, Y.H.; Zhang, L.; Zhang, C.H.; Yang, R.P. Preparation and in vitro transdermal diffusion characteristics of Centella asiatica total glucosides liposome. *Chin. Tradit. Herbal Drugs* **2018**, *49*, 2041–2048. https://doi.org/10.7501/j.issn.0253-2670.2018.09.010.
102. Zhai, L.J.; Yuan, H.X.; Wang, W.; Song, G.J.; Ling, X.; Li, L. Preparation and Structural Characterization of Madecassoside-Phospholipid Complexes. *Chem. World* **2026**, *67*, 148–158. https://doi.org/10.19500/j.cnki.0367-6358.20240605.
103. Li, Z.; Liu, M.; Wang, H.; Du, S. Increased cutaneous wound healing effect of biodegradable liposomes containing madecassoside: Preparation optimization, in vitro dermal permeation, and in vivo bioevaluation. *Int. J. Nanomed.* **2016**, *11*, 2995–3007. https://doi.org/10.2147/ijn.S105035.
104. Boonyarattanasoonthorn, T.; Kongratanapasert, T.; Maiuthed, A.; Hamlin, R.; Kijtawornrat, A.; Khemawoot, P. Bioenhancing effects of piperine and curcumin on triterpenoid pharmacokinetics and neurodegenerative metabolomes from Centella asiatica extract in beagle dogs. *Sci. Rep.* **2022**, *12*, 20789. https://doi.org/10.1038/s41598-022-24935-7.
105. Yang, J.Q.; Zhu, H.; Zhang, Q.B.; Dai, Y.H.; Yao, Q.Y.; Nie, X.Q. Charting the Phytopharmacological Frontier of Centella asiatica: A Quarter-Century Bibliometric Atlas Unlocking Translational Potential. *Rev. Bras. Farmacogn.-Braz. J. Pharmacogn.* **2026**, *36*, 23. https://doi.org/10.1007/s43450-026-00747-y.
106. Pumkathin, S.; Hanlumyuang, Y.; Wattanathana, W.; Laomettachit, T.; Liangruksa, M. Investigating pharmacokinetic profiles of Centella asiatica using machine learning and PBPK modelling. *J. Biopharm. Stat.* **2025**, *35*, 588–603. https://doi.org/10.1080/10543406.2024.2358797.
107. Kim, O.T.; Kim, S.H.; Ohyama, K.; Muranaka, T.; Choi, Y.E.; Lee, H.Y.; Kim, M.Y.; Hwang, B. Upregulation of phytosterol and triterpene biosynthesis in Centella asiatica hairy roots overexpressed ginseng farnesyl diphosphate synthase. *Plant Cell Rep.* **2010**, *29*, 403–411. https://doi.org/10.1007/s00299-010-0831-y.
108. Kim, O.T.; Seong, N.S.; Kim, M.Y.; Hwang, B. Isolation and characterization of squalene synthase cDNA from *Centella asiatica* (L.) Urban. *J. Plant Biol.* **2005**, *48*, 263–269. https://doi.org/10.1007/bf03030521.
109. Song, W.L.; Chen, B.Z.; Feng, L.; Chen, G.; He, S.M.; Hao, B.; Zhang, G.H.; Dong, Y.; Yang, S.C. Telomere-to-telomere genome assembly and 3D chromatin architecture of Centella asiatica insight into evolution and genetic basis of triterpenoid saponin biosynthesis. *Hortic. Res.* **2025**, *12*, uhaf037. https://doi.org/10.1093/hr/uhaf037.
110. Kim, O.T.; Kim, M.Y.; Huh, S.M.; Bai, D.G.; Ahn, J.C.; Hwang, B. Cloning of a cDNA probably encoding oxidosqualene cyclase associated with asiaticoside biosynthesis from *Centella asiatica* (L.) Urban. *Plant Cell Rep.* **2005**, *24*, 304–311. https://doi.org/10.1007/s00299-005-0927-y.
111. Kim, O.T.; Bang, K.H.; Shin, Y.S.; Lee, M.J.; Jung, S.J.; Hyun, D.Y.; Kim, Y.C.; Seong, N.S.; Cha, S.W.; Hwang, B. Enhanced production of asiaticoside from hairy root cultures of *Centella asiatica* (L.) Urban elicited by methyl jasmonate. *Plant Cell Rep.* **2007**, *26*, 1941–1949. https://doi.org/10.1007/s00299-007-0400-1.
112. Bonfill, M.; Mangas, S.; Moyano, E.; Cusido, R.M.; Palazón, J. Production of centellosides and phytosterols in cell suspension cultures of *Centella asiatica*. *Plant Cell Tissue Organ Cult.* **2011**, *104*, 61–67. https://doi.org/10.1007/s11240-010-9804-7.

113. Hernandez-Vazquez, L.; Bonfill, M.; Moyano, E.; Cusido, R.M.; Navarro-Ocaña, A.; Palazon, J. Conversion of α-amyrin into centellosides by plant cell cultures of Centella asiatica. *Biotechnol. Lett.* **2010**, *32*, 315–319. https://doi.org/10.1007/s10529-009-0143-x.
114. de Costa, F.; Barber, C.J.; Reed, D.W.; Covello, P.S. From Plant Extract to a cDNA Encoding a Glucosyltransferase Candidate: Proteomics and Transcriptomics as Tools to Help Elucidate Saponin Biosynthesis in Centella asiatica. *Methods Mol. Biol.* **2016**, *1405*, 43–48. https://doi.org/10.1007/978-1-4939-3393-8_5.
115. James, J.T.; Tugizimana, F.; Steenkamp, P.A.; Dubery, I.A. Metabolomic analysis of methyl jasmonate-induced triterpenoid production in the medicinal herb *Centella asiatica* (L.) urban. *Molecules* **2013**, *18*, 4267–4281. https://doi.org/10.3390/molecules18044267.
116. Yoo, N.H.; Kim, O.T.; Kim, J.B.; Kim, S.H.; Kim, Y.C.; Bang, K.H.; Hyun, D.Y.; Cha, S.W.; Kim, M.Y.; Hwang, B. Enhancement of centelloside production from cultured plants of Centella asiatica by combination of thidiazuron and methyl jasmonate. *Plant Biotechnol. Rep.* **2011**, *5*, 283–287. https://doi.org/10.1007/s11816-011-0173-4.
117. Alcalde, M.A.; Cusido, R.M.; Moyano, E.; Palazon, J.; Bonfill, M. Metabolic gene expression and centelloside production in elicited Centella asiatica hairy root cultures. *Ind. Crop. Prod.* **2022**, *184*, 114988. https://doi.org/10.1016/j.indcrop.2022.114988.
118. Ranjith, G.P.; Jisha, S.; Hemanthakumar, A.S.; Saji, C.V.; Shenoi, R.A.; Sabu, K.K. Impact of potential stimulants on asiaticoside and madecassoside levels and expression of triterpenoid-related genes in axenic shoot cultures of *Centella asiatica* (L.) Urb. *Phytochemistry* **2021**, *186*, 112735. https://doi.org/10.1016/j.phytochem.2021.112735.
119. Loc, N.H.; Giang, N.T.; Huy, N.D.; Lan, T.T.P. Accumulation of madecassoside—A major component of centelloside—In centella (*Centella asiatica* (L.) Urban) cells elicited by salicylic acid. *Period. Biol.* **2017**, *119*, 81–85. https://doi.org/10.18054/pb.v119i1.4386.
120. Chungloo, D.; Theerawitaya, C.; Tisarum, R.; Praseartkul, P.; Pipatsitee, P.; Himanshu, S.K.; Datta, A.; Cha-um, S. Mitigation of water-deficit stress in Indian pennywort (*Centella asiatica*) using exogenous foliar application of methyl jasmonate. *J. Plant Biochem. Biotechnol.* **2025**, *34*, 893–905. https://doi.org/10.1007/s13562-025-00995-4.
121. Kim, O.T.; Um, Y.; Jin, M.L.; Kim, Y.C.; Bang, K.H.; Hyun, D.Y.; Lee, H.S.; Lee, Y. Analysis of expressed sequence tags from *Centella asiatica* (L.) Urban hairy roots elicited by methyl jasmonate to discover genes related to cytochrome P450s and glucosyltransferases. *Plant Biotechnol. Rep.* **2014**, *8*, 211–220. https://doi.org/10.1007/s11816-013-0311-2.
122. Sritongkul, J.; Srilaong, V.; Uthairatanakij, A.; Kanlayanarat, S.; Chalermglin, P. Effect of Light Intensity on Chemical Composition of Asiatic Pennywort (*Centella asiatica* L. Urban). In Proceedings of the Asia Pacific Symposium on Assuring Quality and Safety of Agri-Foods, Bangkok, Thailand, 25 June 2009; pp. 87–93.
123. Srithongkul, J.; Kanlayanarat, S.; Srilaong, V.; Uthairatanakij, A.; Chalermglin, P. Effects of light intensity on growth and accumulation of triterpenoids in three accessions of Asiatic pennywort (*Centella asiatica* (L.) Urb.). *J. Food Agric. Environ.* **2011**, *9*, 360–363.
124. Shin, Y.K.; Lee, J.G. Effects of light intensity and temperature on growth and secondary metabolite production of Centella asiatica in vertical farms. *Hortic. Environ. Biotechnol.* **2025**, *66*, 1437–1456. https://doi.org/10.1007/s13580-025-00755-2.
125. Harakotr, B.; Charoensup, L.; Rithichai, P.; Jirakiattikul, Y. Growth, Triterpene Glycosides, and Antioxidant Activities of Centella asiatica L. Urban Grown in a Controlled Environment with Different Nutrient Solution Formulations and LED Light Intensities. *Horticulturae* **2024**, *10*, 71. https://doi.org/10.3390/horticulturae10010071.
126. Buraphaka, H.; Kitisripanya, T.; Yusakul, G.; Putalun, W. Impact of UV-A and UV-C radiation to enhance triterpenoids and related gene expression in triterpenoid pathway of Centella asiatica postharvest. *Ind. Crop. Prod.* **2024**, *214*, 118579. https://doi.org/10.1016/j.indcrop.2024.118579.
127. Shin, Y.K.; Song, J.W.; Lee, J.G. Controlled Application of Far-Red Light to Improve Growth and Bioactive Compound Yield in Centella asiatica. *Horticulturae* **2025**, *11*, 728. https://doi.org/10.3390/horticulturae11070728.
128. Soun-udom, M.; Garcia, M.R.; Oliveira, A.P.; Andrade, P.B.; Vajrodaya, S.; Duangsrisai, S.; Gomes, N.G.M. LED light treatments enhance neuroprotective properties and differentially impact phenolic compounds and triterpenoid content in Gotu Kola (*Centella asiatica* (L.) Urb.). *Curr. Plant Biol.* **2024**, *40*, 100386. https://doi.org/10.1016/j.cpb.2024.100386.
129. Pipatsitee, P.; Praseartkul, P.; Theerawitaya, C.; Taota, K.; Tisarum, R.; Chungloo, D.; Singh, H.P.; Cha-um, S. Impact of Temperature on Centelloside Content, Growth Characters, Physio-morphological Adaptations, and Biochemical Changes in Indian Pennywort (*Centella asiatica*). *J. Plant Growth Regul.* **2023**, *42*, 6776–6787. https://doi.org/10.1007/s00344-023-11022-y.
130. Rohini, M.R.; Rao, V.K.; Sreenu, B.; Smitha, G.R.; Sridhar, G. Enhanced metabolite yield with compensatory biomass reduction revealed by moisture stress induction in *Centella asiatica* (L.). *J. Hortic. Sci.-India* **2024**, *19*, 5. https://doi.org/10.24154/jhs.v19i1.2460.

131. Praseartkul, P.; Tisarum, R.; Sotesaritkul, T.; Chungloo, D.; Theerawitaya, C.; Taota, K.; Singh, H.P.; Cha-um, S. Arbuscular Mycorrhizal Fungi Improve Tolerance to Water Deficit in Indian Pennywort (*Centella asiatica*) by Promoting Physio-morphological and Biochemical Adaptations. *Agric. Res.* **2024**, *13*, 718–732. https://doi.org/10.1007/s40003-024-00725-7.
132. Pipatsitee, P.; Praseartkul, P.; Theerawitaya, C.; Taota, K.; Tisarum, R.; Singh, H.P.; Cha-um, S. Exogenous NaCl salt elicitor improves centelloside content and physio-morphological adaptations in indian pennywort (*Centella asiatica*). *J. Plant Biochem. Biotechnol.* **2022**, *31*, 777–787. https://doi.org/10.1007/s13562-021-00716-7.
133. Mukherjee, S.; Biswas, D.; Ghosh, B. Carbohydrates acting as enhancers of secondary metabolites synthesis in in vitro cultures of *Centella asiatica* (L.) Urb. *Plant Cell Tissue Organ. Cult.* **2025**, *161*, 16. https://doi.org/10.1007/s11240-025-03055-w.
134. Alqahtani, A.; Tongkao-on, W.; Li, K.M.; Razmovski-Naumovski, V.; Chan, K.; Li, G.Q. Seasonal Variation of Triterpenes and Phenolic Compounds in Australian *Centella asiatica* (L.) Urb. *Phytochem. Anal.* **2015**, *26*, 436–443. https://doi.org/10.1002/pca.2578.
135. Mohapatra, P.; Ray, A.; Jena, S.; Nayak, S.; Mohanty, S. Influence of various drying methods on physicochemical characteristics, antioxidant activity, and bioactive compounds in Centella asiatica L. leaves: A comparative study. *Biotechnologia* **2022**, *103*, 235–247. https://doi.org/10.5114/bta.2022.118666.
136. Ryu, D.; Cho, J.Y.; Hamayun, M.; Lee, S.H.; Cha, H.H.; Jung, J.H.; Kim, H.Y. Optimizing drying time for *Centella asiatica* (L.) Urban: Metabolomic insights into dehydration effects on primary and secondary metabolites. *Chem. Biol. Technol. Agric.* **2025**, *12*, 26. https://doi.org/10.1186/s40538-025-00745-7.
137. Plengmuankhae, W.; Tantitadapitak, C. Low temperature and water dehydration increase the levels of asiaticoside and madecassoside in *Centella asiatica* (L.) Urban. *S. Afr. J. Bot.* **2015**, *97*, 196–203. https://doi.org/10.1016/j.sajb.2015.01.013.
138. Kim, M.C.; Jo, H.; Lim, K.; Kim, I.; Kim, H.B.; Kim, S.; Nho, Y.; Kim, M.; Kim, H.; Baek, C.; et al. Metabolome Shift in Centella asiatica Leaves Induced by the Novel Plant Growth-Promoting Rhizobacterium, Priestia megaterium HyangYak-01. *Plants* **2024**, *13*, 2636. https://doi.org/10.3390/plants13182636.
139. Amprayn, K.O.; Chanchula, N.; Piriyapattarakit, A.; Sunthorn, N.; Premrit, S. Influence of Varieties and Elicitors on Biomass and Bioactive Compound Yield of *Centella asiatica* Growing in Pathumthani. *Int. Trans. J. Eng. Manag. Appl. Sci. Technol.* **2022**, *13*, 10. https://doi.org/10.14456/itjemast.2022.124.
140. Gupta, S.; Bhatt, P.; Chaturvedi, P. Determination and quantification of asiaticoside in endophytic fungus from *Centella asiatica* (L.) Urban. *World J. Microbiol. Biotechnol.* **2018**, *34*, 111. https://doi.org/10.1007/s11274-018-2493-9.
141. Ryu, D.H.; Cho, J.Y.; Jung, J.W.; Cha, H.H.; Kim, H.M.; Park, N.Y.; Ahn, N.H.; Lee, J.H.; Park, J.S.; Lee, D.S.; et al. Lactic Acid Bacteria-Mediated Fermentation Drives Metabolic Remodeling of *Centella asiatica* (L.) Urb. toward Acidic Triterpenoids with Neuroinflammation-Related Bioactivity. *ACS Omega* **2026**, *11*, 28607–28618. https://doi.org/10.1021/acsomega.6c00935.
142. Zhang, Y.; Wei, H.; Chen, X.; Lei, R.; Yin, C.; Huang, Y.; Liu, Y.; Zhou, Q.; Liu, Y.; Shu, P.; et al. CaOSC5-CaOSC7 module governs metabolic partitioning between asiaticoside and asiaticoside B in Centella asiatica. *Plant Physiol. Biochem.* **2025**, *229*, 110411. https://doi.org/10.1016/j.plaphy.2025.110411.
143. Hassanabad, M.K.; Mirjalili, M.H.; Mohajeri, M. Boosted centellosides production in Gotu kola (*Centella asiatica*) transgenic hairy roots elicited by gold and zinc nanoparticles. *Ind. Crop. Prod.* **2025**, *227*, 120796. https://doi.org/10.1016/j.indcrop.2025.120796.
144. Gallego, A.; Ramirez-Estrada, K.; Vidal-Limon, H.R.; Hidalgo, D.; Lalaleo, L.; Kayani, W.K.; Cusido, R.M.; Palazon, J. Biotechnological production of centellosides in cell cultures of *Centella asiatica* (L) Urban. *Eng. Life Sci.* **2014**, *14*, 633–642. https://doi.org/10.1002/elsc.201300164.
145. Mandal, S.; Das, T.; Nandy, S.; Ghorai, M.; Saha, S.C.; Gopalakrishnan, A.V.; Kumar, M.; Radha; Ghosh, A.; Mukerjee, N.; et al. Biotechnological and endophytic-mediated production of centellosides in Centella asiatica. *Appl. Microbiol. Biotechnol.* **2023**, *107*, 473–489. https://doi.org/10.1007/s00253-022-12316-z.
146. Baek, S.; Han, J.E.; Ho, T.T.; Park, S.Y. Development of Hairy Root Cultures for Biomass and Triterpenoid Production in Centella asiatica. *Plants* **2022**, *11*, 148. https://doi.org/10.3390/plants11020148.
147. Aziz, Z.A.; Davey, M.R.; Power, J.B.; Anthony, P.; Smith, R.M.; Lowe, K.C. Production of asiaticoside and madecassoside in Centella asiatica in vitro and in vivo. *Biol. Plant.* **2007**, *51*, 34–42. https://doi.org/10.1007/s10535-007-0008-x.
148. Baek, S.; Ho, T.T.; Lee, H.; Jung, G.; Kim, Y.E.; Jeong, C.S.; Park, S.Y. Enhanced biosynthesis of triterpenoids in Centella asiatica hairy root culture by precursor feeding and elicitation. *Plant Biotechnol. Rep.* **2020**, *14*, 45–53. https://doi.org/10.1007/s11816-019-00573-w.
149. Karimi, Z.; Mirjalili, M.H.; Esmaeili, H. Long-term hairy root culture of *Centella asiatica* (Apiaceae) for enhanced biomass accumulation and centellosides production. *Ind. Crop. Prod.* **2025**, *234*, 121494. https://doi.org/10.1016/j.indcrop.2025.121494.

150. Arnesen, J.A.; Belmonte Del Ama, A.; Jayachandran, S.; Dahlin, J.; Rago, D.; Andersen, A.J.C.; Borodina, I. Engineering of Yarrowia lipolytica for the production of plant triterpenoids: Asiatic, madecassic, and arjunolic acids. *Metab. Eng. Commun.* **2022**, *14*, e00197. https://doi.org/10.1016/j.mec.2022.e00197.
151. Zhou, P.N.; Chen, B.; Shu, C.J.; Li, Z.H.; Chen, P.; Fei, C.H. [Research progress on biosynthesis of triterpenoids in Centella asiatica]. *Zhongguo Zhong yao za zhi = Zhongguo zhongyao zazhi = China J. Chin. Mater. Medica* **2025**, *50*, 609–619. https://doi.org/10.19540/j.cnki.cjcmm.20241114.103.
152. Thomas, M.T.; Kurup, R.; Johnson, A.J.; Chandrika, S.P.; Mathew, P.J.; Dan, M.; Baby, S. Elite genotypes/chemotypes, with high contents of madecassoside and asiaticoside, from sixty accessions of Centella asiatica of south India and the Andaman Islands: For cultivation and utility in cosmetic and herbal drug applications. *Ind. Crop. Prod.* **2010**, *32*, 545–550. https://doi.org/10.1016/j.indcrop.2010.07.003.
153. Prasad, A.; Dhawan, S.S.; Mathur, A.K.; Prakash, O.; Gupta, M.M.; Verma, R.K.; Lal, R.K.; Mathur, A. Morphological, chemical and molecular characterization of Centella asiatica germplasms for commercial cultivation in the Indo-Gangetic plains. *Nat. Prod. Commun.* **2014**, *9*, 779–784.
154. Deng, Q.; Ma, X.Y.; Dai, J.X.; Li, G.S.; Wu, F.; Liu, Z.M.; Wang, Z.B.; Li, M. Development of EST-SSR markers in Centella asiatica: Insights into genetic diversity and terpenoid biosynthesis. *Sci. Hortic.* **2026**, *360*, 114820. https://doi.org/10.1016/j.scienta.2026.114820.
155. Srivastava, S.; Verma, S.; Gupta, A.; Rajan, S.; Rawat, A.K.S. Studies on Chemotypic Variation in *Centella asiatica* (L.) Urban from Nilgiri Range of India. *JPC-J. Planar Chromatogr.-Mod. TLC* **2014**, *27*, 454–459. https://doi.org/10.1556/jpc.27.2014.6.9.
156. Kunjumon, R.; Johnson, A.J.; Remadevi, R.K.S.; Baby, S. Influence of ecological factors on asiaticoside and madecassoside contents and biomass production in Centella asiatica from its natural habitats in south India. *Ind. Crop. Prod.* **2022**, *189*, 115809. https://doi.org/10.1016/j.indcrop.2022.115809.
157. Rafi, M.; Handayani, F.; Darusman, L.K.; Rohaeti, E.; Wahyu, Y.; Sulistiyani; Honda, K.; Putri, S.P. A combination of simultaneous quantification of four triterpenes and fingerprint analysis using HPLC for rapid identification of Centella asiatica from its related plants and classification based on cultivation ages. *Ind. Crop. Prod.* **2018**, *122*, 93–97. https://doi.org/10.1016/j.indcrop.2018.05.062.
158. Yang, F.; You, Q.; Ma, Y.; Sun, Z.; Li, L.; Li, W. Evaluation of Centella asiatica Germplasm Resources in Yunnan, China, Based on Phenotypic Traits, SSR Markers, and Chemical Profiling. *Plants* **2026**, *15*, 2345. https://doi.org/10.3390/plants15152345.
159. Singh, J.; Sangwan, R.S.; Gupta, S.; Saxena, S.; Sangwan, N.S. Profiling of triterpenoid saponin content variation in different chemotypic accessions of *Centella asiatica* L. *Plant Genet. Resour.-Charact. Util.* **2015**, *13*, 176–179. https://doi.org/10.1017/s1479262114000860.
160. Prasad, A.; Yadav, K.S.; Yadav, N.P.; Mathur, A.; Sreedhar, R.V.; Lal, R.K.; Mathur, A.K. Biomass and centellosides production in two elite Centella asiatica germplasms from India in response to seasonal variation. *Ind. Crop. Prod.* **2016**, *94*, 711–720. https://doi.org/10.1016/j.indcrop.2016.09.022.
161. Noppradit, B.; Klinnawee, L.; Leeratiwong, C.; Praparatana, R.; Puttarak, P. *Centella asiatica* (L.) Urb. and Hydrocotyle umbellata L. identification and quality assessment: A methodology comparison. *Phytochem. Anal.* **2024**, *35*, 1383–1398. https://doi.org/10.1002/pca.3371.
162. Maulidiani; Abas, F.; Khatib, A.; Shaari, K.; Lajis, N.H. Chemical characterization and antioxidant activity of three medicinal Apiaceae species. *Ind. Crop. Prod.* **2014**, *55*, 238–247. https://doi.org/10.1016/j.indcrop.2014.02.013.
163. H, M.; Khatib, A.; Shaari, K.; Abas, F.; Shitan, M.; Kneer, R.; Neto, V.; Lajis, N.H. Discrimination of three Pegaga (Centella) varieties and determination of growth-lighting effects on metabolites content based on the chemometry of 1H nuclear magnetic resonance spectroscopy. *J. Agric. Food Chem.* **2012**, *60*, 410–417. https://doi.org/10.1021/jf200270y.
164. Chua, L.S.; Abdullah, F.I.; Sari, E. Comparing herbal phytochemicals in different Pegaga: Centella asiatica and Hydrocotyle verticillata. *Future Food* **2022**, *10*, 13. https://doi.org/10.17170/kobra-202204136015.
165. Prasad, A.; Pragadheesh, V.S.; Mathur, A.; Srivastava, N.K.; Singh, M.; Mathur, A.K. Growth and centelloside production in hydroponically established medicinal plant-*Centella asiatica* (L.). *Ind. Crop. Prod.* **2012**, *35*, 309–312. https://doi.org/10.1016/j.indcrop.2011.06.020.
166. Jat, R.S.; Gajbhiye, N.A. Secondary Metabolites Production Influenced with Soil Fertility and Irrigation in Medicinal Plant; Mandukaparni (*Centella asiatica* L.). *Natl. Acad. Sci. Lett.-India* **2017**, *40*, 87–90. https://doi.org/10.1007/s40009-016-0531-4.
167. Razzaq, W.; Mazzitelli, J.B.; Fabiano Tixier, A.S.; Vian, M.A. Centella asiatica as a Model Biomass for Sustainable Production of Biochemicals via Green Extraction and Purification Technologies: A Comprehensive Field-to-Market Review. *Molecules* **2026**, *31*, 526. https://doi.org/10.3390/molecules31030526.

168. Nurlaily, A.; Baitee, A.R.N.; Musalmah, M. Comparative Antioxidant and Anti-inflammatory Activity of Different Extracts of *Centella asiatica* (L.) Urban and Its Active Compounds, Asiaticoside and Madecassoside. *Med. Health-Kuala Lumpur* **2012**, *7*, 62–72.
169. Yingngam, B.; Chiangsom, A.; Brantner, A. Modeling and optimization of microwave-assisted extraction of pentacyclic triterpenes from Centella asiatica leaves using response surface methodology. *Ind. Crop. Prod.* **2020**, *147*, 112231. https://doi.org/10.1016/j.indcrop.2020.112231.
170. Thong-On, W.; Pathomwichaiwat, T.; Boonsith, S.; Koo-Amornpattana, W.; Prathanturarug, S. Green extraction optimization of triterpenoid glycoside-enriched extract from *Centella asiatica* (L.) Urban using response surface methodology (RSM). *Sci. Rep.* **2021**, *11*, 22026. https://doi.org/10.1038/s41598-021-01602-x.
171. Shen, Y.; Liu, A.L.; Ye, M.D.; Wang, L.; Chen, J.H.; Wang, X.R.; Han, C. Analysis of Biologically Active Constituents in Centella asiatica by Microwave-Assisted Extraction Combined with LC-MS. *Chromatographia* **2009**, *70*, 431–438. https://doi.org/10.1365/s10337-009-1152-6.
172. Sabaragamuwa, R.; Perera, C.O. Total Triterpenes, Polyphenols, Flavonoids, and Antioxidant Activity of Bioactive Phytochemicals of Centella asiatica by Different Extraction Techniques. *Foods* **2023**, *12*, 3972. https://doi.org/10.3390/foods12213972.
173. Hiranpradith, V.; Therdthai, N.; Soontrunnarudrungsri, A.; Rungsuriyawiboon, O. Optimisation of Ultrasound-Assisted Extraction of Total Phenolics and Flavonoids Content from Centella asiatica. *Foods* **2025**, *14*, 291. https://doi.org/10.3390/foods14020291.
174. Khursheed, T.; Khalil, A.A.; Akhtar, M.N.; Khalid, A.; Tariq, M.R.; Alsulami, T.; Mugabi, R.; Nayik, G.A. Ultrasound-assisted solvent extraction of phenolics, flavonoids, and major triterpenoids from Centella asiatica leaves: A comparative study. *Ultrason. Sonochem.* **2024**, *111*, 107091. https://doi.org/10.1016/j.ultsonch.2024.107091.
175. Monton, C.; Settharaksa, S.; Luprasong, C.; Songsak, T. An optimization approach of dynamic maceration of Centella asiatica to obtain the highest content of four centelloids by response surface methodology. *Rev. Bras. Farmacogn.-Braz. J. Pharmacogn.* **2019**, *29*, 254–261. https://doi.org/10.1016/j.bjp.2019.01.001.
176. Rafamantanana, M.H.; Rozet, E.; Raoelison, G.E.; Cheuk, K.; Ratsimamanga, S.U.; Hubert, P.; Quetin-Leclercq, J. An improved HPLC-UV method for the simultaneous quantification of triterpenic glycosides and aglycones in leaves of *Centella asiatica* (L.) Urb (APIACEAE). *J. Chromatogr. B Analyt Technol. Biomed Life Sci.* **2009**, *877*, 2396–2402. https://doi.org/10.1016/j.jchromb.2009.03.018.
177. Jang, Y.; Lee, N.; Jo, W.J.; Choi, J.; Ha, S.H. Analytical evaluation of the effects of hydrogen-bond acceptor (HBA) structure and deep eutectic solvent (DES) composition on terpenoid extraction efficiency from Centella asiatica. *Anal. Sci. Technol.* **2025**, *38*, 383–391. https://doi.org/10.5806/ast.2025.38.6.383.
178. Choi, J.; Kim, S.J.; Ha, S.H. Effect of Water Content in Deep Eutectic Solvent (DES)-based Extraction on the Extraction Efficiency of Phytochemicals. *Korean Chem. Eng. Res.* **2025**, *63*, 350–354. https://doi.org/10.9713/kcer.2025.63.3.105125.
179. Phaisan, S.; Makkliang, F.; Putalun, W.; Sakamoto, S.; Yusakul, G. Development of a colorless Centella asiatica (L.) Urb. extract using a natural deep eutectic solvent (NADES) and microwave-assisted extraction (MAE) optimized by response surface methodology. *RSC Adv.* **2021**, *11*, 8741–8750. https://doi.org/10.1039/d0ra09934a.
180. Choi, J.; Jeon, Y.; Ha, S.H. Effect of deep eutectic solvent (DES) on the extraction of asiaticoside and madecassoside from Centella asiatica. *Anal. Sci. Technol.* **2023**, *36*, 128–134. https://doi.org/10.5806/ast.2023.36.3.128.
181. Lee, Q.; Xu, L.; Zhou, W.; Yu, M.; Zeng, D.; Zhu, S. Non-thermal preparation, component identification, and in vivo antioxidant activity mechanism exploration of polyphenols and derivatives from *Ananas comosus* (L.) flesh. *Food Res. Int.* **2025**, *222*, 117735. https://doi.org/10.1016/j.foodres.2025.117735.
182. Komaikul, J.; Ruangdachsuwan, S.; Juntarapornchai, S.; Wanlayaporn, D.; Ketsuwan, K.; Masrinoul, P.; Yoksan, S.; Puthavathana, P.; Kitisripanya, T. Effectiveness of neutral electrolyzed water in inactivating HCoV-OC43 and SARS-CoV-2 on the surfaces of plastic and the medicinal plant *Centella asiatica* (L.) urban. *Heliyon* **2022**, *8*, e10294. https://doi.org/10.1016/j.heliyon.2022.e10294.
183. Rosli, S.Z.; Adzahan, N.M.; Karim, R.; Ab Rashid, N.K.M. Effect of Acidic Electrolysed Water and Pulsed Light Technology on the Sensory, Morphology and Bioactive Compounds of Pennywort (*Centella asiatica* L.) Leaves. *Molecules* **2023**, *28*, 311. https://doi.org/10.3390/molecules28010311.
184. Zhang, D.D.; Nie, X.Q.; Zhang, H.; Zhao, J.F.; Shi, X.J.; Yang, J.W. Study on the Extraction Technology of Asiaticosides from *Centella asiatica* by Ultrasonic-enzyme Method. *China Pharm.* **2017**, *28*, 1816–1819. https://doi.org/10.6039/j.issn.1001-0408.2017.13.25.

185. Chysirichote, T.; Aroonsong, S. pH-driven mechanistic segmentation and enzyme-assisted deconstruction for the selective release of centelloids from Centella asiatica. *Food Biosci.* **2026**, *79*, 108866. https://doi.org/10.1016/j.fbio.2026.108866.
186. Rachpirom, M.; Pichayakorn, W.; Puttarak, P. Preparation, development, and scale-up of standardized pentacyclic triterpenoid-rich extract from *Centella asiatica* (L.) Urb. and study of its wound healing activity. *Heliyon* **2023**, *9*, e17807. https://doi.org/10.1016/j.heliyon.2023.e17807.
187. Ruksiriwanich, W.; Khantham, C.; Sringarm, K.; Sommano, S.; Jantrawut, P. Depigmented Centella asiatica Extraction by Pretreated with Supercritical Carbon Dioxide Fluid for Wound Healing Application. *Processes* **2020**, *8*, 277. https://doi.org/10.3390/pr8030277.
188. Yuan, Y.; Qiao, Y.; Zheng, X.; Yu, X.; Dong, Y.; Wang, H.; Sun, L. Simultaneous determination of four active compounds in Centella asiatica by supramolecular solvent-based extraction coupled with high performance liquid chromatography-tandem mass spectrometry. *J. Chromatogr. A* **2023**, *1708*, 464298. https://doi.org/10.1016/j.chroma.2023.464298.
189. Dorni, A.I.C.; Peter, G.; Jude, S.; Arundhathy, C.A.; Jacob, J.; Amalraj, A.; Pius, A.; Gopi, S. UHPLC-Q-ToF-MS-guided enrichment and purification of triterpenoids from *Centella asiatica* (L.) extract with macroporous resin. *J. Liq. Chromatogr. Relat. Technol.* **2017**, *40*, 13–25. https://doi.org/10.1080/10826076.2017.1280681.
190. Du, Q.Z.; Jerz, G.; Chen, P.; Winterhalter, P. Preparation of ursane triterpenoids from Centella asiatica using high speed countercurrent chromatography with step-gradient elution. *J. Liq. Chromatogr. Relat. Technol.* **2004**, *27*, 2201–2215. https://doi.org/10.1081/jlc-200025707.
191. Diallo, B.; Vanhaelenfastre, R.; Vanhaelen, M. Direct coupling of high-speed countercurrent chromatography to thin-layer chromatography—application to the separation of asiaticoside and madecassoside from centella-asiatica. *J. Chromatogr.* **1991**, *558*, 446–450. https://doi.org/10.1016/0021-9673(91)80013-7.
192. Gao, M.Z.; Yuan, X.Y.; Xiao, H.B. Preparation of asiaticoside and m adecassoside from the extract of Centella a sia tica(L) Urb using preparative high perfomance liquid chromatography. *Chin. J. Chromatogr.* **2008**, *3*, 362–365.
193. Gao, M.; Yuan, X.; Xiao, H. [Preparation of asiaticoside and madecassoside from the extract of *Centella asiatica* (L.) Urb using preparative high performance liquid chromatography]. *Se Pu* **2008**, *26*, 362–365.
194. Schieffer, G.W. Use of solid-phase extraction for improving HPLC assays of triterpene glycosides in gotu kola (*Centella asiatica*), parthenolide in feverfew (*Tanacetum parthenium*), and valerenic acids in valerian (*Valeriana officinalis*). *J. Liq. Chromatogr. Relat. Technol.* **2005**, *28*, 581–592. https://doi.org/10.1081/jlc-200047215.
195. Eilstein, J.; Nair, V.; Moore, K.; Pannakal, S.T.; Grégoire, S.; Ekhar, P.; Guy, R.H.; Delgado-Charro, M.B.; Roy, N. Non-destructive, reverse iontophoretic extraction of phytochemicals from Mangifera indica, Centella asiatica, Punica granatum, and Citrus sinensis. *Phytochem. Anal.* **2023**, *34*, 408–413. https://doi.org/10.1002/pca.3219.
196. Charoenchaitrakool, M.; Niamnuy, C.; Dittanet, P.; Chantes, O.; Chuangyang, P. Statistical optimization for precipitation of bioactive compounds from extracted Centella asiatica using gas anti-solvent technique. *J. Food Process Eng.* **2020**, *43*, e13318. https://doi.org/10.1111/jfpe.13318.
197. Zhao, N.; Wu, Z.S.; Wu, C.Y.; Wang, S.Y.; Zhan, X.Y. Performance evaluation of variable selection methods coupled with partial least squares regression to determine the target component in solid samples. *J. Near Infrared Spectrosc.* **2022**, *30*, 171–178. https://doi.org/10.1177/09670335221097236.
198. Liu, H.; Ye, X.L.; Yang, G.; Qi, Y.P.; Fan, G.R. [Near-infrared spectroscopy technology for online monitoring of the column separation and purification process of active components of *Centella asiatica* L. Urban]. *Guang pu xue yu guang pu fen xi = Guang pu* **2013**, *33*, 98–101.
199. Schaneberg, B.T.; Mikell, J.R.; Bedir, E.; Khan, I.A. An improved HPLC method for quantitative determination of six triterpenes in Centella asiatica extracts and commercial products. *Die Pharm.* **2003**, *58*, 381–384.
200. Wang, H.D.; Xu, W.C.; Wang, Y.; Kong, X.W.; Sun, L.J. Determination of asiaticoside and madecassoside in *Centella asiatica* (L.) Urban by HPLC-ELSD. *China Surfactant Deterg. Cosmet.* **2023**, *53*, 976–980. https://doi.org/10.3969/j.issn.2097-2806.2023.08.015.
201. Inamdar, P.K.; Yeole, R.D.; Ghogare, A.B.; deSouza, N.J. Determination of biologically active constituents in *Centella asiatica*. *J. Chromatogr. A* **1996**, *742*, 127–130. https://doi.org/10.1016/0021-9673(96)00237-3.
202. Günther, B.; Wagner, H. Quantitative determination of triterpenes in extracts and phytopreparations of Centella asiatica (L.) urban. *Phytomedicine* **1996**, *3*, 59–65. https://doi.org/10.1016/s0944-7113(96)80011-0.
203. Yang, L.; Marney, L.; Magana, A.A.; Choi, J.; Wright, K.; McFerrin, J.; Gray, N.E.; Soumyanath, A.; Stevens, J.F.; Maier, C.S. Quantification of Caffeoylquinic Acids and Triterpenes as Targeted Bioactive Compounds of Centella asiatica in Extracts and Formulations by Liquid Chromatography Mass Spectrometry. *J. Chromatogr. Open* **2023**, *4*, 100091. https://doi.org/10.1016/j.jcoa.2023.100091.

204. Sabaragamuwa, R.; Perera, C.O.; Fedrizzi, B. Ultrasound assisted extraction and quantification of targeted bioactive compounds of Centella asiatica (Gotu Kola) by UHPLC-MS/MS MRM tandem mass spectroscopy. *Food Chem.* **2022**, *371*, 131187. https://doi.org/10.1016/j.foodchem.2021.131187.
205. Raj, D.; Kielisz, P. High-Performance Thin-Layer Chromatographic-Densitometric Determination of the Major Triterpene Saponins and Their Aglycones from *Centella asiatica*. *JPC-J. Planar Chromatogr.-Mod. TLC* **2019**, *32*, 25–30. https://doi.org/10.1556/1006.2019.32.1.3.
206. James, J.; Dubery, I. Identification and Quantification of Triterpenoid Centelloids in *Centella asiatica* (L.) Urban by Densitometric TLC. *JPC-J. Planar Chromatogr.-Mod. TLC* **2011**, *24*, 82–87. https://doi.org/10.1556/jpc.24.2011.1.16.
207. Tassanawat, P.; Putalun, W.; Yusakul, G.; Sritularak, B.; Juengwatanatrakul, T.; Tanaka, H. Production of polyclonal antibody against madecassoside and development of immunoassay methods for analysis of triterpene glycosides in *Centella asiatica*. *Phytochem. Anal.* **2013**, *24*, 256–262. https://doi.org/10.1002/pca.2406.
208. Juengwatanatrakul, T.; Sritularak, B.; Amornnopparattanakul, P.; Tassanawat, P.; Putalun, W.; Tanaka, H.; Morimoto, S. Preparation of a specific monoclonal antibody to asiaticoside for the development of an enzyme-linked immunosorbent assay. *Analyst* **2011**, *136*, 1013–1017. https://doi.org/10.1039/c0an00868k.
209. Lu, Q.; Li, W.H.; Hu, S.Q. [Studies on fingerprints of Centella asiatica by HPLC]. *Zhong yao cai = Zhongyaocai = J. Chin. Med. Mater.* **2011**, *34*, 46–50.
210. Jia, Z.W.; Mao, X.H.; Chen, K.; Wang, K.; Ji, S. Quantitative analysis and HPLC specific chromatogram of Centellae Herba and its total glucosides by chiral mobile phase additives. *Chin. Tradit. Herb. Drugs* **2010**, *41*, 2070–2074.
211. Xin-wei, T. Determination ofmadecassoside in SD rats plasma by solid-phase extraction RP- HPLC. *J. Chongqing Med. Univ.* **2010**, *35*, 884–887. https://doi.org/10.13406/j.cnki.cyxb.2010.06.053.
212. Han, W.J.; Xia, Y.F.; Dai, Y. Development and validation of high-performance liquid chromatography/electrospray ionization mass spectrometry for assay of madecassoside in rat plasma and its application to pharmacokinetic study. *Biomed. Chromatogr.* **2012**, *26*, 26–32. https://doi.org/10.1002/bmc.1620.
213. Wright, K.M.; Bollen, M.; David, J.; Speers, A.B.; Brandes, M.S.; Gray, N.E.; Alcázar Magaña, A.; McClure, C.; Stevens, J.F.; Maier, C.S.; et al. Pharmacokinetics and Pharmacodynamics of Key Components of a Standardized Centella asiatica Product in Cognitively Impaired Older Adults: A Phase 1, Double-Blind, Randomized Clinical Trial. *Antioxidants* **2022**, *11*, 215. https://doi.org/10.3390/antiox11020215.
214. Wright, K.M.; Bollen, M.; David, J.; Mepham, B.; Alcázar Magaña, A.; McClure, C.; Maier, C.S.; Quinn, J.F.; Soumyanath, A. Bioanalytical method validation and application to a phase 1, double-blind, randomized pharmacokinetic trial of a standardized *Centella asiatica* (L.) Urban water extract product in healthy older adults. *Front. Pharmacol.* **2023**, *14*, 1228030. https://doi.org/10.3389/fphar.2023.1228030.
215. Songvut, P.; Chariyavilaskul, P.; Tantisira, M.H.; Khemawoot, P. Safety and Pharmacokinetics of Standardized Extract of Centella asiatica (ECa 233) Capsules in Healthy Thai Volunteers: A Phase 1 Clinical Study. *Planta Med.* **2019**, *85*, 483–490. https://doi.org/10.1055/a-0835-6671.
216. Boonyarattanasoonthorn, T.; Kijtawornrat, A.; Songvut, P.; Nuengchamnong, N.; Buranasudja, V.; Khemawoot, P. Increase water solubility of Centella asiatica extract by indigenous bioenhancers could improve oral bioavailability and disposition kinetics of triterpenoid glycosides in beagle dogs. *Sci. Rep.* **2022**, *12*, 2909. https://doi.org/10.1038/s41598-022-06967-1.
217. Yang, Y.Y.; Wan, J.Y.; Luo, F.L.; Zhang, Z.; Li, H.Z.; Zhou, Q.X. Effect of Madecassoside on Activation of Synovial Fibroblasts from Rats with Adjuvant Arthritis. *Chin. J. Exp. Tradit. Med. Formulae* **2014**, *20*, 173–177. https://doi.org/10.13422/j.cnki.syfjx.2014080173.
218. Luo, Y.; Yang, Y.P.; Liu, J.; Li, W.H.; Yang, J.; Sui, X.; Yuan, X.; Nie, Z.Y.; Liu, Y.Q.; Chen, D.; et al. Neuroprotective effects of madecassoside against focal cerebral ischemia reperfusion injury in rats. *Brain Res.* **2014**, *1565*, 37–47. https://doi.org/10.1016/j.brainres.2014.04.008.
219. Luo, Y.; Wang, C.; Li, W.H.; Liu, J.; He, H.H.; Long, J.H.; Yang, J.; Sui, X.; Wang, S.; You, Z.; et al. Madecassoside protects BV2 microglial cells from oxygen-glucose deprivation/reperfusion-induced injury via inhibition of the toll-like receptor 4 signaling pathway. *Brain Res.* **2018**, *1679*, 144–154. https://doi.org/10.1016/j.brainres.2017.11.030.
220. Liu, S.; Li, G.; Tang, H.; Pan, R.; Wang, H.; Jin, F.; Yan, X.; Xing, Y.; Chen, G.; Fu, Y.; et al. Madecassoside ameliorates lipopolysaccharide-induced neurotoxicity in rats by activating the Nrf2-HO-1 pathway. *Neurosci. Lett.* **2019**, *709*, 134386. https://doi.org/10.1016/j.neulet.2019.134386.

221. Monton, C.; Luprasong, C.; Suksaeree, J.; Songsak, T. Preparation and evaluation of film forming polymeric dispersion containing Centella asiatica extract for skin application. *Adv. Tradit. Med.* **2021**, *21*, 73–81. https://doi.org/10.1007/s13596-020-00451-9.
222. Suhail, M.; Chiu, I.H.; Ullah, A.; Khan, A.; Ullah, H.; Al-Sowayan, N.S.; Wu, P.C. Formulation and In Vitro Assessment of Polymeric pH-Responsive Nanogels of Chitosan for Sustained Delivery of Madecassoside. *ACS Omega* **2024**, *9*, 19345–19352. https://doi.org/10.1021/acsomega.4c00461.
223. Liu, M.; Chen, W.; Zhang, X.; Su, P.; Yue, F.; Zeng, S.; Du, S. Improved surface adhesion and wound healing effect of madecassoside liposomes modified by temperature-responsive PEG-PCL-PEG copolymers. *Eur. J. Pharm. Sci.* **2020**, *151*, 105373. https://doi.org/10.1016/j.ejps.2020.105373.
224. Chiu, I.H.; Vu, Q.L.; Wu, P.C. Development and evaluation of madecassoside-loaded microemulsion for enhanced topical drug delivery. *Int. J. Pharm. X* **2026**, *12*, 100649. https://doi.org/10.1016/j.ijpx.2026.100649.
225. Winitthana, T.; Niwattisaiwong, N.; Patarapanich, C.; Tantisira, M.H.; Lawanprasert, S. In vitro inhibitory effects of asiaticoside and madecassoside on human cytochrome P450. *Toxicol. Vitr. Int. J. Publ. Assoc. BIBRA* **2011**, *25*, 890–896. https://doi.org/10.1016/j.tiv.2011.02.010.
226. Wu, Y.; Zhao, M.; Zhang, P.; Ho, C.T. Microbiota-Mediated Conversion of Asiaticoside to Asiatic Acid Restores Intestinal Homeostasis in Mice with Chronic Intestinal Inflammation. *J. Agric. Food Chem.* **2026**, *74*, 24277–24291. https://doi.org/10.1021/acs.jafc.5c17587.
227. Wei, L.L.; Bai, F.C.; Lin, W.J.; Lin, Y.T.; Qiu, Y.; Wei, J.B.; Wang, D.D. Effect of madecassoside on gut microbiota in mice with alcoholic liver disease. *Chin. Pharmacol. Bull.* **2026**, *42*, 1686–1693. https://doi.org/10.12360/CPB202510073.
228. Zhao, G.; Liu, Y.J.; Bai, J.R.; Song, Y.; Liu, Y. Protective Effects of Madecassoside on the Acute Spinal Cord Injury in Rats. *J. LI-Shizhen Tradit. Chin. Med.* **2011**, *22*, 2129–2131. https://doi.org/10.3969/j.issn.1008-0805.2011.09.034.
229. Tawinwung, S.; Junsaeng, D.; Utthiya, S.; Khemawoot, P. Immunomodulatory effect of standardized C. asiatica extract on a promotion of regulatory T cells in rats. *BMC Complement. Med. Ther.* **2021**, *21*, 220. https://doi.org/10.1186/s12906-021-03394-z.
230. Wannasarit, S.; Puttarak, P.; Kaewkroek, K.; Wiwattanapatapee, R. Strategies for Improving Healing of the Gastric Epithelium Using Oral Solid Dispersions Loaded with Pentacyclic Triterpene-Rich Centella Extract. *AAPS PharmSciTech* **2019**, *20*, 277. https://doi.org/10.1208/s12249-019-1488-7.
231. Xu, B.; Chen, J.M.; Gao, Y.H.; Fan, N.Q.; Zhang, S.H. Design and evaluation of complex plant extract-loaded dissolving microneedle for improving periocular wrinkles. *J. Drug Deliv. Sci. Technol.* **2025**, *113*, 107355. https://doi.org/10.1016/j.jddst.2025.107355.
232. He, Y.; He, D.; Ren, S.; Fan, L.; Wang, L.; Sun, J. 3D-printed microneedles loaded with madecassoside for periodontal soft tissue regeneration. *Int. J. Pharm.* **2025**, *676*, 125569. https://doi.org/10.1016/j.ijpharm.2025.125569.
233. Zhou, W.; Wu, W.H.; Si, Z.L.; Liu, H.L.; Wang, H.; Jiang, H.; Liu, Y.F.; Alolga, R.N.; Chen, C.; Liu, S.J.; et al. The gut microbe Bacteroides fragilis ameliorates renal fibrosis in mice. *Nat. Commun.* **2022**, *13*, 6081. https://doi.org/10.1038/s41467-022-33824-6.
234. Bian, D.; Liu, M.; Li, Y.; Xia, Y.; Gong, Z.; Dai, Y. Madecassoside, a triterpenoid saponin isolated from Centella asiatica herbs, protects endothelial cells against oxidative stress. *J. Biochem. Mol. Toxicol.* **2012**, *26*, 399–406. https://doi.org/10.1002/jbt.21434.
235. Wright, K.M.; Magana, A.A.; Laethem, R.M.; Moseley, C.L.; Banks, T.T.; Maier, C.S.; Stevens, J.F.; Quinn, J.F.; Soumyanath, A. Centella asiatica Water Extract Shows Low Potential for Cytochrome P450-Mediated Drug Interactions. *Drug Metab. Dispos.* **2020**, *48*, 1053–1063. https://doi.org/10.1124/dmd.120.090860.

Disclaimer/Publisher's Note: The statements, opinions and data contained in all publications are solely those of the individual author(s) and contributor(s) and not of MDPI and/or the editor(s). MDPI and/or the editor(s) disclaim responsibility for any injury to people or property resulting from any ideas, methods, instructions or products referred to in the content.